Classification of Tropical Vegetation

by

Dominica Elaine Harrison

A thesis submitted in partial fulfillment of the requirements for the degree of

Master's of Science

Earth and Atmospheric Sciences
University of Alberta

Thesis abstract

The increasing anthropogenic pressure on biodiversity in the tropics is resulting in changes to ecosystem structure and increasing species extinction rates (Collen et al. 2013). These issues are heightened in the tropics where 50% of the world's biodiversity is held in 7% of the world's terrestrial landmass (Urquhart 2001). The biodiversity of vegetation has been used as an indicator of the overall health and processes occurring in a biological system. This thesis explores ways to quantify the biodiversity of vegetation using different avenues of vegetation classification.

In the second chapter of this thesis the leaf economic spectra (LES), a vegetation classification that attempts to provide a general framework to assess plant functional diversity, is used to explore the relationships between the conventional plant functional traits with the newly applied anatomical traits (Wright et al. 2004). This system uses economic principles to help understand plant ecology trade-offs and performance strategies. The LES was used to discern two plant functional groups (PFG), lianas and tree species, at two different Panamanian tropical sites, a tropical wet forest and a tropical dry forest. This was accomplished by examining the interactions between commonly used whole-leaf traits from the LES and newly applied anatomical traits. The addition of anatomical traits to the LES is a new approach (Reich 2014). The findings of this investigation support the hypothesis that trees are resource conservative when compared to their liana counterpart, which are thought to be resource acquisitive (Schnitzer 2005; Asner and Martin 2012). Additionally, the interaction of whole-leaf and anatomical traits provide insight into the foliar mechanisms and cellular organization such as: the amount of palisade and nutrients dictates leaf growth rates, the amount of airspace in the spongy mesophyll and potassium regulate water uptake, and cell size and cell numbers affects the defences against

herbivores. Furthermore, variations across sites demonstrated that more resource availability will result in conservative traits and fewer resources will result in acquisitive traits. Future research in the field should focus on the implementation of anatomical traits on different PFGs and at different sites in the tropics.

The third chapter of this thesis takes a remote sensing perspective to vegetation classification by exploring a region of the electromagnetic spectrum that has not been exploited extensively for vegetation investigations, namely the long-wave infrared (LWIR; 8.0 μm-12.5 μm; Ribeiro da Luz and Crowley 2007). Focusing on species discrimination through spectral signature sampling, a Fourier Transform Infrared (FTIR) spectrometer was used to collect the LWIR spectra of 26 tropical dry forest tree species in Costa Rica. To begin, a spectral library of cuticle and cell wall compounds collected by Ribeiro da Luz and Crowley (2007) was used to identify spectral features in the spectra of each species. Then the species were divided into groups based on similarities between spectral features and main compound(s) driving their spectra. Linear discriminant analysis (LDAs) was applied to each group to discriminate species within a group with accuracy rates ranging from 0-67% after validation. A random forest boot-strapping analysis was then applied to entire suite of species to discriminate species resulting in an out-of-bag error rate of 11%. This investigation is a first step in the application of LWIR to environmental monitoring. Advances in technology and airborne sensors will facilitate future remote sensing investigations in species discrimination from imagery and at regional scales.

These two studies demonstrate different approaches to vegetation classification, PFT`s and RS. Together they emphasise the need to classify vegetation to assess damage resulting from biodiversity loss. Future research should focus on a standardization of wide-scale classification techniques.

Preface

This thesis is an original work completed by Dominica Elaine Harrison. Whole-leaf trait data for Chapter 2 was collected by Dr. Joseph Wright and company at the Smithsonian Tropical Research Institute in Panama. Leaf samples for Chapter 2 were collected by Dr. Karen Castro at the Smithsonian Tropical Research Institute in Panama. All sample histological preparations and data collection of the anatomical traits from Chapter 2 were prepared by me. All collection and preparation for Chapter 3 was my original work.

Acknowledgements

Foremost, I would like to acknowledge my co-supervisors, Dr. Benoit Rivard and Dr. Arturo Sanchez-Azofeifa for the constant support and guidance they have provided. This opportunity given to me would not otherwise be possible without their expertise and financial assistance. Thank you for all the time and effort put into this thesis with me, it has helped grow as a scientist and an individual.

I greatly appreciate the advice and involvement of Dr. Janice Cooke, Dr. Joseph Wright and Dr. Andreas Hamann. A special thanks to Sofia Calvo-Rodriguez, Sandra Duran and Kayla Stan. I would also like to thank Mei Mei Chong and all my colleagues in the CEOS lab at the University of Alberta. I would like to acknowledge those who helped in the field when I was far from home: Julio Calvo-Alvarado, Mario Santos, Ana Julieta Calvo, Branko Hilje, Maria Rodriguez and Thiago Silva

Furthermore, I would like to thank my friends and family who have been supporting me the entire two and a half years, specifically, to my parents for their constant proud support. Finally, I would like to acknowledge the financial and institutional support of the University of Alberta, NSERC and the Inter-American Institute for Global Change Research (IAI).

Table of Contents

List of Tables

List of Figures

1.0 Introduction

Tropical ecosystems hold two third of the worlds terrestrial biodiversity, 44% of all plant species and all 25 of the defined biodiversity hot spots around the globe (Gardner et al 2009; Myer et al. 2000). Biodiversity related services are crucial for human survival and economic stability; ecosystem services related to biodiversity such as: forest products, tourism, recreation, genetic resources, disturbance buffers and even medicinal opportunities (Chazdon 2008). Despite the importance of tropical ecosystems, deforestation and climate change still are serious threats. One fifth of the world's green house gas emissions are a result of tropical deforestation and the rate is still increasing with few regulations be put in place or enforced (Burgess et al. 2011; 2012). The loss of tropical ecosystems not only impacts carbon dioxide emission but the loss of biodiversity and its sequential resources is accelerating. Changes to structure composition, and woody plant diversity are associated with deforestation and tropics' degradation (Chazdon 2008). Rather than attempting to understand the current roles biodiversity plays in the tropics, little oversight is occurring while these detrimental losses take place. The need to quantify and calculate biodiversity in the tropics is pertinent to our survival both economically and environmentally.

Species extinction rates are at an all time high as a result of increasing anthropogenic activity. The impacts on the environment are detrimental and are also ever increasing (Collen et al. 2012). The available conservation resources are not sufficient to reverse the effects let alone catalog all the species that are being loss (Houghton et al. 2001). One of the most important consequences from climate change is the ecosystem alterations occurring at the base of the trophic system, changes at the vegetation level (Mucina 1997). To understand these shifts in the ecosystem structure and composition research is being focused on understanding biodiversity (Schlapfer

and Schmidt 1999). Biodiversity of vegetation is paramount to the general health of the environment and to the provisional well being of humans (Winter 2012; Gardner et al 2009) as it provides vital ecosystem services and acts as a buffer in both natural and anthropogenic disturbances (Peterson 1998). Despite its role in human's welfare there are still many anthropogenic threats to biodiversity (Gardner et al 2009). Extinctions are accelerating at a dangerous rate due to societal activities that include agriculture, deforestation, over exploitation of resources, expansion of invasive species, pollution etc (Houghton et al. 2001). To most effectively understand how biodiversity is being impacted it is necessary to be able to identify and quantify the variety of life, particularly the extent of vegetation as it forms the foundation in all trophic systems.

How to monitor biodiversity is still an opened question and there are no standardize methods. Issues include: 1) locating the boundaries of a community, 2) the identification of hot spots and, 3) defining the criteria of species vs plant functional groups that varies from the scale and focal point of a study or question at hand (Myers et al. 2000; Mucina 1997). One field of study with an emphasis to find a solution to these questions is vegetation classification. The need to order and arrange the environment is an inherently anthropogenic trait tied to advancing the understanding of biological systems. More specifically, vegetation classification is the process of systematically organizing plant communities and it is essential in understanding the structural dynamics of ecosystems (Mucina 1997). When examining ecosystem processes (such as soil fertility, long term weather stressors, carbon or energy flow and capture etc) vegetation diversity is chosen most often as an indicator of function of these processes because it is readily quantifiable and relatively static (Dybzinski et al. 2008; Mucina 1997). Furthermore, grouping vegetation based on patterns and trends in response to their environment is essential in our

ecosystem management practices to maintain sustainability and map the extent of our renewable forest resources.

The methodologies applied in vegetation classification are not uniform across scientific fields and therefore different approaches can lead to a different but equally sounds answers. Vegetation classification has undergone some changes over the course of history and most dramatically in the early 70's. The main topics of discussion revolved around (Mucina 1997): 1) continuum vs. discrete, ordering vegetation as discrete communities and functional groups or along a continuum based on traits and genetics; 2) naturalness vs. arbitrariness of traits or classifiable units regarding the temporal aspects of a plant community, are only climax or stable communities truly classifiable?; 3) hierarchical classification (taxonomy) systems in vegetation is biased towards a specific biome or region and cannot be effectively transferred between regions; 4) classical vs. numerical techniques in data collection with advances in technology, where classical identification techniques are very subjective and advances in technology increase the objectivity through numerical measurements. From these discussions a myriad of methods in which vegetation is grouped has arisen.

The scale at which classification is occurring is important towards the purpose of the question at hand. Community classification techniques are generally associated with plant attributes and then grouped accordingly as plant functional groups (PFG) (Domingues et al. 2006; Pierce et al 2012). PFG's are groupings of plants based on their physical, phylogenetic and phenological characteristics. These characteristics are measured by the trends of their plant functional traits (PFT), which are physiological and morphological traits. Some of the main classification approaches associated with PFGs are: physiognomic, environmental, physiognomico-environmental, socio-ecological and floristic (De Cáceres et al. 2009). Physiognomic

classification is very commonly used and utilizes functional and morphological traits to group communities. Environmental classification is when communities in a shared environment are generally grouped together; more specifically the soil and climate are the main drivers. Physiognomico-environmental combines the surrounding soil climate and biogeography with functional and morphological traits. Socio-ecological classification is groups of plants that have similar ecological requirements. Floristic classification is the taxonomical identification of plants communities and generally contains a list of species (De Cáceres et al. 2009).

A popularized concept of PFT classification has been the Leaf Economic Spectrum (LES; Wright et al. 2004); An idea that leaf traits can be categorized depending on their resource investment strategies (Wright et al 2004). The grouping of PFTs along this spectrum is thought to be dependant of the rate of return of a resource: some species being fast investors and others being slow investors or resource acquisitive and conservative, respectively. Reich (2014) took this concept one step further suggesting that the rate of return should be equal at all scales (cellular, organ, individual and ecosystem) and locations (root, stem, leaf, and branch). The application of this concept to PFT categorization will be discussed in detail in the second chapter of this thesis.

A more systematic approach to classification is taxonomy. Specifically, species distributions and inventories are key to providing a quantifiable numerical value to the biodiversity of a classifiable plant community. There are many classical ecological approaches to this problem such as: expert taxonomists, dichotomous keys for the non experts, metamorphic and image processing and until more recently, DNA fingerprinting (Jensen and Bourgeron 1994; Whittaker 1982). All these techniques are generally done at the local scale where identification occurs within a plot.

From a global or ecosystem level perspective remote sensing (RS) and land-use mapping have widely been used to map and attempt to identify species distributions and compositions. RS of the environment uses leaf optics and the interaction with light to characterize and categorize plants' health and distribution (Ustin and Gamon 2010). In general, three primary regions of the electromagnetic spectrum (EM) are utilized in RS: the visible (VIS; 0.4-0.7 μm) and near and shortwave infrared (NIR: 0.7-1.4 μm; SWIR: 1.4-2.5 μm). Both airborne and satellite sensors have been used to capture surface information in these regions of the EM (VIS, NIR and SWIR). This information for the most part has been limited to the characterization of growth form, fractional cover and phenology (Ustin and Gamon 2010). This information is most often captured through the use of spectral indices that use spectral band ratio or other spectral math to measure vegetation properties. Some of the most common indices are: NDVI, EVI and the red-edge index. Generally, analysis of satellite imagery will use indices due to the limitations of space-borne multi-spectral sensors where more recent airborne sensors offer hyper-spectral sensors. The most commonly used satellite sensors being: 1) Landsat Thematic Mapper for environmental monitoring; 2) AVHRR and MODIS for vegetation structure and phenology; and 3) fine spatial scale sensors such as Worldview, GeoEye, Ikonos, Quickbird and TerraSAR-X (Jones and Vaughan 2010).

A few studies have aimed to identify tropical tree species (Zhang et al. 2006; -Esau et al. 2006 & 2008, Feret and Asner 2011). Zhang et al (2006) found that wavelet transformation on tree-crown airborne hyperspectral imagery was much more successful at species identification of 5 TDF tree species when compared to spectral angle mapping. Castro-Esau et al. (2006) were able to identify tropical dry forest tree species within a single site and season using forward feature selection and patter recognition. Furthermore, Feret and Asner (2011) used field spectroscopy

and radiative transfer models to identify tropical Hawaiian tree species with and accuracy rate of 50-80%. A novel and relatively recent study by Ribeiro da Luz and Crowley (2006; 2007 & 2010) utilized laboratory long-wave spectroscopy signatures to discriminate nine temperate tree species. The third chapter of this thesis builds on the work of Ribeiro da Luz and Crowley (2007) with the application of long-wave infrared spectroscopy species discrimination in a high biodiversity site, a tropical dry forest.

The overall objective of this thesis was to explore different modes of categorization of vegetation species in the tropics for the purpose of ecosystem mapping and biodiversity quantification. To this end, I attempted to discern plant functional groups using the leaf economic spectrum (Chapter 2) and then explore the distinction of tree species through their long-wave infrared spectral signatures (Chapter 3).

Chapter 2. **An anatomical application to Leaf Economic Spectrum (LES) through liana and tree whole-leaf trait analysis**, explores the plant functional group (PFG) category of classification. In an attempt to understand the trends associated with resource investment, two opposing groups are examined lianas and trees, along the well established trait analysis system known as the LES (Wright et al. 2004; Reich 2014). The LES attempts to classify PFGs based on their resource strategies along an economic spectrum. This spectrum assesses plant ecology trade-off and performance strategies based on the rate of return of an investment. This trade-off hypothesis suggests that these different strategies in PFTs help explain give rise to niche partitioning, the process which competing species use the environment differently to enable co-existence (Sterk et al 2011). The trade-offs are between light vs. nutrients or light vs. water gradients. The traits used in the LES are functional traits including both foliar physiological and morphological attributes of the plant: nitrogen, phosphorous and potassium concentrations;

photosynthesis and dark respiration rates; and leaf mass area, leaf longevity, and laminar toughness (Asner and Martin 2012; Reich 2014; Batcheler 1985). However, the LES does not encompass the anatomy of the leaf which can dictate the functional consequences and process from the morphological and physiological traits. In this chapter cross sections of leaves from26 lianas species and 25 trees species were created, both from two different tropical wet and dry forest sites, and measured the following anatomical parameters: 1) upper and lower epidermis thickness and cell occupied area and 2) palisade and spongy mesophyll thickness, cell count, cell size, cell-occupied area and airspace area. With the anatomical traits and the whole leaf traits the differences of PFT groups (lianas and trees) and site (wet and dry) were examined. The whole leaf traits were examined with general linear models, the anatomical traits with linear mixed model and a linear discriminate analysis. Finally, the interactions between anatomical and whole-leaf traits were examined through analyses of co-variances. The main objective of this chapter was to examine the interactions between whole leaf and anatomical traits of lianas and trees in two different climatic conditions: a tropical wet forest (Mean Annual Precipitation, MAP > 3000 mm) and a tropical dry forest (MAP < 1800 mm) in the context of their relative position in the LES.

Chapter 3, **Long-wave infrared spectral feature characterization of tropical dry forest tree species and use for species discrimination**, focused on species level classification through new techniques in remote sensing of the environment. Classical vegetation monitoring techniques have used the visible (VIS; 0.4-0.7 μm), near and shortwave infrared (NIR: 0.7-1.4 μm; SWIR: 1.4-2.5 μm) regions of the electromagnetic (EM) spectrum for the remote sensing of vegetation. From these region scientists have been able to map the extent, health and vigour of ecosystems globally with the help of vegetation indices (Kokaly et al. 1999 & 2009). These indices,

however, provide information that is not taxonomically specific. A novel study from Ribeiro da Luz and Crowley (2006; 2007; 2010) found that the long wave infrared (LWIR, 8.5-12.5 μm) region of the EM produced unique "finger-print" spectra for nine different temperate tree species. From these findings this chapter attempts to identify internal cuticular and epidermal compounds in the LWIR spectra of 26 tree species from a tropical dry forest. Compounds are attributed to the observed spectral features and the spectral fingerprints measured are thought to be unique to species (Salisbury 1986; Ribeiro da Luz and Crowley 2006). From these signatures this chapter attempts to classify species through multivariate statistics such as random forest boot-strapping analyses and linear discriminant analyses.

1.1 References

Asner, G. P., & Martin, R. E. (2012). Contrasting leaf chemical traits in tropical lianas and trees: Implications for future forest composition. *Ecology Letters*, *15*(9), 1001–1007.

Batcheler, C. L. (1985). Note on measurement of woody plant diameter distributions. *New Zealand Journal of Ecology*, *8*, 129–132.

Burgess, K. S., Fazekas, A. J., Kesanakurti, P. R., Graham, S. W., Husband, B. C., Newmaster, S. G., Barrett, S. C. H. (2011). Discriminating plant species in a local temperate flora using the rbcL+matK DNA barcode. *Methods in Ecology and Evolution*, *2*(4), 333–340.

Burgess, R., Hansen, M., Olken, B. A., Potapov, P., & Sieber, S. (2012). The political economy of deforestation in the tropics. *Quarterly Journal of Economics*, *127*(4), 1707–1754.

Castro-Esau, K. L., & Sanchez-Azofeifa, G. A. (2008). Changes in Spectral Properties, Chlorophyll Content and Internal Mesophyll Structure of Senescing Populus balsamifera and Populus tremuloides Leaves. *Sensors*, *8*, 51–69.

Castro-Esau, K. L., Sanchez-Azofeifa, G. A., Rivard, B., Wright, S. J., & Quesada, M. (2006). Variability in leaf optical properties of mesoamerican trees and the potential for species classification. *American Journal of Botany*, *93*(4), 517–530.

Chazdon, R. L. (2008). Beyond deforestation: restoring forests and ecosystem services on degraded lands. *Science (New York, N.Y.)*, *320*(5882), 1458–1460.

Clark, R. N., Despain, D. G., Kokaly, R. F., & Livo, K. E. (2003). Mapping vegetation in Yellowstone National Park using spectral feature analysis of AVIRIS data, *Remote Sensing of the Environment 84*, 437–456.

Collen, B., Pettorelli, N., Bailie, J. E. M., Durant, S. 2013. *Biodiversity monitoring and conservation: bridging the gap between global commitment and local action*. Wiley-Blackwell publications.

De Cáceres, M., Font, X., Vicente, P., & Oliva, F. (2009). Numerical reproduction of traditional classifications and automatic vegetation identification. *Journal of Vegetation Science*, *20*(4),

Domingues, T. F., Martinelli, L. A., & Ehleringer, J. R. (2007). Ecophysiological traits of plant functional groups in forest and pasture ecosystems from eastern Amazonia, Brazil. *Plant Ecology*, *193*(1), 101–112.

Dybzinski, R., Fargione, J. E., Zak, D. R., Fornara, D., & Tilman, D. (2008). Soil fertility increases with plant species diversity in a long-term biodiversity experiment. *Oecologia*, *158*(1), 85–93.

Féret, J. B., & Asner, G. P. (2012). Semi-supervised methods to identify individual crowns of lowland tropical canopy species using imaging spectroscopy and lidar. *Remote Sensing*, *4*(8), 2457–2476.

Gardner, T. A., Barlow, J., Chazdon, R., Ewers, R. M., Harvey, C. A., Peres, C. A., & Sodhi, N. S. (2009). Prospects for tropical forest biodiversity in a human-modified world. *Ecology Letters*, *12*(6), 561–582.

Houghton, J. T., Ding, Y., Griggs, D. J., Noguer, M., Van der Linden, P. J.,Dai, X., Johnson, C. A. (2001). Climate Change 2001: The Scientific Basis. *Climate Change 2001: The Scientific Basis*

Jensen, M., & Bourgeron, P. (1994). Volume II: ecosystem management: principles and applications. *General Technical Report PNW-GTR 318*, 376.

Jones, H. G., Vaughan, R. A. (2010). *Remote sensing of vegetation*. Ch. 7.2 Spectral indices.164-182, Oxford, New York, *Oxford University Press*.

Kiang, N. Y., Siefert, J., Govindjee, & Blankenship, R. E. (2007). Spectral signatures of photosynthesis I review of earth organisms. *Astrobiology*, *7*(1), 222–251.

Kokaly, R. F., Asner, G. P., Ollinger, S. V., Martin, M. E., & Wessman, C. A. (2009). Characterizing canopy biochemistry from imaging spectroscopy and its application to ecosystem studies. *Remote Sensing of Environment*, *113*(SUPPL. 1), S78–S91.

Kokaly, R. F., & Clark, R. N. (1999). Spectroscopic determination of leaf biochemistry using band-depth analysis of absorption features and stepwise multiple linear regression. *Remote Sensing of Environment*, *67*(3), 267–287.

Mucina, L. (1997). Classification of vegetation: Past, present and future, Journal of Vegetation Science 8 751–760.

Myers, N., Mittermeier, R. A., Mittermeier, C. G., da Fonseca, G. A. B., & Kent, J. (2000). Biodiversity hotspots for conservation priorities. *Nature*, *403*(6772), 853–858.

Peterson, G., Allen, C. R., Holling, C. S. (1997). Ecological resilience, Biodiversity and Scale. Ecosystems 1: 6-18.

Pierce, S., Brusa, G., Vagge, I., & Cerabolini, B. E. L. (2013). Allocating CSR plant functional types: The use of leaf economics and size traits to classify woody and herbaceous vascular plants. *Functional Ecology*, *27*(4), 1002–1010.

Reich, P. B. (2014). The world-wide "fast-slow" plant economics spectrum: A traits manifesto. *Journal of Ecology*, *102*(2), 275–301.

Ribeiro da Luz, B. (2006). Attenuated total reflectance spectroscopy of plant leaves: A tool for ecological and botanical studies. *New Phytologist*, *172*(2), 305–318.

Ribeiro da Luz, B., & Crowley, J. K. (2007). Spectral reflectance and emissivity features of broad leaf plants: Prospects for remote sensing in the thermal infrared (8.0-14.0um). *Remote Sensing of Environment*, *109*(4), 393–405.

Ribeiro da Luz, B., & Crowley, J. K. (2010). Identification of plant species by using high spatial and spectral resolution thermal infrared (8.0-13.5 [mu]m) imagery. *Remote Sensing of Environment*, *114*(2), 404–413.

Sanchez-Azofeifa, G. A., Castro, K., Wright, S. J., Gamon, J., Kalacska, M., Rivard, B., … Feng, J. L. (2009). Differences in leaf traits, leaf internal structure, and spectral reflectance between two communities of lianas and trees: Implications for remote sensing in tropical environments. *Remote Sensing of Environment*, *113*(10), 2076–2088.

Sanchez-Azoffeifa, G.A., Kalacska, M., Quesada, M., Calco-Alvarado, J. C., Nassar, J.M., Rodriguez, J.P. (2005). Need for Integrated Research for a Sustainable Future in Tropical Dry Forests, *19*(2), 285–286.

Salisbury, J. W. (1986). Preliminary measurements of leaf spectral reflectance in the 8-14 μm region. *International Journal of Remote Sensing*, *7*(12), 1879–1886.

Schläpfer, F., & Schmid, B. (1999). Ecosystem Effects of Biodiversity : a Classification of. *Ecological Applications*, *9*(3), 893–912.

Schnitzer, S. A. (2005). A mechanistic explanation for global patterns of liana abundance and distribution. *The American Naturalist*, *166*(2), 262–276.

Séné, F. C., B., Mccann, M. C., Wilson, R. H., & Crinter, R. (1994). Fourier-Transform Raman and Fourier-Transform lnfrared Spectroscopy '. *Plant Physiology*, *106*, 1623–1631.

Sterk, F., Markesteijn, L., Chieving, F., & Poorter, L. (2011). Functional traits determine trade-offs and niches in a tropical forest community. Proceedings of the National Academy of Sciences 51: 2062-20632.

Urquhart, G., Chomentowski, W.S. (2001). Tropical deforestation. Technical report, NASA Earth Observatory (Burgess)

Ustin, S. L., & Gamon, J. A. (2010). Remote sensing of plant functional types. *New Phytologist*, *186*(4), 795–816.

Whittaker, R. H. 1998. *Ordination of plant communities*. Dr.W Junk Publishes. The Hague Boston-London.

Winter, S. (2012). Forest naturalness assessment as a component of biodiversity monitoring and conservation management. *Forestry*, *85*(2), 291–304.

Wright, I. J., Reich, P. B., Westoby, M., Ackerly, D. D., Baruch, Z., Bongers, F., Gulias, J. (2004). The worldwide leaf economics spectrum, Nature, 12, 821–827.

Zhang, J., Rivard, B., Sánchez-Azofeifa, A., & Castro-Esau, K. (2006). Intra- and inter-class spectral variability of tropical tree species at La Selva, Costa Rica: Implications for species identification using HYDICE imagery. *Remote Sensing of Environment*, *105*(2), 129–141.

2.0 An anatomical application to Leaf Economic Spectrum through liana and tree whole-leaf trait analysis

2.1 Abstract

The physiology and morphology of leaves have been used extensively in classification and characterization of taxa and plant functional groups (PFG). One of the more common classification systems was developed by Wright et al. (2004) called the Leaf Economic Spectrum (LES). This system uses economic principals to assess plant functional diversity. Moreover, the LES is defined as the rate of return from a resource investment where plant functional traits (physiological and morphological traits) are treated like currency that fall along a fast to slow continuum (Wright et al. 2004; Reich 2014). In an attempt to understand the mechanisms behind these whole-leaf traits this investigation breaks down the leaf into anatomical sections through measurement of anatomical traits such as the epidermis, mesophyll (palisade and spongy mesophyll): cell occupied areas, air space area, thicknesses, number of cells and average size of the individual cells. Two PFGs at two different site types, trees and lianas at wet and dry sites, were used because they are thought to be at opposing ends of the spectrum, trees are considered slow resource investors and lianas are thought to be fast resource investors. Furthermore, opposing sites provided the perspective role water availability plays on resource investment strategies. Linear models (General linear models and linear mixed models) were constructed for each trait and then whole-leaf and anatomical traits interactions were examined with analyses of co-variance. The results support the hypothesis that lianas are resource inquisitive and trees are resource conservative and provided some mechanistic points of view not yet seen before. For example: trees have thicker, denser leaves with more palisade mesophyll cell occupied area and lianas had thin, less dense, more air area in the spongy mesophyll. Therefore, trees invest more into infrastructure while lianas invest more in fast growth mechanisms and are cheaper

investments than those of tree leaves. The results of the site type demonstrated an unexpected result that the interaction between palisade and nutrients on growth form was negligible but significantly different between site type. This suggests that water stress, for some traits, could have more influence on anatomical variation than competition between growth form. This circumstantial experiment enabled the addition of anatomical traits into the LES with two PFGs that are thought to be at opposing ends of the spectrum. Furthermore, the knowledge of the co-existence of lianas and trees was advanced. It is imperative as lianas are increasing in abundance with climate change and are thought to be negatively impacting their host trees through increased mortality and competition.

2.2 Introduction

Leaves are the most variable organ of plants as they vary widely in shape, size, and anatomical organization (Hudson and Jeffree 2001). This variability is reflected in their internal adaptations to external pressures (eg. thickness of the mesophyll dictates the diffusion time of CO_2 into the photosynthetic pathway or sunken stomata suggest a windy or hot environment to prevent evapo-transpiration loss). As such, each layer of a given leaf (upper epidermis, palisade mesophyll, spongy mesophyll and lower epidermis) is responsible for particular processes, for example: provision of protective cells, the promotion of the bulk of primary metabolic functions, photosynthesis, and gas exchange among many other processes (Pyke 2012; Hopkins and Huner 2009; Taiz and Zeiger 2006). Furthermore, at the micro-scale level, variations in anatomy and physiology in leaves are used in intra- and inter-specific functional group classifications (Wright et al 2004).

In tropical forests, high levels of species diversity result in increased rates of competition or niche-differentiation between different functional groupings of plants (Hopkins and Huner

2009). This high level of plant biodiversity also translates into differences among anatomic properties between self-supported (Trees) and non-supported systems (Lianas; Sanchez-Azofeifa et al 2009). Thus differences on anatomic properties contribute to overall differences on plant functional diversity; which in turn influence the position of a given species or functional grouping on the Leaf Economic Spectrum (LES).

The LES is a classification system that attempts to provide a general framework to assess plant functional diversity (Wright et al. 2004). This theory uses economic principles to help understand plant ecology trade-offs and performance strategies. The LES is, in general, defined as the rate of return from a resource investment, where plant functional traits are treated like currency that fall along a fast to slow continuum (Wright et al. 2004; Reich 2014). As such, fast investment species have high resource acquisition and allocation rates and most traits are aimed to increase growth and productivity. Fast tactics mostly occur in resource-rich environments. Slow investment species have slow resource movement and turnover, and traits are aimed at survival and conservation mechanisms. Slow tactics are usually due to biophysical constraints directly related to low or limiting resource availability (Wright et al 2004; Reich 2014). Table 2.2 presents eight of the whole leaf traits commonly used to assess leaf economics.

In the context of the LES, Reich (2014) hypothesized that the speed of resource investment tactics in plants is conserved across all scales and locations. He suggested that functional traits should reflect such speed. Reich (2014) also revised the LES by adding different scales (organ, individual and ecosystem), locations (root, stem and leaf), as well as including all the essential resources (carbon, water and nutrients). Along the LES, species from similar functional groups generally fall together to one side of the spectrum (Reich 2014). As such, lianas and trees are hypothesized to be at opposing ends of the LES (Schnitzer and Bonger 2005; Wright et al 2004;

Reich 2014) since lianas are thought to be resource acquisitive and trees resource conservative (Sanchez-Azofeifa et al. 2009; Schnitzer et al. 2015).

The parasitic nature of lianas enables them to be considered a species that allocates resources related to growth and productivity for leaf production because their host tree species provides them with structure and support (Sanchez-Azofeifa et al. 2009; Schnitzer 2015). Lianas have been found to have low Leaf Mass Area (LMA), thin leaves, with high nitrogen, phosphorous, photosynthetic rates, and hydraulic conductance (An explanation of each trait can be found on Table 2.2; Cai et al. 2009; Sanchez-Azofeifa et al. 2009, Schnitzer et al. 2015); however these trends can vary depending on environmental conditions and global locations. On the other hand, trees invest more in survival and structure and are slow strategists (Schnitzer et al. 2015). Conservative plant species, such as trees, generally have high density, expensive and tough leaves, low nutrient concentrations, low photosynthesis and respiration rates, and low hydraulic conductance (Reich 2014; Schnitzer et al. 2005). Although there are important differences in liana/tree traits, the variations among them are very large and have considerable overlap (Gilbert et al 2006).

As the differences between functional groups of plants are explored, the climatic and external pressures must simultaneously be investigated. Climate influences leaf traits and thus impacts the resource rate of return (Wright et al 2004). Wright et al. (2004) found that co-existence between species to have more of an effect on trait variation than climate. However, the impact of climate was not null and traits varied with mean annual rainfall (MAR) and mean annual temperature (MAT). Therefore, site conditions cannot be ignored, and presumably, a more stressed environment will lead to lower energy investments into leaf infrastructure. For instance, Leaf longevity (LL) and Leaf Mass Area (LMA) were found to be lower in sites with less rainfall

(Wright et al 2004). This suggests that the return of a unit of investment is lower in more resource poor environments.

Reich (2014) suggested that, despite the fact that leaf size and shape are highly studied, their involvement in the LES remains unclear. One of the problems in the LES is that most of the whole leaf traits it uses are physiological or morphological; in contrast, anatomical traits (epidermis area and thicknesses; palisade and spongy mesophyll cell-occupied area, air space area and layer thicknesses; see Table 2.3) are still not included in this classification system (Reich 2014). This knowledge gap extends to liana and tree studies, where the relationships between anatomical and whole leaf traits are also not well understood.

In this context, the goal of this paper is to examine the interactions between whole leaf and anatomical traits of lianas and trees in two different climatic conditions. This analysis was conducted from leaves collected in a tropical wet forest (Mean Annual Precipitation (MAP) > 3000 mm) and a tropical dry forest (MAP < 1800 mm) in the context of their relative position in the LES. This was done by exploring leaf traits as a function of resource abundance and scarcity. As such, whole leaf traits are explored using General Linear Models (GLMs); anatomical traits are examined through Linear Mixed Models (LMMs) and a linear discriminant analysis (LDA); and the interactions between whole leaf and anatomical traits are examined with the use of Analyses of Covariance (ANCOVA's) and standardize major axis regressions. From these analyses I hypothesize trends in the whole leaf and anatomical traits of lianas will exhibit an overall metabolic strategy of fast growth and low investment and trees trait will be resource conservative (Wright et al 2004; Schnitzer et al. 2005); and a lack of water stressed in wet sites should result in more investments in their leaves than dry sites (Reich 2014).

2.3. Methods

2.3.1. Study area and sample preparation

This investigation took place at two canopy crane systems in Panama, one in the Parque Natural Metropolitano (PNM) and the other in at the San Lorenzo National Park (SLNP) (See Castro-Esau et al. (2004) or Slot et al. (2013) for a complete description). The PNM is a tropical dry forest with an average rainfall of 1740 mm a year. The dry season extends from December until early May, and the wet season from May until early December. The vegetation at this site is roughly 80 to 100 years old. The canopy tower at this site is 42m high with a boom radius of 51m. The SLNP is a tropical wet forest with an average annual rainfall of 3300 mm. The dry season extends from January to March, and the wet season April to December. The vegetation at the SLNP site was roughly 200-300 years of old growth forest. The canopy tower for this site is 56m high with a boom radius of 54m.

Sun leaves were collected from the top of the canopy with the use of the cranes. Samples were collected from 39 species in total. Twenty-one lianas species and nineteen tree species were collected from the PNM crane. Sixteen liana species and twenty-four tree species were collected from the SLNP crane. Each leaf sample immediately upon clipping (early morning) was placed in a plastic bag with a moist paper towel, and transferred within 1-hour to a dry ice cooler for transportation to a laboratory. Three small sections (5 mm in width and 20 mm in length) were cut from each leaf while avoiding the presence of prominent vascular areas. The cut-out sections were treated for two weeks with formalin aceto-alcohol in a vacuum oven. After, the two weeks the samples were run through an ethanol processing center and transferred to a hot paraffin bath for embedding into paraffin blocks. A detail description of the process can be found in Sanchez-Azofeifa et al. (2009).

2.3.2 Leaf histology

Seven μm sections were prepared from each leaf sample with a Leica microtome from a paraffin block and mounted onto microscope slides. The slides were placed in an oven at 37°C overnight for roughly 10-12 hours. The following morning, slides were de-waxed with a series of diluted ethanol concentrations, and then soaked in toluene for 2 minutes (Bandcroft and Cook 1984). The slides were then submersed into a toluene blue stain for 22 seconds. Cover slips were placed over stained samples using DPX mounting medium. Slides were again placed in 37°C oven for 10-12 hours to dry and set the DPX (Bandcroft and Cook 1984). Finally, cross section photos were taken using a Zeiss M1 Axio Imager microscope. For each species three leaves were mounted, stained and photographed giving 63 and 57 lianas and tree pictures, respectively or 48 and 72 for dry and wet site species photos respectively.

2.3.3 Leaf metrics

All Whole-leaf traits were collected by Dr. Joseph Wright and Smithsonian Tropical Research Center colleagues and all anatomical metrics were calculated from black and white photos obtained from the histology approach (ImageJ 1.46, Ferreira and Rasband 2012). This process first involved the estimation of cell-occupied space and airspaces where the contrast of all color plates was enhanced and then transformed to black and white. Second, the area and percentage of the blackened material was calculated with the tool "analyzed particles" (ImageJ, Ferreira and Rasband 2012). Cell-occupied space was obtained the original black and white photo while the airspace is an inverted version of this image. The area of each individual layer was then manually selected with the Region of Interest tool, and the "analyze particles" tool was used to calculate the area of the blackened material of the selected layer (upper and lower epidermis, palisade or spongy mesophyll). Total and layer thicknesses were calculated by taking the average of 5 measurements per photo.

Cell counts were estimated using the edge effect rules (MBF Bioscience 2015). A 3,000 μm^2 central area was established with a 1,500 μm^2 buffer zone. Next, each cell was counted in the selected area. For cells to be included they needed to be entirely encompassed in the central area and the buffer zone. Once the cell count was established, the total numbers of cells per mesophyll layer (palisade and spongy mesophyll) were estimated. The former was accomplished by dividing the total area of the mesophyll by the estimates cell counts in the central area and the buffer zone (Equation 1, Table 2.3).

$$PCC \text{ or } SCC = \frac{PCA \text{ or } SCA}{Cell\ count\ in\ 3000\ \mu m2\ area} \quad (1)$$

The individual cell areas were estimated with the cell count results. This was accomplished by dividing the cell counts by the total mesophyll area (Equation 2; Table 2.3):

$$PAC \text{ or } SAC = \frac{PCC \text{ or } SCC}{PCA \text{ or } SCA} \quad (2)$$

2.3.4 Statistical analyses All Statistical analyses were run in R studio 3.3.1. Each analysis used the package MASS (Venables and Ripley 2002);with the exception of the standardize major axis regression the package CRAN was used (Venables and Ripley 2002).

2.3.4.1 General Linear Models (GLMs):

GLMs were performed on the whole-leaf traits. The goal of the GLMs was to test whether whole-leaf traits differed significantly with site and growth form *(McCune and Grace 2002)*. The whole-leaf traits included photosynthesis (A_{max}); dark respiration (R_d); nitrogen, phosphorous and potassium leaf concentrations; lamina toughness; LMA and leaf longevity (Table 2.2). The grouping factors were growth form and site (*Equation 3*). We predict that lianas and dry site

species will exhibit greater values of A_{max}, R_d and leaf nutrient concentrations (N, P and K) and lower values of LMA, LL and laminar toughness than tree and wet site species.

*GLM=Whole-leaf trait ~ growth form * site (3)*

2.3.4.2 Linear Mixed Models (LMMs)

LMMs were performed on all anatomical traits. The goal of the LMMs was to test whether anatomical traits differed significantly with site and growth form. The anatomical traits included: thickness, cell area, individual cell size and cell counts for the entire leaf, the palisade mesophyll, the spongy mesophyll, and the upper and lower epidermises, and airspace in the spongy mesophyll (Table 2.3). The grouping factors were growth form and site, and the random effect was species (*Equation 4*). It is predicted that lianas and dry site species will have lower values for thicknesses, cell areas and cell counts than trees and wet site species. It is also predicted that liana and dry site species will have higher values for individual cell sizes and spongy mesophyll airspaces than tree and wet site species.

*LMM= anatomic trait ~ growth form * site, random= ~1|Species (4)*

2.3.4.3 Analysis of covariance (ANCOVA)

ANCOVA were performed to explore the interactions of whole-leaf and anatomical traits. The goal of the ANCOVAs was to examine whole-leaf traits by growth form and site while controlling for the anatomical traits *(McCune and Grace 2002)*. The response variables were the whole-leaf traits, the covariates were the anatomical traits and the grouping factors were site and growth form. It is predicted that:

1) There will be a significant effect of A_{max}, R_d, P and N on site type and functional grouping when controlling for palisade mesophyll cell-occupied areas and thicknesses; lianas and dry sites will have higher whole-leaf traits in lower palisade mesophyll abundances;

2) There will be a significant effect of R_d and K on site type and functional grouping when controlling for spongy mesophyll cell occupied areas, thickness and airspace areas; lianas and dry sites will have higher whole leaf traits in lower spongy mesophyll cell occupied area and thickness and they will also have higher air space areas with higher rates of K and Rd;

3) There will be a significant effect of Fractal laminar toughness (Lamtuff; Table 2.2) on site type and functional grouping when controlling for mesophyll cell sizes and counts; where lianas and dry sites will have lower laminar toughness and fewer but larger cells.

4) There will be a significant effect of LL and LMA on site type and functional grouping when controlling for spongy and palisade mesophyll abundances; where trees and wet sites have higher rates of LMA and LL with more mesophyll.

2.3.4.4 Standardized major axis regression

Standardized major axis regressions were performed (Figure 2.1). The goal of these regressions is to examine the correlation coefficients (R^2) between the whole-leaf traits and palisade mesophyll abundances at the site level *(McCune and Grace 2002)*. The dependent variables are nitrogen and phosphorous concentrations, the independent variables are thickness and cell area of the palisade mesophyll, and the grouping factor is site type. I predict negative relationships between nitrogen and phosphorous with the palisade mesophyll and that in dry sites the

concentrations of P and N will be greater in lower amounts of palisade mesophyll compared to the wet sites.

2.3.4.5 Linear discriminant analysis (LDA)

The goal of the LDA was to classify growth form and site based on the mesophyll anatomical traits. The independent variables are the mesophyll anatomical traits and the categorical dependent variables are growth form and site. The output is the optimal rotation of data where the most variance is explained. The amount of variance explained is numerically quantified through a proportion of trace for the descending linear discriminant functions. The proportion of trace is the ratio of between class variance to the within class variance. Furthermore, for each anatomical variable there is a co-efficient of linear discriminant which is a score for their influence in the linear discriminant classification. I predict four clusters: lianas in wet sites, lianas in dry sites, trees in wet sites and trees in dry sites.

2.4 Results

Results from the GLMs, LMMs and ANCOVAs all demonstrate that there is no interaction between growth form and site type. Therefore, all results discussed will referred to growth form species and site type species as two separate categories independent of the other, such as: 1) lianas species and dry site species or wet site species and tree species. The lack of interactions is due to the small sample size and this should be subject to improvement in future investigations.

2.4.1 Whole-leaf traits

I calculated the means, standard errors, f and p-values for each whole-leaf trait (Table 2.3). The General Linear Models from the whole-leaf trait analyses show that lianas species and dry sites species have significantly elevated levels of nitrogen (N), phosphorous (P) and potassium (K) ($P<0.05$; Figure 2.1; Table 2.4 & 2.5). Tree species and wet sites species have higher LMA and increased leaf longevity ($P<0.05$; Figure 2.1, Table 2.4 & 2.5). Photosynthetic rates are only marginally significantly different between sites ($P=0.06$), but not significant between growth forms ($P>0.05$). A_{max} is higher in dry sites ($P<0.05$, Table 2.4 & 2.5). Dark respiration rates are significantly higher in lianas, and laminar toughness is significantly higher in trees ($P <0.05$; $P <0.05$ respectively). Sites show no significant role on either respiration or laminar toughness ($P>0.05$).

2.4.2 Anatomical traits

I calculated the means, standard errors, f and p-values for each anatomical trait (Table 2.4 & 2.5). The Linear Mixed Models with significant growth form effects for the anatomical traits were: TCA, PCA, SCA, TTT, TPM, SAC, PAC, SCC, PCC (a full description for these variables can be found on Table 2.3). In all cases trees show significantly greater anatomical size except for PAC and SAC which were significantly higher in all lianas species ($P<0.05$; Table 2.4 & 2.5). Trees have significantly more cell-occupied space, thicker leaves, thicker palisade mesophyll and thicker spongy mesophyll ($P<0.05$). Trees have significantly smaller mesophyll cells than lianas but have higher cell counts ($P<0.05$). Lianas have significantly smaller leaves and smaller layers: less cell-occupied space, thinner leaves, and thinner mesophyll layers where $P<0.05$. Lianas have larger mesophyll cells with a lower cell count than trees ($P<0.05$; Table 2.4 & 2.5).

The LMMs with significant site effects contained the following variables: TCA, PCA, SCA, TTT, TSM, SCC ($P<0.05$, Table 2.4 & 2.5). In all traits the wet site species had higher values: the leaves are larger, they have more cell occupied space (in total, palisade and spongy mesophyll) and the leaves are thicker (in total, palisade and spongy mesophyll). There are higher spongy mesophyll cell counts in the wet sites species; however, the individual mesophyll cell areas and palisade mesophyll cell counts are not significantly different ($P>0.05$). Dry sites species show opposing trends ($P<0.05$): smaller and thinner leaves with less cell-occupied space (in total, palisade and spongy mesophyll). Upper and lower epidermises are not significantly different for growth form or site ($P>0.05$). There were no significant interactions between the growth form and site for any of the anatomical traits (Table 2.5).

2.4.3 Whole-leaf and anatomical interactions

2.4.3 1 Palisade mesophyll

The ANCOVA's results showed that the relationships between the whole-leaf and anatomic traits were all significant between the palisade mesophyll and Amax, Rd, N and P ($P<0.05$, Table 2.6). The assumption of homogeneity of slopes was met, and there were no significant interactions between the two fixed effects, growth form and site, with the anatomical traits ($P>0.05$). Site was significant but not growth form on the whole-leaf traits while controlling for the anatomic traits ($P<0.05$ and $P>0.05$, respectively). The significant effects of site were between P and N with palisade mesophyll cell area and thickness ($P<0.05$, Table 2.6). From the standardized major axis regressions between sites is it clear that a negative correlation exists between nitrogen and phosphorous with palisade mesophyll size ($P<0.05$; Figure 2.1). Dry site species have high rates of nitrogen and phosphorous with smaller palisade mesophyll areas and thicknesses than wet site species (Figure 2.1). R^2 of each site were all quite low thought still all found to be significant

(Figure 2.1; A) N and PCA: (p=6.9e-3) FS: R^2=0.06; PMN: R^2=0.31 B) N and TPM: (p=5.5e-3) FS: R^2=0.013; PMN: R^2=0.08; C) P and PCA: (p=7.1e-3) FS: R^2=0.18; PMN: R^2=0.07 D) P and TPM: (p=9.6e-3) FS: R^2=0.15; PMN: R^2=0.07)

2.4.3.2 Spongy mesophyll

The ANCOVA results showed that the relationships between spongy mesophyll area, thickness and air with Rd and K were all significant (P<0.05, Table 2.7). The assumption of homogeneity of slopes was met and there were no significant interactions between growth form and site with the anatomical traits (P>0.05; Table 2.7). There was a significant interaction of growth form but not site on the dark respiration trait while controlling for the spongy mesophyll traits (P<0.05 and P>0.05 respectively; Table 2.7). There was a significant effect of site and growth form on K concentrations while controlling for the spongy mesophyll traits (P<0.05).

2.4.3.3 Infrastructure

The ANCOVA results demonstrated that the relationships between whole-leaf and anatomical traits associated with infrastructure were all significant (P<0.05, Table 2.8). The assumption of homogeneity of slopes was met and there were no significant interactions between growth form and site with the anatomical traits (anatomical traits; P>0.05). Growth form was significant and site was marginally significant for laminar toughness while controlling for the mesophyll individual cell areas (P<0.05, P=0.06, respectively; Table 2.8). Growth form was significant but not for site on laminar toughness while controlling for mesophyll cell counts (P<0.05, P>0.05, respectively; Table 2.8). The size of the leaf and the size of its layers influence the longevity of the leaf and its density/LMA (Table 2.8; P<0.05). Trees and wet site species have thicker, larger

and denser leaves (higher LMA) that are longer lived (Table 2.8; $P<0.05$). Lianas and dry site species exhibit opposing trends: thin, smaller, less dense/lower LMA leaves that are short lived (Table 2.8; $P<0.05$).

2.4.3.4 Linear Discriminant Analysis

The results of the LDA highlight the anatomical separation between growth forms and sites (Figure 2.2). Four distinct clusters are clearly defined: lianas in dry sites (LPMN), lianas in wet sites (LFS), trees in dry sites (TPNM) and trees in wet sites (TFS; Figure 2.2). The first two linear discriminants explain 90% of the variation in the data (Table 2.9). The anatomical trends show that: 1) trees species and wet species have larger palisade and spongy mesophyll areas and higher thicknesses, 2) trees have more but smaller mesophyll cells, 3) lianas species and the dry site species have smaller mesophyll areas and thicknesses 4) lianas have larger and fewer individual mesophyll cells.

2.5 Discussion

The results support my a-priori hypothesis that trees are resource conservative and lianas are resource acquisitive at the foliar level. By performing a comprehensive analysis of common whole-leaf traits from the LES with novel anatomical traits I have revealed the underlying mechanisms at the local level of known life history and investment strategies. Lianas exhibit a high metabolism and inexpensive infrastructure. Conversely, trees have a slow metabolism to support an expensive infrastructure. Water availability is an important environmental stressor that affects the rate of return in a resource investment and was considered when documenting placement of growth forms along the LES. The data also indicate water availability significantly

influences the anatomical and whole-leaf trait investments into leaves. Drier environments have fewer water resources and therefore smaller leaves with less physiological investment.

2.5.1 Palisade mesophyll functions

Whole leaf traits with specific functional consequences in the palisade mesophyll are: A_{max}, R_d, nitrogen and phosphorous concentrations (Table 2.4 & 2.5). A_{max} is the direct measure of photosynthetic capacity in the palisade mesophyll and both A_{max} and R_d reflect Rubisco's activity in the palisade mesophyll. Furthermore, Nitrogen is an essential component of the internal cellular machinery involved in growth and light capture such as: amino acids, proteins, co-enzymes, and nucleic acids. Phosphorous plays a key role in the chemical reactions and physical storage of light capture and growth: P is used for energy storage, structural integrity and reactions associated with ATP (Taiz and Zieger 2006; Armstrong et al. 1998). Furthermore, there are no significant effects for A_{max} between growth forms and only a marginally significant effect on site ($P>0.05$, $P=0.06$ respectively; Table 2.4 & 2.5).

My findings beg the question whether water stress of a site is the limiting factor for photosynthetic rates. The results show through the addition of anatomical traits water competition between growth forms is low if not null. These results are both supported and contradicted in the literature because other studies have found either no differences in A_{max} between lianas and trees, or a higher A_{max} in lianas (Castellanos et al. 1991, Zotz and Winter 1996; Cai et al 2009). The results also demonstrate that phosphorous and nitrogen concentrations are higher in lianas and dry site species (Table 2.4 & 2.5). Asner and Martin (2012) suggest that elevated concentrations of nutrients in lianas are a result of higher nutrient cycling; therefore, the nitrogen and phosphorous sources are concentrated in their leaves. However, Asner and Martin

(2012) do not make a significant characterization by site or water availability as conducted in this study. Cai et al. (2009) found no differences between nitrogen and phosphorous mass-based concentrations during the wet season but found higher levels of nitrogen and lower levels of phosphorous mass-based concentrations in lianas during the dry season. Cai et al. (2009) attributed their results to lianas' competitive advantage in a seasonal forest. Our results support Asner and Martin's (2012) hypothesis of high nutrient cycling in lianas; however similar to Cai et al. (2009), I highlight the important role environmental stressors can play on light capture and growth traits in the palisade mesophyll, an element not considered by Asner and Martin (2012).

The relationships between the area and thickness of the palisade mesophyll with the N and P concentrations show that the effect of growth form disappears while the effect of site is significant and negatively correlated ($P<0.05$; Table 2.6, Figure 2.1). The N and P concentrations are higher in dry sites species due to higher photosynthetic performances. A_{max} was marginally significant for site and higher in dry site species ($P=0.06$; Table 2.4 & 2.5). Higher levels of N suggest more investments into photosynthetic enzymes and higher P suggest more energetic output as ATP (Schnitzer et al. 2015; Kazda and Mehltreter 2001; Wright et al. 2001). Concentrated N and P into less palisade mesophyll is reflective of the water stress of the environment. Growth will be restricted and nutrients will be concentrated into the palisade because more energy is required to obtain sufficient resources in a resource scarce environment. Furthermore, I suggest that the differences in the whole-leaf traits disappear between lianas and trees in this category when controlling for anatomic traits because water stress puts greater pressure on photosynthetic strategies rather than competition pressure between growth forms in a stressed environment.

2.5.2 Spongy mesophyll functions

The results show that dark respiration (R_d) concentrations are higher in lianas species and there is no significant effect associated with site (Table 2.4 & 2.5). There is evidence that lianas generally have C3 pathways and many tropical trees tend to have C4 pathways (Domingues et al. 2006). I suggest that lianas higher respiration rates are a result of this lack of Kranz anatomy that is specialized for warmer climates. Since lianas have lower investments in their leaves, C4 adaption pathways are limited in their functional group. In high temperature climates like the tropics, Rubisco's affinity to oxygen is greater than its affinity to CO_2 (Taiz and Zeiger 2006). Kranz anatomy in C4 plants creates a physical separation to maintain Rubisco's carboxylase properties. However, the limitation of C3 anatomy in the tropics suggest Rubisco's activity as an oxygenase will be elevated in the lianas, resulting in elevated rates of respiration.

The results also show that potassium concentrations are higher in lianas species and dry sites species; whereas spongy mesophyll cell-occupied areas, thicknesses and airspaces are all significantly greater in tree and wet site species (Table 2.4 & 2.5). It should be noted that over all, trees have greater spongy mesophyll air space due to leaf size; yet when comparing trees and lianas within the same site, lianas have higher levels of spongy mesophyll air space. This is particularly interesting because lianas and dry site species: 1) have higher levels of potassium with less spongy mesophyll, and 2) K is positively associated with spongy mesophyll air space. This particular group of findings highlights lianas' ability to conduct water more efficiently than trees.

High levels of potassium help maintain turgor pressure within the spongy mesophyll cells and inadvertently maintain negative water potentials outside of the cell (Taiz and Zeiger 2006). This

is a useful strategy during times of water stress such as those associated with dry forests. Negative water potentials are also maintained with large spongy mesophyll air spaces. A film of water around the exterior of the spongy mesophyll cells creates minute menisci between cells that cause a negative water potential. Greater spongy mesophyll air space causes more surface area for these menisci to form. This in turn creates more tension in the interstitial space of the interior of the leaf and thus decreases the water potential (Taiz and Zeiger 2006). One of the functions of potassium in the spongy mesophyll is to manage water conductance by pulling water into the cells to maintain turgor pressure (Armstrong et al. 1998). This movement of water into the cells enhances the effect of the miniscule menisci and thus resulting in more negative water potentials (Taiz and Zeiger 2006). These two processes provide a microscopic mechanistic explanation to hypotheses that suggest lianas have better WUE strategies than trees (Schnitzer 2005; Schnitzer 2015; Sanchez-Azofeifa et al 2009). For example, Schnitzer (2005) found evidence that lianas draw more water up their extensive root system than trees during times of water stress and Sanchez-Azofeifa et al. (2009) found that lianas prolonged senescence in the dry season of a tropical dry forest.

Finally, since potassium in the spongy mesophyll facilitates gas exchange processes I suggest that stomatal conductance is highly regulated in lianas (Taiz and Zeiger 2006; Schnitzer 2005). Potassium is transported into the leaf via the vascular tissues and must diffuse through the spongy mesophyll to reach the stomata in the lower epidermis (Taiz and Zeiger 2006). Therefore, high levels potassium in lower amounts of spongy mesophyll in lianas promotes greater control over stomatal conductance. (Cai et al. 2009; Schnitzer et al. 2015). These findings support the evapo-transpiration hypothesis that lianas have more control over their stomata which is crucial for seasonality, elevated temperatures and less precipitation associated with climate change

(DeWalt et al. 2010; Swaine and Grace 2007; Schnitzer 2005). In summary, the wide spread functions of potassium and their association with the spongy mesophyll potentially give lianas the competitive advantage during times of water stress and gas exchange regulation.

2.5.3 Infrastructure functions

The anatomical and whole-leaf traits related to the infrastructure are laminar fractal toughness, individual cell areas and cell counts of mesophyll (palisade and spongy mesophyll; Table 2.8). These traits make up the physical integrity of the plant, and leaf structure is a direct reflection of the economic investments and it also doubles as the first line of defense against herbivory. Trees are thought to invest more into infrastructure and structural defenses (Asner and Martin 2012; Wright et al. 2004). It is also necessary they invest more into structure because they do not have the parasitic advantage like that of lianas (Granados and Korner 2002; Letcher and Chazdon 2009). My findings support the idea that trees are resource conservative because they invest more into the anatomical integrity of theirs leaves with: thicker leaves, higher laminar toughness and in general stronger barrier defenses (Table 2.8). In this context the results demonstrate a structural anatomical mechanism for the differences in the economic investments into whole-leaf traits not documented before. Trees have more mesophyll cells (palisade and spongy mesophyll) but their cells are smaller and lianas have larger but less mesophyll cells (Table 2.8).

The results show that trees have higher laminar toughness in relation to more cell area and more mesophyllic cell counts (Table 2.4, 2.5 & 2.8). The organization of cells in the mesophyll layers support the idea of greater energy investment in structure and barrier defenses (John et al. 2010). An increased cell count in trees means more cell walls and cell area for a greater distribution of

resistance against applied force (John et al. 2010). Therefore, trees have a solid barrier defensive strategy and greater infrastructural investment into their leaves (Reich 2014; John et al. 2010).

Growth form and site have a significant effect on LMA with while controlling for total, palisade and spongy mesophyll cell areas (Table 2.9). Also, growth forms had a significant effect and site had a marginally significant effect on leaf longevity when controlling for TCA, PCA and SCA (Table 2.9). Trees and wet site species both have large leaves that are long lived with high LMAs. Dry site species and liana species have smaller leaves are shorter lived with lower LMAs. The novelty of these findings is that LMA and LL can be directly attributed to the growth strategies of the plants through leaf dimensions. Trees' long lived, dense, thick leaves show their resource investment mechanism is one of conservation and survival. Their long lived leaves suggest carbon gain is slow and nutrient cycling is low. Tree's high LMA suggest it is inherent to this functional group and that a lot of energy is invested into their leaves (Wright et al. 2004). The large area and thicknesses of tree leaves are a direct consequence of these two growth strategies involving long lived and dense leaves. More mesophyll, as seen in trees, is required to fulfill this high resource investment and energy demand. The same inverse conclusion can be made for lianas: short lived, less dense and small leaves are cheap to make and is evidence for resource allocation to productive strategies and high growth rates. This generally occurs when construction cost is low, photosynthesis is high or the rate of photosynthesis decreases over time (Kikuzawa 1995)

The differences between sites can be attributed to the severity of stressors in the environment type (Bongers and Popma 1990; Popma et al. 1992). The wet site has less seasonality, more water availability and thus more nutrients (Castro-Eseau et al. 2004). This enables the wet site species access to more resources to grow thick denser and stronger leaves (Swaine and Grace

2007; Mediavilla et al 1999; Milla-Moreno 2010). Dry sites species have to deal with harsher conditions, high seasonality, long periods without water, and lower level of nutrients in the soil (Swaine and Grace 2007; Popma et al 1992). Thus, there are fewer resources available which put more limits on growth in dry sites compared to wet sites.

2.5.4 Importance of mesophyll

The differences in anatomical traits are highlighted in the LDA (Figure 2.2; Table 2.9). The results demonstrated that the differences in palisade and spongy mesophyll were highly characteristic of both growth form and site (Figure 2.2). I argue that mesophyll dimensions are important for the physiological functions of each tissue type because the first two linear discriminants of the LDA explained 90% of the variance (Table 2.9). Together the mesophyll satisfies the two processes of photosynthesis: The palisade mesophyll is the light capture center of the leaf and the spongy mesophyll regulates gas exchange and water conduction. The anatomical differences reflected the life history mechanisms of each growth form; trees allocate more energy to structure and defense while lianas allocate energy to growth and productivity.

The differences between the life history strategies of lianas and trees highlight the tradeoffs each growth form has taken in order to gain a strategic advantage. The results demonstrate these tradeoffs because lianas show favorability toward metabolism and growth, while trees have stronger infrastructure traits. Productivity is given up for safety and strong defenses are sacrificed for fast growth. Sterck et al. (2011) suggested that trait trades-off along a light and a water gradient result in the co-existence between acquisitive species and conservative species. I attempt to argue in favor of this hypothesis with the use of two opposing growth forms, each that roughly fall into one of the two resource use categories. Trees and lianas use different strategies

to cope with water stress environments and thus potentially occupy different niches. There are conflicting hypotheses on lianas and tree competition: 1) some studies have suggested competition for water is high in dry forest environments (Schnitzer 2005). 2) while others hypothesized niche differentiation is occurring in extreme dry seasonal forests (Duran et al 2015). The data in this investigation potentially provide some evidence in support niche differentiation because our findings demonstrate the traits of each growth form falling at opposing ends of the spectrum.

2.6 Conclusions

Whole-leaf and anatomic trait interactions have shed new light onto the differences between lianas and trees. Palisade mesophyll and nutrient traits were more influenced by site than growth form differences. This was an unexpected result, the extremes in water availability imply that there are more evolutionary pressures from water stress than competition between growth forms in this category. These findings deviated from the original hypothesis because the resource pressure has a greater influence than functional grouping competitive strategies. Spongy mesophyll and high dark respiration rates hint at the differentiation between C4 and C3 plants of lianas and trees. Furthermore, liana species and dry sites species are able to keep their water potential more negative by having greater potassium levels in lower amounts of spongy mesophyll. Infrastructure traits revealed that trees invest more in to a physical mechanism for the first line of defense against herbivores. LMA and leaf age directly to growth strategies of plants through leaf size and density. Trees' mesophyll layers caused their leaves to be denser and longer lived.

I fostered support and introduced cellular mechanisms to the theory that lianas are fast growth species and trees are slow growth. The addition of anatomical traits to the leaf economic spectrum provides unique insights into leaf-level functions that had not yet been examined. This circumstantial experiment enabled me to explore where anatomical traits fit into the LES with two functional groups that are thought to be at opposing ends of the spectrum. Furthermore, I enhanced the understanding of the co-existence of lianas and trees. This is imperative because lianas play an important role in tropical ecosystem structure and have consequences on their host trees. I argue to fully understand ecosystem functions we must also have a firm grasp of processes occurring at all scales: organ, individual and ecosystem.

2.7 References

Armstrong, D. L., Griffin, K. P., Danner, M., Mees, C., Nguyen, D. (1998). *Better crops with plant food*. Potash & phosphate institute, Norcross, GA.

Asner, G. P., & Martin, R. E. (2012). Contrasting leaf chemical traits in tropical lianas and trees: Implications for future forest composition. *Ecology Letters*, *15*(9), 1001–1007.

Bancroft, J. D., Cook, H. C. (1984) Manual of Histology Techniques. New York, NY, Churchill Livingstone

Bongers, F., Popma, (1990). Leaf characteristics of the tropical rain forest flora of Los Tuxtlas, Mexico. Botanical Gazette 151: 354-365.

Cai, Z., Schnitzer, S. A., Bongers, F. (2009). Seasonal difference in leaf-level physiology give lianas competitive advantage over trees ina tropical seasonal forest. Oecologia 161: 25-33

Castellanos, J., Maass, M., Kummerow, J. (1991). Root biomass of a dry deciduous tropical forest in Mexico. Plant and Soil 131: 225-228

Castro-Esau, K. L., Sanchez-Azofeifa, G. A., Caelli, T. (2004) Discrimination of lianas and trees with leaf level hyperspectral data. Remote sensing of the Environment 90: 353-372

Castro-Esau, K. L., Sanchez-Azofeifa, G. A., Rivard, B., Wright, S. J., & Quesada, M. (2006). Variability in leaf optical properties of mesoamerican trees and the potential for species classification. *American Journal of Botany*, *93*(4), 517–530.

Castro, K. L., & Sanchez-Azofeifa, G. A. (2008). Changes in Spectral Properties, Chlorophyll Content and Internal Mesophyll Structure of Senescing *Populus balsamifera and Populus tremuloides* Leaves. *Sensors*, *8*, 51–69.

Chazdon, R. L. (2008). Beyond deforestation: restoring forests and ecosystem services on degraded lands. *Science (New York, N.Y.)*, *320*(5882), 1458–1460.

Choog, A., Lucas, P. W, Ong, J. S. Y., Perreira, B., Tan, H. T. W., Turner, I. M. (1992). Leaf fracture toughness and sclerophylly: their correlations and ecological implications. New phytologist 121: 597-610.

DeWalt, S.J., Schnitzer, S. A.,Chave, J., Bongers, F., Burnham R. J., Cai, Z., Chuyong, G., Clark, D. B., Ewango, C. E. N., Gerwing, J., Gortaire, E., Hart, T., Ibarra-Manrıquez, G., Ickes, K., Kenfack, D., Macıa, M. J., Makana, J. R., Martınez-Ramos, M., Mascaro, J., Moses, S., Muller-Landau, H. C., ParrenM. P., Parthasarathy, N.,Perez-Salicrup, D. R. Putz, F. E., Romero-Saltos, H., & Thomas, D. (2010). Annual rainfall and seasonality predict pan-tropical patterns of liana density and basal area. Biotropica 42: 309-317

Domingues, T. F., Martinelli, L. A., & Ehleringer, J. R. (2007). Ecophysiological traits of plant functional groups in forest and pasture ecosystems from eastern Amazonia, Brazil. *Plant Ecology*, *193*(1), 101–112.

Duran, S., & Sanchez Azofeifa, G. A. (2015). Lianas effects on carbon storage and uptake in mature and secondary tropical forests. *Biodiversity of Lianas, Sustainable Development.* Springer International Publishing Switzerland.

Ferreira, T., & Rasband, W. (2012). ImageJ user guide1.46r.

Fortunel, C., Fine, P. V A., Baraloto, C. (2012). Leaf stem and root tissue strategies across 758 neotropical tree species. Functional Ecology 26: 1153-1161.

Gilbert, B., Wright, S. J., Muller Landau, H. C., Kitajima, K., Hernandez, A. (2006). Life history trade-offs in tropical trees and lianas. Ecological Society of America 87: 1281-1288.

Granados, J. and Korner, C. 2002. In deep shade, elevated CO2 increases the vigor of tropical climbing plants. Global Change Biology 8: 1109-1117.

Hopkins, W. G. Hüner, N. P. A. (2004) *Introduction to plant physiology*. Ontario, John *Wiley & Son publishing*.

Hudson, A., Jeffree, C. (2001). Leaf and Internode. *Encyclopedia of Life Science 1,* 1-6.

John, G. P., Scoffoni, C., Sack, L. (2010). Allometry of cells and tissues within leaves. American Journal of Botany 100: 1936-1948.

Kazda, M., and K. Mehltreter. "Contrasting leaf nutrition, and leaf mass per unit area in lianas, and trees from the subtropical Island Martin Garcia, Argentina." *Diss Bot* 346 (2001): 131-139.

Kikuzawa, K., (1995). The basis for variation in leaf longevity of plants. Vegetatio 121:89-100

Letcher, S., & Chazdon, R. (2009). Lianas and self-supporting plants during tropical forest succession. Forest Ecology and Management 257: 2150-2156.

McCune, B. and J. B. Grace. 2002. *Analysis of Ecological Communities*. MjM Software, Gleneden Beach, Oregon, USA (www.pcord.com) 304 page

Mediavilla, S., Escudero, A., Heilmeier, H. (1999). Internal leaf anatomy and photosynthetic resource-use efficiency: interspecific and intraspecific comparisons. Tree Physiology 21: 251-259.

MBF Bioscience (2015) Autospine. http://www.mbfbioscience.com/autospine

Milla-Moreno, E. (2010). Structural properties related to mesophyll conductance and underlying variation in leaf mass area of Balsam Poplar (Populus balsamifera). MSc Thesis University of British Columbia.

Poorter, H.,Niinemets, U., Pooter, L., Wright, I. J., Villar, R., Causes and consequences of variation in leaf per mass area (LMA): a meta-analysis. New Phytologist 182: 565-588.

Popma, J., & Bongers, F., Werger, M. J. A. (1992). Gap-dependence and leaf characteristics of trees ina tropical lowland rain forest in Mexico. Oikos 63: 207-2014.

Portillo-Quintero, C., Sanchez-Azofeifa, A., Calvo-Alvarado, J., Quesada, M., & do Espirito Santo, M. M. (2015). The role of tropical dry forests for biodiversity, carbon and water conservation in the neotropics: lessons learned and opportunities for its sustainable management. *Regional Environmental Change*, *15*(6), 1039–1049.

Pyke, K., (2012) Mesophyll. In: eLS. John Wiley & Sons, Ltd: Chichester

Reich, P. B. (2014). The world-wide "fast-slow" plant economics spectrum: A traits manifesto. *Journal of Ecology*, *102*(2), 275–301.

Sanchez-Azofeifa, G. A., Castro, K., Wright, S. J., Gamon, J., Kalacska, M., Rivard, B., Feng, J. L. (2009). Differences in leaf traits, leaf internal structure, and spectral reflectance between two communities of lianas and trees: Implications for remote sensing in tropical environments. *Remote Sensing of Environment*, *113*(10), 2076–2088.

Sanchez-Azoffeifa, G.A., Kalacska, M., Quesada, M., Calco-Alvarado, J. C., Nassar, J.M., Rodriguez, J.P. (2005). Need for Integrated Research for a Sustainable Future in Tropical Dry Forests, *19*(2), 285–286.

Schnitzer, S. A. (2005). A mechanistic explanation for global patterns of liana abundance and distribution. *The American Naturalist*, *166*(2), 262–276.

Schnitzer, S., & Bongers, F. (2002). The ecology of lianas and their role in forests. Trends in Ecology & Evolution, 17(5), 223–230.

Schnitzer. S., Bongers, F., Burnham, R. J., Putz, F. (2015). *Ecology of lianas*. John Wiley & Sons, Ltd, Chichester, UK

Slot, M., Wright S. J., Kitajima, K. (2013). Foliar respiration and its temperature sensitivity in trees and lianas: in situ measurements in the upper canopy of a tropical forest. Tree physiology 33: 505-515.

Sterk, F., Markesteijn, L., Chieving, F., & Poorter, L. (2011). Functional traits determine trade-offs and niches in a tropical forest community. Proceedings of the National Academy of Sciences 51: 2062-20632.

Swaine,, M. D., & Grace, J. (2007). Lianas may be favoured by low rainfall evidence from Ghana. Plant Ecology 192: 271-276.

Venables, W. N. & Ripley, B. D. (2002) Modern Applied Statistics with S. Fourth Edition. Springer, New York. ISBN 0-387-95457-0

Wright, I. J., Reich, P. B., Westoby, M., Ackerly, D. D., Baruch, Z., Bongers, F., Gulias, J. (2004). The worldwide leaf economics spectrum, *Nature, 12*, 821–827.

Zotz, Gerhard, and Klaus Winter. "Diel patterns of CO2 exchange in rainforest canopy plants." *Tropical forest plant ecophysiology*. Springer US, 1996. 89-113.

Tables Chapter 2

Table 2.1*. Species of lianas and trees collected from Panama. Locations PNM (Parque Natural Metropolitano) and SL (San Lorenzo).*

Species	**Family**	**Growth form**	**Site (Forest type)**
Bonamia maripoide	Convolvulaceae	Liana	PMN (dry)
Vitis tiliifolia	Vitaceae	Liana	PMN (dry)
Serjania mexicana.	Sapindaceae	Liana	PMN (dry)
Stigmaphyllon hypargyreum	Malpighiaceae	Liana	PMN (dry)
Machaerium riparium	Fabaceae (Papilionoideae)	Liana	PMN (dry)
Passiflora vitifolia	Passifloraceae	Liana	PMN (dry)
Arrabidaea candidans	Bignoniaceae	Liana	PMN (dry)
Aristolochia maxima	Aristolochiaceae	Liana	PMN (dry)
Stizophyllum riparium	Bignoniaceae	Liana	PMN (dry)
Jacquemontia sp.	Convolvulaceae	Liana	PMN (dry)
Gouania lupuloides	Rhamnaceae	Liana	PMN (dry)
Mikania leiostachya	Asteraceae	Liana	PMN (dry)
Phryganocydia corymbosa	Bignoniaceae	Liana	SL (wet)
Tontelea ovalifolia	Hippocrateaceae	Liana	SL (wet)
Maripa panamensis	Convolvulaceae	Liana	SL (wet)
Doliocarpus multiflorus	Dilleniaceae	Liana	SL (wet)
Arrabidaea verrucosa	Bignoniaceae	Liana	SL (wet)
Forsteronia myriantha	Apocynaceae	Liana	SL (wet)
Pleonotoma variabilis	Bignoniaceae	Liana	SL (wet)
Odontadenia puncticulosa	Apocynaceae	Liana	SL (wet)
Dioclea wilsonii	Fabaceae-Papilionoideae	Liana	SL (wet)
Luehea seemannii	Tiliaceae	Tree	PMN (dry)
Cordia alliodora	Boraginaceae	Tree	PMN (dry)
Astronium graveolens	Anacardiaceae	Tree	PMN (dry)
Annona spraguei	Annonaceae	Tree	PMN (dry)
Cordia bicolor	Boraginaceae	Tree	SL (wet)
Brosimum utile	Moraceae	Tree	SL (wet)
Matayba apetala	Sapindaceae	Tree	SL (wet)
Tocoyena pittieri	Rubiaceae	Tree	SL (wet)
Virola surinamensis	Myristicaceae	Tree	SL (wet)
Manilkara bidentata	Sapotaceae	Tree	SL (wet)
Carapa guianensis	Meliaceae	Tree	SL (wet)
Simarouba amara	Simaroubaceae	Tree	SL (wet)
Lonchocarpus longifolium	Fabaceae-Papilionoideae	Tree	SL (wet)

Tachigali versicolor	Fabaceae-Caesalpiniodeae	Tree	SL (wet)
Ficus nymphaeifolia	Moraceae	Tree	SL (wet)
Marila laxiflora	Clusiaceae	Tree	SL (wet)
Aspidosperma cruenta	Apocynaceae	Tree	SL (wet)
Ficus insipida	Moraceae	Tree	SL (wet)
Porouma dianensis	Cecropiaceae	Tree	SL (wet)

Table 2.2. *Whole leaf trait abbreviations, units, description and processes.*

Whole-leaf trait	Abbreviation	Unit	Description and processes
Photosynthetic capacity	Amax	μmoles (m^{-2} s^{-1})	The maximum rate at which plants fix carbon. A measure of carbon assimilation rates and energetic productivity (Reich 2014; Ort and Kramer 2009)
Dark respiration rates	Rd	μmoles (m^{-2} s^{-1})	Rate of respiration in the dark use to measure by-product of Rubisco's dual enzymatic properties (Taiz and Zeiger 2006)
Nitrogen concentration	N_Mass	g cm^{-2}	Nitrogen per unit mass. N concentrations reflect development and growth strategies of the plant. In leaves, N is essential in the activation and structural make-up of photosynthetic enzymes and proteins like Rubisco (Reich 2014).
Phosphorous concentrations	P_Mass	g cm^{-2}	Phosphorous per unit mass. P has many functions such structural composition of membranes and DNA material (Taiz and Zeiger 2006). One of its primary functions in the leaf is its role in the production of energetic molecules such as ATP, NADP or NADPH.
Potassium concentrations	K_PCT	Fraction (%)	Percentage of potassium. Have many functional consequences such as: enzyme activation, maintenance of turgor pressure, suppression of respiration (to prevent energy loss), sugar translocation, cellulose and protein construction (Taiz and Zeiger 2006; Armstrong et al 1998).
Leaf Mass Area	LMA	g cm^{-2}	Leaf dry mass per area. LMA has extensively been used as a key trait in understanding plant growth strategies: Up to 36% of the variation in LMA can be attributed to the specific plant functional group, LMA is a decomposed product of density and it varies with temperature light, CO2 and water (Poorter et al. 2009).
Leaf Longevity	LL	days	Average life span of leaves. Used as an indicator for growth strategies and as such longevity is used to understand the optimal maximization of carbon gain, nutrient cycling strategies and phenology (Kikuzawa 1995).
Fractal Laminar toughness	LAMTUFF	J m^{-2}	Lamtuff is the amount of force it takes to break apart the lamina of a leaf (John et al. 2010). This trait has widely been used to determine resistance to herbivores in the field of ecology (Choog et al. 1992, Fortunel et al. 2012).

Table 2.3. *Anatomical trait abbreviations, units and descriptions.*

Anatomical traits	**Abbreviation**	**Units**	**Description**
Total cell area	TCA	microns^2 (μm^2)	Total cell-occupied area
Upper epidermis cell area	UCA	microns^2 (μm^2)	Upper epidermis cell-occupied area
Lower epidermis cell area	LCA	microns^2 (μm^2)	Lower epidermis cell-occupied area
Palisade cell area	PCA	microns^2 (μm^2)	Palisade mesophyll cell-occupied area
Spongy cell area	SCA	microns^2 (μm^2)	Spongy mesophyll cell-occupied area
Spongy air area	SAA	microns^2 (μm^2)	Spongy mesophyll air-space-occupied area
Total leaf thickness	TTT	microns^2 (μm^2)	Total thickness of entire leaf cross section
Thickness upper epidermis	TUE	microns^2 (μm^2)	Thickness of upper epidermis
Thickness lower epidermis	TLE	microns^2 (μm^2)	Thickness of lower epidermis
thickness palisade mesophyll	TPM	microns^2 (μm^2)	Thickness of palisade mesophyll
Thickness spongy mesophyll	TSM	microns^2 (μm^2)	Thickness of spongy mesophyll
Spongy individal area of each cell	SAC	microns^2 (μm^2)	Calculated average of individual cell area of spongy mesophyll
Palisade individal area of each cell	PAC	microns^2 (μm^2)	Calculated average of individual cell area of palisade mesophyll
Spongy cell count	SCC	microns^2 (μm^2)	Estimated cell count from spongy mesophyll
Palisade cell count	PCC	microns^2 (μm^2)	Estimated cell count from palisade mesophyll

Table 2.4. *Mean and standard deviation of whole-leaf and anatomical traits. Mean and standard error (SE) are given for each group. See Table 1 for trait definitions and units.*

Traits	**Growth form**				**Site**			
	Lianas		**Trees**		**FS (Wet)**		**PMN (Dry)**	
Whole-leaf traits								
	Mean	**SE**	**Mean**	**SE**	**Mean**	**SE**	**Mean**	**SE**
AMAXMASS	162.556	11.527	137.64	14.22	133.701	11.336	176.586	13.232
RESPMASS	0.017	0.002	0.01	0.002	0.011	0.001	0.018	0.003
N_MASS	0.024	0.002	0.019	0.001	0.018	0.001	0.028	0.002
P_MASS	1.40E-03	1.00E-04	1.10E-03	5.00E-04	9.70E-04	1.00E-04	1.20E-03	5.00E-04
K_PCT	1.456	0.128	0.915	0.122	0.896	0.081	1.638	0.153
LMA	69.335	4.65	101.968	6.132	98.767	5.168	65.674	5.647
LIFETIME	209.05	24.167	306.971	29.765	315.659	25.873	163.667	14.455
LAMTUF	472.61	10.6	824.52	21.48	753.75	16.621	453.09	12.685
Anatomical traits								
TCA	60192.39	1696.52	77089.05	2864.46	78310.98	2196.37	53869.64	1387.87
UCA	7713.61	367.82	9659.92	498.75	9530.59	456.77	7345.42	341.17
LCA	5292.41	156.78	5183.19	206.3	5454.03	171.8	4961.63	180.44
PCA	21137.65	986.03	27763.95	1247.12	27407.78	1223.23	19771.91	711.48
SCA	20348.08	1073.34	27071.39	1569.5	28240.88	1343.01	16921.18	725.16
SAA	3733.95	411.41	5534.47	871.74	5991.36	712.16	2624.63	363.71
TTT	169.62	5.06	221.32	9.67	225.19	7.38	150.1	4.15
TUE	22.06	1.08	23.34	1.07	24.22	1.1	20.54	0.95
TLE	14.71	0.53	14.36	0.67	15.36	0.59	13.48	0.54
TPM	59.44	2.46	79.41	3.02	76.96	3.1	57.16	1.72
TSM	71.71	4.07	94.92	6.61	101.4	5.31	56.63	3.14
SAC	210.66	7.36	161.99	6.15	183.6	6.65	195.37	8.74
PAC	297.66	14.92	215.81	11.3	265.49	15.94	254.16	11.19
SCC	103.64	5.86	169.55	8.29	161.37	7.39	96.23	6.1
PCC	86.9	7.09	145.69	8.73	133.52	9.36	86.8	5

Table 2.5. Linear models for whole-leaf and anatomical traits and their fixed effects. The model constructed had the whole-leaf or anatomical trait as the response variable and growth form (Lianas and Trees) and site (wet site: Fort Sherman- FS and dry site: Natural Metropolitan Park -PNM) as the fixed variables. Whole leaf traits were constructed with general linear models while anatomical traits used linear mixed models. The anatomical traits species were accounted for as the random effect in the model. The significance for p-values > 0.05 are indicated as such: 0 (***) 0.001 (**), 0.01(*), 0.05 (.). See Table 2.1 for trait definitions and units.

Traits	**Growth form**			**Site**			**Interaction**
	Df	**f-value**	**p-value**	**df**	**f-value**	**p-value**	**p-value**
Whole-leaf traits							
AMAXMASS	31	1.84	0.18	31	3.8	0.06.	0.13
RESPMASS	26	5.26	0.03*	26	2.36	0.13	0.69
N_MASS	26	4.46	0.044*	26	14.3	8.00E-04***	0.39
P_MASS	26	5.53	0.027*	26	36.5	2.23E-06***	0.9
K_PCT	32	11.93	0.0016**	32	13.86	7.56E-04***	0.46
LMA	26	19.43	1.60E-04***	26	11.426	2.29E-03***	0.97
LIFETIME	34	9.07	4.90E-03***	34	14.78	5.05E-04***	0.83
LAMTUF	31	12.63	1.23E-03***	31	2.63	0.097	0.82
Anatomical traits							
TCA	35	8.65	0.0057**	35	14.38	0.0005***	0.42
UCA	36	2.97	0.09	36	2.01	0.16	0.88
LCA	36	0.0919	0.76	36	2.11	0.155	0.21
PCA	35	4.45	0.039*	35	3.55	0.063.	0.97
SCA	36	3.55	0.0676.	36	9.67	0.0037**	0.45
SAA	36	0.61	0.44	36	3.34	0.0756.	0.32
TTT	36	7.16	0.0111*	36	12.53	0.0011**	0.4
TUE	36	0.1	0.75	36	1.49	0.22	0.45
TLE	36	0.21	0.6496	36	2.72	0.1073	0.82
TPM	36	6.85	0.013*	36	3.15	0.0844	0.72
TSM	36	2.15	0.15	36	9.79	0.0035**	0.61
SAC	36	10.49	0.0026**	36	0.77	0.385	0.42
PAC	36	6.41	0.0159*	36	2.11	0.15	0.15
SCC	36	17.87	0.0002***	36	7.56	0.0093**	0.75
PCC	36	1.47	0.0086**	36	7.74	0.23	0.67

Table 2.6. *ANCOVA between whole-leaf traits associated palisade function. Where the anatomical traits are the predictor variables in the second column, the whole-leaf traits are the response variables in the first column and the fixed variables were life form and site also in the second column. Reported is the degrees of freedom (Df), the sum of squares, mean of squares, f-value (F) and P value (P). Life form is divided into lianas and trees and site are the wet (FS) and dry (PNM) sites. The homogeneity of slopes assumption was met by the non-significant results between life form: predictor and site: predictor interactions. The significance for p-values > 0.05 are indicated as such: 0 (***) 0.001 (**), 0.01(*), 0.05 (.). Description and units of each variable can be found in Table 2.1.*

Palisade functions

Response	Interactions	Df	Sum of squares	Mean squares	F	P
N_MASS						
	PCA	1	2.73E-05	0.000273	7.23	0.013*
	Life_form	1	3.27E-05	3.27E-05	0.87	0.36
	SITE	1	4.18E-04	0.000418	11.05	2.84E-3**
	Life_form:PCA	1	2.00E-05	1.98E-05	0.50	0.49
	SITE:PCA	1	1.93E-05	1.93E-05	0.49	0.49
	Life_form:SITE	1	3.62E-05	3.62E-05	0.96	0.34
	Residuals	24	9.07E-04	3.78E-05		
P_MASS						
	PCA	1	1.69E-06	1.69E-06	16.04	5.21E-4***
	Life_form	1	2.91E-08	2.91E-08	0.28	0.60
	SITE	1	2.98E-06	2.98E-06	28.37	1.82E-5***
	Life_form:SITE	1	1.09E-08	1.09E-08	0.10	0.75
	Life_form:PCA	1	2.97E-08	2.97E-08	0.26	0.61
	SITE:PCA	1	2.00E-10	2.00E-10	0.00	0.97
	Residuals		2.52E-06	1.05E-07		
AMAXMASS						
	PCA	1	22713.00	22713.30	9.43	4.6E-3**
	Life_form	1	1049.00	1048.80	0.44	0.51
	SITE	1	4360.00	4360.40	1.81	0.19
	Life_form:SITE	1	6975.00	6975.20	2.90	0.10.
	Life_form:PCA	1	72.00	72.00	0.03	0.87
	SITE:PCA	1	74.00	73.50	0.03	0.87
	Residuals	29	69824.00	2407.70		
N_MASS						
	TPM	1	1.71E-04	1.71E-04	4.40	0.04*
	Life_form	1	5.27E-05	5.27E-05	1.36	0.26
	SITE	1	4.79E-04	4.79E-04	12.33	1.79E-3**
	Life_form:SITE	1	3.25E-05	3.25E-05	0.84	0.37

	Life_form:TPM	1	1.00E-08	1.00E-08	3.00E-04	0.99
	SITE:TPM	1	1.50E-05	1.50E-05	0.36	0.55
	Residuals	24	9.32E-04	3.88E-05		
P_MASS						
	TPM	1	1.43E-06	1.43E-06	13.53	1.18E-3**
	Life_form	1	3.42E-08	3.42E-08	0.32	0.58
	SITE	1	3.21E-06	3.21E-06	30.27	1.17E-5***
	Life_form:SITE	1	1.44E-08	1.44E-08	0.14	0.72
	Life_form:TPM	1	5.18E-08	5.18E-08	0.46	0.51
	SITE:TPM	1	0.00E+00	0.00E+00	0.00	1.00
	Residuals	24	2.54E-06	1.06E-07		
AMAXMASS						
	TPM	1	20198.00	20198.40	8.01	8.36E-3**
	Life_form	1	603.00	603.30	0.24	0.63
	SITE	1	5160.00	5159.60	2.05	0.16
	Life_form:SITE	1	5837.00	5836.60	2.31	0.14
	Life_form:TPM	1	1303.00	1303.40	0.50	0.49
	SITE:TPM	1	730.00	729.50	0.28	0.60
	Residuals	29	73124.00	2521.50		

Table 2.7. *ANCOVA between whole-leaf traits associated with spongy mesophyll function. Where the anatomical traits are the predictor variables in the second column, the whole-leaf traits are the response variables in the first column and the fixed variables were life form and site also in the second column. Reported is the degrees of freedom (Df), the sum of squares, mean of squares, f-value (F) and the P value (P). Life form is divided into lianas and trees and site are the wet (FS) and dry (PNM) sites. The homogeneity was slopes assumption was met by the non-significant results between life form: predictor and site: predictor interactions. The significance for p-values > 0.05 are indicated as such: 0 (***) 0.001 (**), 0.01(*), 0.05 (.). Description and units of each variable can be found in Table 2.1.*

Spongy Functions						
Response	Interactions	Df	Sum of squares	Mean squares	F	P
RESPMASS						
	SCA	1	4.16E-04	4.16E-04	5.16	0.03*
	Life_form	1	3.15E-04	3.15E-04	3.91	0.05.
	SITE	1	2.99E-05	2.99E-05	0.37	0.55
	Life_form:SCA	1	7.39E-05	7.39E-05	0.89	0.36
	SITE:SCA	1	3.07E-05	3.07E-05	0.37	0.55
	Life_form:SITE	1	5.09E-06	5.09E-06	0.06	0.80
	Residuals	24	1.93E-03	8.05E-05		
RESPMASS						
	TSM	1	3.91E-04	3.91E-04	4.85	0.04*
	Life_form	1	3.36E-04	3.36E-04	4.18	0.05.
	SITE	1	3.22E-05	3.22E-05	0.40	0.53
	Life_form:SITE	1	7.68E-06	7.68E-06	0.10	0.76
	Life_form:TSM	1	2.60E-04	2.60E-04	3.42	0.07.
	SITE:TSM	1	1.44E-06	1.44E-06	0.02	0.89
	Residuals	24	1.93E-03	8.05E-05		
RESPMASS						
	SAA	1	4.40E-04	4.40E-04	5.65	0.03*
	Life_form	1	3.34E-04	3.34E-04	4.29	0.05*
	SITE	1	5.44E-05	5.44E-05	0.70	0.41
	Life_form:SITE	1	2.03E-06	2.03E-06	0.03	0.87
	Life_form:SAA	1	3.34E-04	3.34E-04	5.66	0.03*
	SITE:SAA	1	2.38E-04	2.38E-04	4.03	0.05.
	Residuals	24	1.87E-03	7.78E-05		
K_PCT						
	SCA	1	0.93	0.93	4.14	0.05.
	Life_form	1	2.09	2.09	9.36	4.64E-3**
	SITE	1	2.53	2.53	11.34	2.10E-3**
	Life_form:SITE	1	0.13	0.13	0.59	0.45

	Life_form:SCA	1	0.37	0.37	1.75	0.20
	SITE:SCA	1	0.43	0.43	2.04	0.16
	Residuals	30	6.71	0.22		
K_PCT						
	TSM	1	0.62	0.62	2.80	0.10
	Life_form	1	2.28	2.28	10.24	3.23E-3**
	SITE	1	2.67	2.67	12.00	1.62E-3**
	Life_form:SITE	1	0.13	0.13	0.59	0.45
	Life_form:TSM	1	0.60	0.60	2.88	0.10
	SITE:TSM	1	0.24	0.24	1.14	0.29
	Residuals	30	6.68	0.22		

Table 2.8. *ANCOVA between anatomical and whole-leaf traits associated with leaf infrastructure. Where the anatomical traits are the predictor variables in the second column, the whole-leaf traits are the response variables in the first column and the fixed variables were life form and site also in the second column. Reported here is the degrees of freedom (Df), the sum of squares, mean of squares, f-value (F) and the P value (P). Life form is divided into lianas and trees and site are the wet (FS) and dry (PNM) sites. The homogeneity was slopes assumption was met by the non-significant results between life form: predictor and site: predictor interactions. The significance for p-values > 0.05 are indicated as such: 0 (***) 0.001 (**), 0.01(*), 0.05 (.). Description and units of each variable can be found in Table 2.1.*

Leaf Infrastructure						
Response	Interactions	Df	Sum of squares	Mean squares	F	P
LAMTUF						
	PAC	1	364134	394134	4.41	0.04*
	Growth form	1	802011	802011	9.71	4.02E-3**
	Site	1	323877	323877	3.92	0.06
	Growth form:Site	1	697	697	8.40E-03	0.93
	Residuals	30	2478449	82315		
LAMTUF						
	SAC	1	428642	428642	5.11	0.031211*
	Life_form	1	707888	707888	8.42	6.90E-3**
	SITE	1	298673	298673	3.55	6.92E-2.
	Growth form:Site	1	10368	10368	0.12	0.73
	Residuals	30	2522596	84087		
LAMTUF						
	PCC	1	293962	293962	3.35	0.07.
	Life_form	1	823550	823550	9.39	4.59E-3**
	SITE	1	216313	216313	2.47	0.13
	Growth form:Site	1	3352	3352	0.04	0.85
	Residuals	30	2631990	87733		
LAMTUF						
	SCC	1	1018014	1018014	12.10	1.56E-3**
	Life_form	1	322534	322534	3.83	5.96E-2.
	SITE	1	104998	104998	1.25	0.27
	Growth form:Site	1	319	319	3.80E-03	0.95
	Residuals	30	2523302	84110		
LMA		LMA				
	PCA	1	9057.40	9057.40	25.50	3.67E-

						5***
	Life_form	1	2344.10	2344.10	6.60	0.02*
	SITE	1	2616.20	2616.20	7.36	0.01*
	Growth form:Site	1	22.40	22.40	0.06	0.80
	Growth form:PCA	1	64.90	64.90	0.17	0.69
	SITE:PCA	1	0.10	0.10	0.00	0.99
	Residuals	24	8525.50	355.20		
LMA						
	SCA	1	3215.40	3215.40	7.57	0.01*
	Life_form	1	6452.60	6452.60	15.18	6.84E-4***
	SITE	1	2697.20	2697.20	6.35	0.01*
	Growth form:Site	1	0.20	0.20	0.00	0.98
	Growth form:SCA	1	60.40	60.40	0.13	0.72
	SITE:SCA	1	207.60	207.60	0.46	0.50
	Residuals	24	10200.20	425.00		
LL						
	PCA	1	57303	57303	5.59	0.02*
	Life_form	1	55064	55064	5.37	0.02*
	SITE	1	121336	121336	11.84	1.63E-3**
	Growth form:Site	1	455	455	0.04	0.83
	Growth form:PCA	1	60548	60548	6.79	0.01*
	SITE:PCA	1	39	39	0.00	0.95
	Residuals	32	327967	10249		
LL						
	SCA	1	105668	105668	10.78	2.68E-3**
	Life_form	1	54756	54756	5.58	0.02*
	SITE	1	83563	83563	8.52	0.01
	Growth form:Site	1	8822	8822	0.90	0.35
	Growth form:SCA	1	15579	15579	1.58	0.22
	SITE:SCA	1	3388	3388	0.35	0.56
	Residuals	29	284334			

Table 2.9. Principal Component Analysis numerical results A) Variance explained of LDA. LD1, LD2 and LD3 are the newly calculate orthogonal variables that have been used to classify the original variables known as linear discriminants. Proportion of trace is the fraction of the variance that is explained by the linear discriminant. B) the co-efficient of each linear discriminant.

A) Proportion of trace		
LD1	LD2	LD3
0.5772	0.3307	0.0921

B) Coefficients of linear discriminant			
	LD1	LD2	LD3
PCA	-2.73E-05	-5.99E-05	5.44E-05
SCA	-6.05E-05	1.79E-05	-1.06E-04
PAA	-3.89E-05	-1.62E-05	-3.72E-04
SAA	5.72E-07	-1.84E-04	1.82E-05
PCC	6.73E-04	1.46E-02	-3.28E-03
SCC	1.28E-02	-8.31E-03	5.76E-03
PAC	8.42E-04	1.29E-02	5.55E-03
SAC	-6.34E-03	7.07E-04	-9.69E-03
TPM	3.25E-02	1.48E-02	7.18E-03
TSM	1.80E-02	2.41E-02	-4.77E-04

Figures Chapter 2

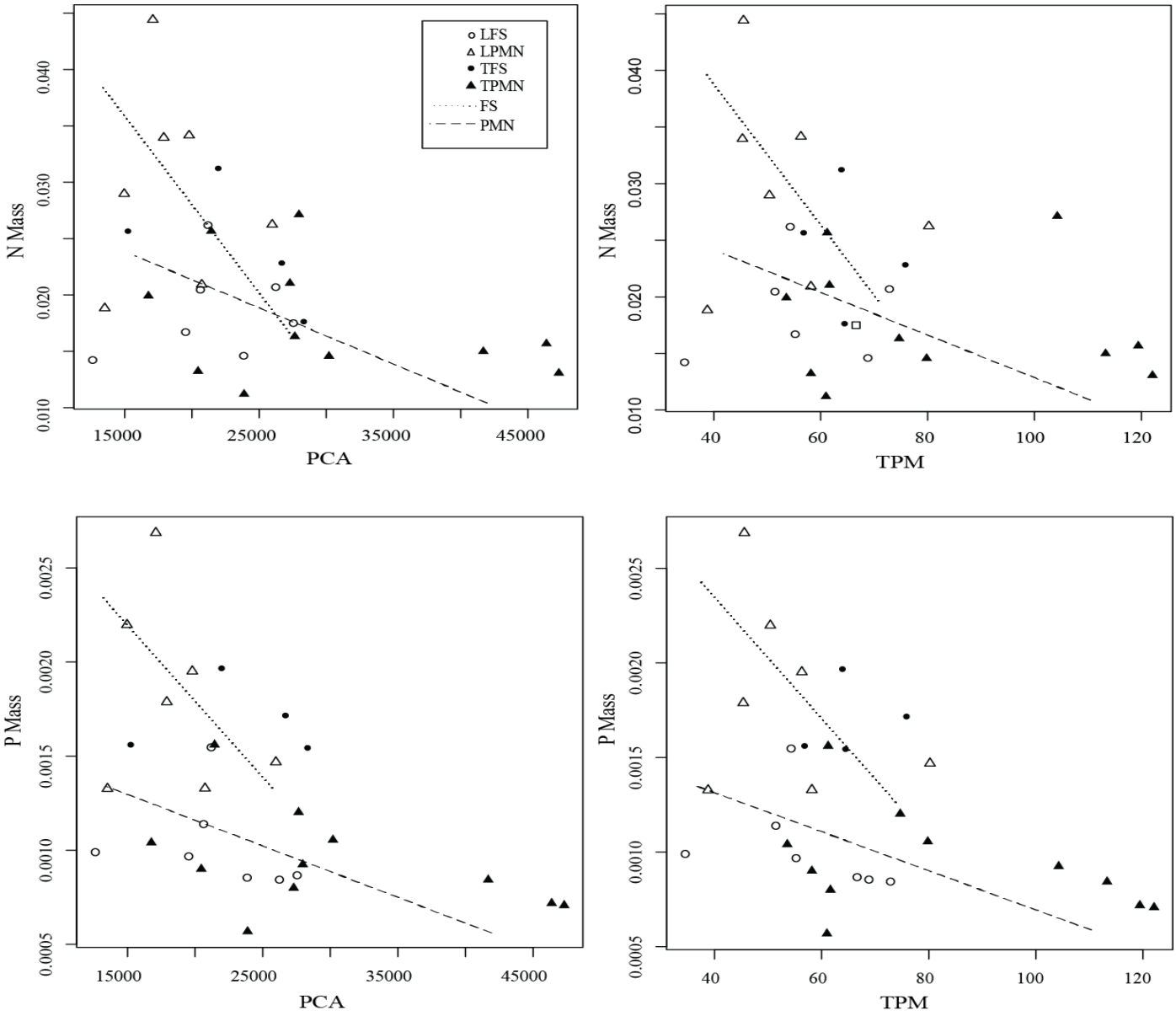

Figure 2.1. *Standardized major axis regressions relationship of palisade anatomical variables and nitrogen and phosphorous variables of wet (FS, solid line, circles) and dry sites (PMN, broken line, triangles). The lines of best fit indicate the slope for each group (wet and dry). A description of each variable can be found in Table 1. A) N and PCA: (p=6.9e-3) FS: R^2=0.06; PMN: R^2=0.31 B) N and TPM: (p=5.5e-3) FS: R^2=0.013; PMN: R^2=0.08; C) P and PCA: (p=7.1e-3) FS: R^2=0.18; PMN: R^2=0.07 D) P and TPM: (p=9.6e-3) FS: R^2=0.15; PMN: R^2=0.07)*

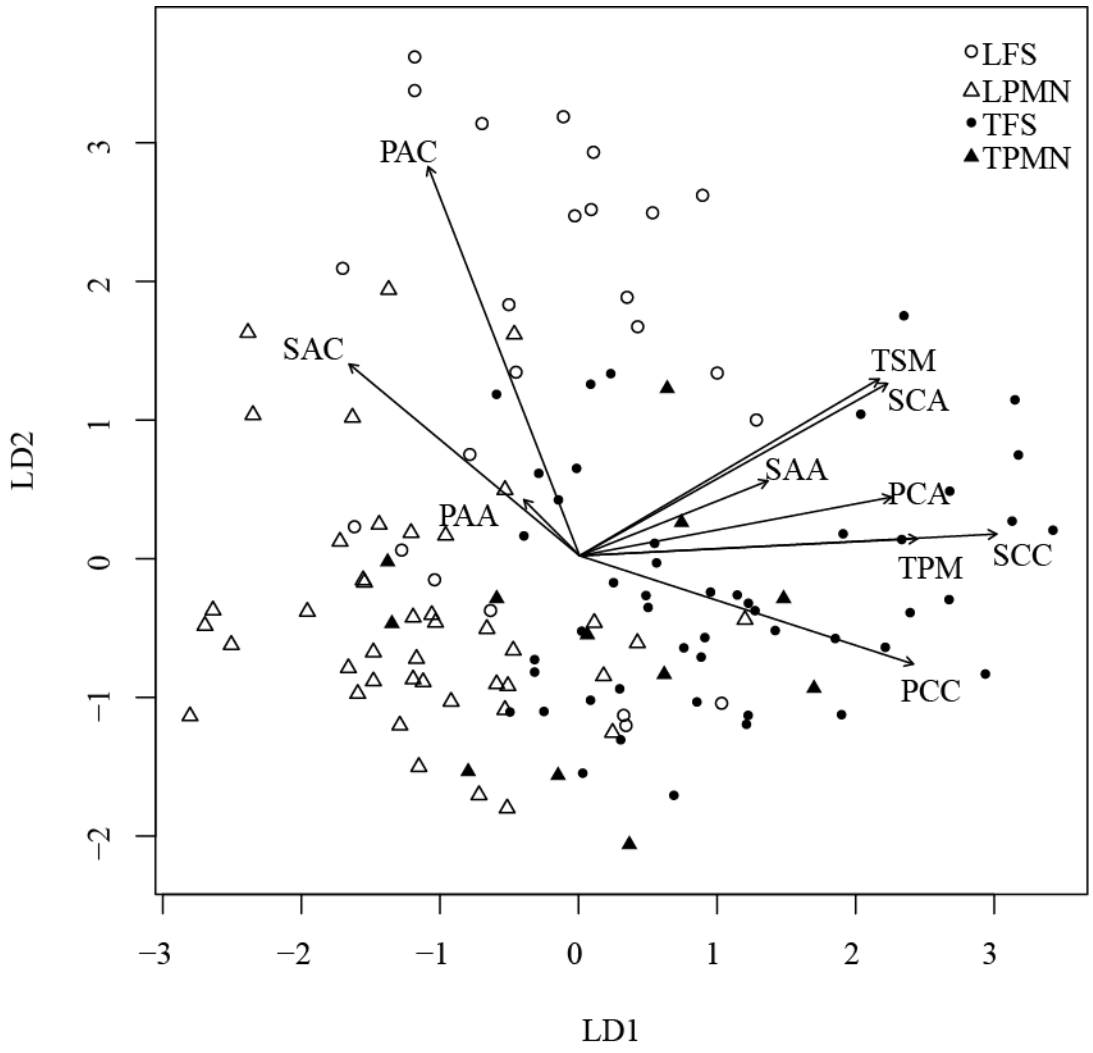

Figure 2.2. *Linear Discriminant Analysis of anatomical parameters of the palisade and spongy mesophyll. Life forms are identified by colors, where green indicates liana (L) species and brown/black represents tree (T) species. Circles are species at the wet forest site (FS) and triangles are species at the dry forest site (PMN). The anatomical parameters used in this analysis are: PCA, SCA, PAA, SAA, PAC, SAC, PCC, SCC, TSM, TPM (description of each variable in Table 1). The arrows indicate correlations between the eigenvector scores and the original variable labelled at the end of the arrow.*

3.0 Longwave infrared spectral feature characterization of tropical dry forest tree species and use for species discrimination

3.1 Abstract

Remote sensing of the environment has utilized the visible, near and short-wave infrared (IR) regions of the electromagnetic (EM) spectrum to characterize vegetation health vigor and distribution. However, little research has been focused on the use of the long-wave infrared (8.5 μm -12.5 μm) region for studies of vegetation. In a leading investigation by Ribeiro da Luz and Crowley (2007; 2010) nine temperate tree species were identified from their longwave spectral signatures acquired with a bench top spectrometer. This chapter attempts to improve and expand on these findings through the use of a portable Fourier Transform IR spectrometer (FTIR; Agilent ExoScan 4100) for in-situ leaf measurements in a high diversity environment, a tropical dry forest in Costa Rica. The spectral signatures of leaves from twenty-six tree species were collected in the field during the summers of 2013 and 2014. A spectral library for leaf or proxy compounds contributed by Ribeiro da Luz (2013) was then used to identify spectral features observed in leaf spectra. Cellulose, cutin, lignin, oleanolic acid and matrix glycans explained most of the features observed for the species of this study. Species were grouped according to spectral similarities and similarities in the compounds driving their spectra. During this analysis a continuous wavelet transformation (CWT) was applied to all spectra to minimize noise and amplitude variations introduced by non-compositional effects. Three classifier techniques were used for the discrimination of trees species: Principal Component Analysis, Linear Discriminant Analysis and Random Forest boot strapping analysis. The groupings established based on a visual assessment of spectral similarity and based on compounds attributable to the observed features were corroborated by RGB combinations of principal components. Each group species was classified with LDAs. The random forest analysis was conducted over the entire species

spectral samples resulting in an 11% out of bag error rate. Cell wall and cuticular compounds drive the longwave infrared spectral signature of tree leaves and from this knowledge the 26 tropical species of this study were classified with spectra obtained from an *in-situ* spectrometer. Future work could be extended to airborne longwave imaging spectroscopy measurements for landscape scale species distribution and ecosystem monitoring.

3.2 Introduction

Environmental monitoring techniques have widely used the visible (VIS; 0.4-0.7 μm), near and shortwave infrared (NIR: 0.7-1.4 μm; SWIR: 1.4-2.5 μm) regions of the electromagnetic (EM) spectrum for remote sensing of vegetation. Each of these spectral regions provides different information based on the interaction of light with the internal foliar components. For instance, in the VIS, *chlorophyll a* reflects in the green (495nm-570nm) and absorbs in the red and blue (620nm-750nm and 450nm-495nm, respectively), and indices have been created that capture this information to indicate photosynthetic capacity and productivity (Kiang et al 2007). In the NIR, which is also known as the NIR plateau, vegetation is strongly reflective (Kiang et al 2007; Kokaly et al. 2003 & 2009) and the NIR is driven by leaf thickness and internal morphology and a few studies have used these traits to successfully classify species in the same site and season (Zhang et al 2006; Castro-Esau et al. 2006; Castro and Sanchez-Azofeifa 2008; Sanchez-Azofeifa et al. 2009). Additionally, spectral features in the NIR resulting from organic bonds of plant biochemical material are detectable in dried and ground matter and are potentially more promising in species classification (Kokaly et al 2003); these features in living, fresh leaves are masked due to internal scattering from the cell walls and strong absorption features from water (water absorption: 0.98 μm &1.3 μm; Kokaly et al. 1999 & 2003). The SWIR region is exploited for the estimation of leaf water content and leaf dry matter content (Kokaly et al. 1999 & 2003 ;

Cheng et al 2012). In regards to the discrimination of species all three regions have limitations: 1) pigments in the VIS are generally not taxonomically unique; 2) the NIR has limited success in one site, in one season and a saturation with a large number of species (Castro-Esau et al. 2006) and cellular biochemical features in the NIR that are potentially species specific can be masked in living and fresh leaves (Clark and Roberts 2012; Kokaly et al. 2003); and 3) water content varies with individual and is also not inherently discernible between species. These issues have encouraged new investigations into alternative regions of the EM spectrum for taxonomic discrimination.

A relatively under-explored yet promising region of the EM spectrum for species identification is the long-wave infrared (8µm-12.5µm; LWIR). The LWIR has been used extensively in chemotaxonomic characterization of vegetation in the fields of biochemistry and chemistry (Wilson et al 2000; Karukova 2000; Szymanska-Chargot 2015). Infrared (vibrational) and Raman spectroscopy have been used to identify plant constituents, compound abundances and starch-deficient mutants (McCann et al 1992; Chen et al. 1998; Wilson et al 2000; Sene et al 1994). However, for the purpose of remote sensing, vegetation was thought to be featureless in the LWIR until the pioneering work of Salisbury (1986) who reported different spectral responses for four tree species albeit low overall reflectance and spectral contrast. Salibury (1986) hypothesized that the observed spectral variability could be due to internal hydrocarbons and the waxy cuticle.

Ribeiro da Luz and Crowley (2006; 2007; 2010) made important strides in LWIR vegetation research providing strengthening evidence towards Salisbury's (1986) hypotheses. They identified the source of the spectral features to be from internal leaf constituents and showed that living leaves have LWIR spectral characteristics that could potentially discriminate tree species

(Ribeiro da Luz and Crowley 2007). Ribeiro da Luz and Crowley (2006 & 2007) found that biochemical and structural constituents within the leaf produce spectral features as a result of the molecular vibrations of functional groups of cellulose, xylan, lignins, cuticular waxes, cutin, silica and terpenes. These spectral features make up a "fingerprint" spectrum that may be unique to a particular tree species (Ribeiro da Luz and Crowley 2006 & 2007). Ribeiro da Luz and Crowley (2007) also found intra-specific variation between development stages of the leaf and its location within the crown (sun versus shade leaves). An experiment by Ullah et al. (2012) paralleled Ribeiro da Luz and Crowley's (2007) findings but did not include compound characterization. Ullah et al. (2012 & 2014) were able to discriminate 13 temperate tree species by using band selection methods applied to mid-infrared (3-6 μm; MIR) and LWIR spectra. These investigations showed the potential of LWIR spectroscopy as a new method to remotely detect vegetative species. However, a limitation of these studies is that they both were conducted in temperate forests - homogeneous and low diversity ecosystems. High diversity biomes could provide a better picture of the spectral diversity and variability in the LWIR signatures among a greater number of vegetation species.

In this study, LWIR remote sensing is applied to tropical dry forests (TDF). TDF is defined as an ecosystem that is dominated by deciduous trees (i.e.: at least 50%) and experiences a mean annual temperature of >25°C, a total annual precipitation between 700 mm and 2000 mm, and 3 or more dry months annually (Sanchez-Azofeifa et al. 2005). The abundance of endemic plant species and their location in the tropical latitudes supports the high diversity index found in these ecosystems (Portillo-Quintero et al. 2014; Sanchez-Azofeifa et al. 2005). A TDF will therefore provide a well-rounded data set to capture inter-specific and intra-specific variability with many more species than that of a temperate forest. TDFs also provide optimal canopy structure for

LWIR remote sensing that is closed planophile canopies with wide and flat leaves that should lead to stronger spectral contrast, (Ribeiro da Luz and Crowley 2010) of relevance to ensuing investigations based on airborne longwave infrared imaging as a continuity to this study. Using LWIR spectra of leaves from TDF tree species this investigation has two specific aims: i) to characterize spectral features based on internal constituents of the epidermis and leaf cuticle and, ii) examine the feasibility to classify tree species or groups of species.

3.3 Methods

3.3.1 Sample site and leaf collection

This investigation took place at Santa Rosa National Park in Costa Rica (10º 53' N, 85º 38' W) over two consecutive wet seasons in 2013 and 2014. This site is a tropical dry forest with a mean annual precipitation of 1390 m and a mean annual temperature of 26.6 °C. The dry season extends from December to April and the wet season from May to November. Data collection was conducted at two sites of secondary growth forest where the vegetation is roughly 50 to 60 years old (1 hectare squared and 20 m by 50 m, respectively). Trees greater than 5 cm of diameter at breast height (DHB) were previously identified at the species level (Batcheler 1985).

3.3.2 Leaf spectral measurements

Leaf samples were collected from each of 3 tree individuals per species for 26 species (Table 3.1). One spectral measurement per leaf was collected from a total of 10 leaves per individual in 2013 (4 sun leaves, 3 mid-canopy and 3 shade leaves) and 3 leaves per individual in 2014 (1 sun, 1 mid-canopy and 1 shade). A diffuse reflectance spectrum of each leaf sampled was acquired with the use of an Agilent 4100 ExoScan FTIR (Fourier transform infrared) spectrometer. This spectrometer has a spectral range of 2.5 to 16 μm (4000-650 cm^{-1}) and a resolution of 4 cm^{-1}. It

is a portable spectrometer with a weight of 3.73 kg, designed for field measurements with minimal to no sample preparation. The FTIR has interchangeable probes that alter the fashion in which the infrared light exits. For this study, an external diffuse reflectance probe with a diffuse infra-gold reference cap for background collection was used. This probe has a field of view (FOV) of roughly 1.5 cm and a maximum depth of light penetration between 20-50 μm, depending on the medium.

Once leaves were clipped from their respective tree, they were placed on a black 2% reflectance panel within minutes of clipping and spectral measurements were taken by contacting the probe to the adaxial side of the leaf. Each diffuse spectral measurement lasted approximately 1 minute and was the result of an average of 64 scans. A further increase in the number of scans did not improve signal to noise because the instrument was sensitive to human movement altering the adequate contact of the sensor with the leaf therefore 64 scans was deemed optimal. Some sample spectra were not retained because of poor quality (e.g. noise due to collection error) or insufficient meta data on the collection location. All spectra retained were imported into a single spectral library, hereby referred to as the species library.

3.3.3 Leaf compounds spectra

A spectral library of pure compounds and proxies for organic compounds was obtained through an online published spectral library from Dr. Ribeiro da Luz at the United States Geological Survey laboratory and the University of Sao Paulo (Ribeiro da Luz 2013). From this collection, a smaller spectral library of compounds relevant to this study comprising 29 spectra from five compounds, referred herein to as the compound library, was produced consisting of spectra of multiple samples of cellulose, matrix glycan/xylan, oleanolic acid (terpenes), lignin, and cutin (3.

2). These compounds have been shown to dominate the LWIR region of the EM spectrum of vegetation (Ribeiro da Luz and Crowley 2007 & 2010). Spectra for cutin included eight proxy spectra of the fruit skin from tomatoes, *Lycoperscion esculentum*. For cellulose nine spectra were collected from cellulose microcrystalline which is refined wood pulp. There were four spectra from corn leaves *(Zea mays)* which were proxies for xylan (a type of matrix glycan). For lignin only one spectrum was collected from sugar cane bagasse; bagasse is the fibrous matter post-juice extract of sugar cane (*Saccharum officinarum*). It should be noted that sugar cane is a monocot therefore it will contain H-lignin (H: p-coumaryl; Seyed 2013) whereas the trees species in this investigation are eucots which have G and S lignin (G: coniferyl; S: sinapyl; Seyed 2013). Finally, for oleanolic acid two spectra were collected for a 97% solution of O. acid and 5 proxy spectra were collected from *Prunus serotine*.

All compound spectra were hemispherical directional reflectance (DHR) measurements taken by Ribeiro da Luz and Crowley (2007). Spectra were collected using a Nexus 670 spectrometer with a 12.7 cm diameter integrating sphere coated internally with Infragold. The spectral range of the Nexus Spectrometer was 2.5-14 μm with a spectral resolution of $4cm^{-1}$ (a full description of the instrument can be found in Ribeiro da Luz and Crowley 2007).

3.3.4 Wavelet transformations

This study made use of a spectral pre-processing methodology, namely continuous wavelet transformations (CWT) used in prior publications by our research group (Rivard et al., 2008, 2010;Rogge 2010; Cheng et al., 2010, 2011; Lyder et al., 2010; Feng et al. 2013). The premise is that any reflectance spectrum may be represented as a sum of similar wave-like functions (wavelets) (Torrence & Gilbert, 1998) each capturing spectral features of different widths, here

referred to as scales. In the initial step, the mean of the reflectance spectrum is calculated over the entire spectral range and is subtracted from each band to ensure that the wavelets are comparable between scales and also that the wavelets from different spectra are comparable at the same scale. The chosen shape of the wavelet base is the second order derivative of Gaussian or DOG (Muraki, 1995) shown in past studies (Rivard et al., 2008; Lyder et al., 2010) to be effective in isolating spectral features from their continuum and for minimizing non-compositional effects (e.g. illumination). For this study, wavelet power spectra were calculated for 9 scales, the lower scales being sensitive to the small-scale structure of spectra (e.g. random noise) and the higher valued scales being sensitive to the large scale structure (e.g. the spectral continuum).

Unless otherwise indicated, all continuous wavelet transformations (CWT) used in this investigation consist of the summation of scales 3, 4 and 5 (S345). These wavelet scales were expected to be largely free of noise associated with the collection of FTIR spectra while maintaining compositional information within the LWIR.

3.4 Results

3.4.1 Spectral enhancements provided by the wavelet transformation

The wavelet transformation of reflectance spectra facilitated the identification of spectral features by minimizing noise and amplitude variations introduces by non-compositional effects (e.g. illumination variability). This is illustrated in Figure 3.1 that displays the reflectance spectra and wavelet representations for two groups of species showing relatively high (left column) and low (right column) spectral variance. The reflectance spectra display random noise and overall amplitude variability due to non-compositional effects associated with internal leaf scattering

and variability in illumination during data collection (Figure 3.1 a & b). This amplitude variability is clearly captured by the sum of wavelet scales 7 and 8 (S78) that highlight how the larger scales capture the broad form of the spectra or continuum and variability in its amplitude (Figure 3.1c & d). For the investigation of feature, the chosen wavelet representation was a summation of S3, S4 and S5 (S345) (Figure 3.1 e & f). This sum of scales enables a view of features while minimizing the intra-species variance that is evident in the larger scale S78 representation (Figure 3.1). In the left column panels of Figure 3.1 the two species can be discerned in both wavelet representations because each species displays not only unique features and feature strength but also very distinct continuums. In this case the S345 highlights differences in feature characteristics difficult to see in reflectance spectra particularly beyond 9 um. In contrast the right column display two species with very similar continuums and much of the spectral variance is captured by S78. Consequently the S345 representation of the entire spectral population for both species is very compact (e.g low intra-class variability) and subtle feature differences between the two species (e.g. inter-species differences) that are not visible in reflectance spectra can be observed (e.g. near 9.5 um).

3.4.2.0 Features observed in the compound spectral library

Significant features from the spectral library of compound samples were identified (Figure 3.2, Table 3.3) based on the wavelength of maximum reflectance and labeled via comparison to features reported in the literature (Ribeiro da Luz and Crowley 2007; Kacurakova et al 2000 & 2001; Poletto 2013; Ramirez 1992; Sammons et al. 2013; Vyas and Argal 2014).

3.4.2.1 Cutin

Cutin is an important constituent of the cuticle of most leaves (Ramirez et al. 1992). There is a high abundance of cutin in the fruit skin of *Lycopersicon esculentum* (tomato fruit) therefore it was used as a proxy (as high as 80%; Ribeiro da Luz and Crowley 2006 &2007; Ramirez et al. 1992) and features (Ft.) at 8.65 µm (Ft. a), 9.14 µm (Ft. b), 10.01 µm (Ft. c) and 10.75 µm (Ft. d) (Figure 3.2C; Table 3.2) are attributed to cutin. Ribeiro da Luz and Crowley (2007) identified Ft. a and b as asymmetrical and symmetrical stretching modes of ester C-O-C bonds. Ft. c and d observed in this study remain unidentified (Table 3.3 and Figure 3.2). Ft. a and b are consistently observed amongst the spectra of our study.

3.4.2.2 Cellulose

Cellulose is the most abundant compound in vegetation (Poletto et al. 2013) and related features are the most consistently observed features in vegetative spectra of this investigation. All measurements from the compound library were for microcrystalline cellulose (refined wood pulp; Table 3.1). Six features (Table 3.3; Figure 3.2C Ft. a-f) are observed centered at 8.19 µm, 8.62 µm, 9.01 µm, 9.44 µm, 9.67 µm, and 10.75 µm (Figure 2C; Table 3.3). Ribeiro da Luz and Crowley (2007) attributed features at 9.44 µm and 9.67 µm to the C-O stretching of primary and secondary alcohol functional groups. However, Poletto et al. (2013) attributed the 9.67 µm feature to in-plane CH deformation. Poletto et al. (2013) further identified features at 8.62 µm and 9.02 µm to asymmetric COC bridge stretching and anhydroglucose ring asymmetric stretching, respectively (Table 3.3). In leaves, cellulose can cause volume scattering and surface scattering varying with amount, location and thickness of cellulose in the cell walls (Ribeiro da Luz and Crowley 2007; Kacurakova et al. 2000) impacting the strength of spectral features.

3.4.2.3 Xylan

Xylan is a type of matrix glycan and in the compounds library by Ribeiro da Luz (2013), this group is represented by xylan. All xylan spectral measurements were proxy samples collected from *Zea mays* (corn) due to corn's high concentration of xylan in the leaf (Hespell 1998; Table 3.1). Xylan binds the cellulose matrix in the cell wall crystalline matrix and is one of many polysaccharides that fall into the matrix glycan family (Taiz and Zeiger 2006). Xylan is one of the more common matrix glycans present in the foliar cell walls. Key features from the corn samples include: 8.35 μm, 8.62 μm, 9.03 μm and 9.67 μm (Figure 2D Ft. a-d). Ft. a and b are not reported in the Ribeiro da Luz and Crowley (2007) and their source is unknown; potentially, these two features could result from other compounds in the corn leaf. Ft. c at 9.03 μm is thought to result from CO, CC stretching in an arabinoxylan, a cousin matrix glycan to xylan (Kacurakova 1994; Poletto et al. 2013; Table 3.3). The source of Ft. d at 9.62 μm for xylan possibly results from the main α-glucan bond in the molecule (Kacurakova et al. 2000). It should be noted that depending on the backbone and side chain combination of the matrix glycans this feature can display shifts in wavelength and amplitude (Kacurakova et al. 2000).

3.4.2.4 *Lignin*

Lignin was not reported in the Ribeiro da Luz and Crowley (2007) investigation though it was included in their online compound library (Ribeiro da Luz 2013). Lignin's primary role is for structural support in secondary cell walls (Taiz and Zeiger 2006). Features are observed at 8.6 μm, 9.29 μm, 10.06 μm and 10.96 μm (Figure 3.2E Ft. a-d). Sammons et al. (2013) assigned these features to C=O stretching in the ester group of HGS lignin, C-O stretching of secondary

alcohols and aliphatic ethers, and CH=CH bending of the aromatic rings, respectively (Table 3.3).

3.2.4.5 Oleanolic acid (terpenes)

Oleanolic acid (O. acid) is a type of terpene and was reported as one of the main internal constituents associated with leaf cuticles by Ribeiro da Luz and Crowley (2007). Terpenes are found in oils, pigments, hormones and cuticular waxes of leaves of some species (Jetter et al. 2006; Ribeiro da Luz and Crowley 2007). The pure oleanolic acid samples in the spectral library were two solutions of 97% O. acid but spectra are also shown for *Prunus serotina,* which is an appropriate proxy as reported by Ribeiro da Luz and Crowley (2007). The following features are attributed to this compound: 8.67 µm, 9.00 µm, 9.27 µm, 9.7 µm, 10.36 µm, and 10.75 µm (Figure 3.2F; Ft. a-f). A vibrational mechanism in the literature could only be found for the feature at 9.00 µm attributed to the stretching vibration of C-O group of carbonic acid (Figure 3.2f; Table 3.3; Vyas and Argal 2014).

3.4.3 Features observed in the spectra of leaves and ensuing species grouping

The spectra of leaves for the 26 species were examined in the context of the features described above for the five following essential compounds: cutin, cellulose, xylan, oleanolic acid and lignin. Features for these compounds were detectable in all species, though in some instances features could not be uniquely assigned between two compounds. Species were then grouped based on similarities in the position and amplitude of spectral features observed in their leaf spectra (Figure 3.3). Probable compounds labels were then attributed to the diagnostic features of each species group (Figure 3.4, Table 3.4). Groups did not result in an even distribution of species amongst groups with as many as a third of the species falling into group 3. Group 1

spectra are variable but two broad features (8.61 μm and 9.19 μm) at the lower wavelengths are the key characteristics. Group 2 only has two species and displays the two features seen in Group 1 but differences are apparent at longer wavelengths. Groups 3 and 4 spectra display a triplet of features (8.78 μm, 9.1 μm and 9.55 μm) but group 3 has a large feature near 10.00 μm. Groups 5 and 6 spectra share a distinctive broad and strong feature near 9.6 μm but differ in the presence of two weaker features (e.g.10 and 10.5 μm in group 6) at longer wavelengths. Group 8 displays the lowest intra-variability. Spectra for group 7 and 8 encompass one species per group and are distinct from the other groups. Though a cursory look at group 7 (species LM) might suggest similarities to group 5, closer look reveals that the large feature near 9.6 μm encompasses a triplet whereas a single broad feature is observed for group 5 (Figures 3.3 and 3.4).

To facilitate comparison of features observed in the spectra of compounds and leaves by grouping, Figure 3.4 displays the average spectra of relevant compounds with the average leaf spectra in a group (dashed line) along with the average spectra of each species in the group. The position of features is denoted by reflectance maxima and the wavelength range encompassed by a feature is marked by a labelled white box (Figure 3.4 top of each panel).

3.4.3.1 Group 1 spectra: driving compound cutin

The species that make up Group 1 are AA, AH, SG and PG (Table 3.3). Features a and b (Figure 3.4) of Group 1 are consistent with features reported for cutin by Ribeiro da Luz and Crowley (2007). Features c and d, present in the spectra of cutin, were not reported by Ribeiro da Luz and Crowley (2007).

3.4.3.2 Group 2 spectra: driving compound lignin

BC and CS are the two species that make up Group 2. Features (Ft.) a, b, c, d and e (Figure 3.4) are broad, most prominent and span similar regions to features observed for lignin (Table 3.3). Ft. c is more distinct in BC and may be part of the broader lignin feature. The features a and b in BC appear to be shifted to lower wavelengths, however this is the result of averaging of spectra. There are a few leaf spectra seen in figure 3.3 with a stark reflectance peak at the lower wavelength range skewing the average of BC.

3.4.3.3 Group 3 spectra: driving compound cellulose

Group 3 contains more than one third of the species: AG, BQ, CAR, CC, CV, GU, LC, LS, SMO, TO, ZG. This is because the driving compound is cellulose, which, as the main component of cell walls, is the most abundant compound in the leaf (Taiz and Zeiger 2006). The most prominent features observed in all species are cited in the literature (Ribeiro da Luz and Crowley 2007; Kacurakova 2000; Poletto 2013) and form a triplet located between 8.53 μm and 9.75 μm (Figure 3.4 G3 Ft. b-d). Wavelength displacements of all three features are observed across species and can be used for species classification as discussed below. Ft. f is prominent in most species but is absent in the cellulose spectra; the origin of this feature is not known.

3.4.3.4 Group 4 spectra: driving compound cellulose

This group contains only two species, ES and MB, and the dominant spectral features are also attributed to cellulose though the wavelength match is notably poorer. These species were separated from the previous group because the conspicuous triplet, between 8.53 μm and 9.75 μm, is shifted far enough to shorter wavelengths that the features appear to be inverted (Figure 3.4). Ribeiro da Luz and Crowley (2007) also reported this phenomenon of inverted cellulose

features and interpreted it as the result of IR light scattering or attenuation. Furthermore, these two species lack feature f of Group 3.

3.4.3.5 Group 5 spectra: driving compounds xylan and matrix glycans

Two species, CAM and BS, form this group. Their spectra are distinctly characterized by a prominent broad feature spanning 9.17-9.65 μm (Figure 3.2 & 3.4). Xylan exhibits a similar feature with a shift towards longer wavelengths at 9.62 μm and but the feature width (9.35-9.95 μm) occupies a smaller wavelength range than that observed for the species of this group. Xylan is a type of matrix glycan and Kacurakova (2000; 2001) suggests that this dominant broad feature of matrix glycan is variable in its wavelength location depending on the backbone and sugar combination; this may explain the observed shift in the feature between the species and the compound in this investigation. This feature may thus represent a different matrix glycan rather than the specific polysaccharide xylan. The smaller Ft. a and c at 8.17-8.61 μm and 10.3-10.77 μm are also consistent amongst spectra of this group.

3.4.3.6 Group 6 spectra: driving compounds xylan, and cutin

The species in this group are CO, MT (A and B separated due to differences in signature of one individual), and SME. The attribution of compounds to the spectra of this group is more difficult as there are no obvious matches of features to any given compound. Here we suggest a combination of xylan and cutin. Ft. c at 9.17μm-9.65μm is the most prominent caused by xylan or a different type of matrix glycan. For CO this feature consists of a doublet and may have another origin or consist of an alternative matrix glycan, other than xylan. Ft. b at 8.62 μm -8.84 μm is likely resulting from cutin. Ft. d and e at 10.02 μm and 10.55 μm are also likely due to

cutin because their overall shape and wavelength position parallels that seen in the cutin average spectrum. The cause of Ft. a at 8.20 μm-8.49 μm is unknown.

3.4.3.7 Group 7 spectra: driving compounds lignin and cellulose

This group has one species, LM, which has a unique spectral signature with consistently high reflectance beyond 9 μm (Figure 3.4, G7). This particular species, as seen below, can be readily classified but labelling of the observed features is more complex. Ft. a, b and c may represent the triplet of cellulose. The high reflectance beyond 9 μm could be due to high surface scattering at the cuticle or the presence of cellulose-rich trichomes (Ft b-d; Ribeiro da Luz and Crowley 2007). The presence of lignin may further explain the relatively uniform reflectance of Ft. a between 8.42-8.67 μm.

3.4.3.8 Group 8 spectra: driving compound oleanolic acid

This group contains one species, RT, with spectral characteristics distinct from the rest of the species. The spectra of RT are alike that of oleanolic acid (o.acid) with a slight displacement of features towards longer wavelengths for all features.

3.4.4 Group Discrimination

A Principal component analysis was performed on the summation of wavelet scales 3,4 and 5 (S345) to corroborate the user-based division of the 26 species into 8 groups describe above (Figure 3.4). The principal components (PCs) were derived from 184 bands spanning the wavelength range of 8.5-11 μm. RGB (red/green/blue) color composite images (Figure 3.5) were constructed with combinations of three PC's and a total of six composites were created using the top eight of the 184 PCs to highlight the groups. Red, green and blue colors correspond to the

order of the PCs indicated (Ex. PC123 would be PC1 red, PC 2 as blue and PC3 as green). Figure 3.5 displays the entire spectral data in a pixel representative image, where each pixel is a leaf sample spectrum and each row is the collection of spectra for a species (Figure 3.5). Similarities in brightness and color represent similarity in variance between pixels and species. Group 1 stands out in red on PCs 456 (Figure 3.5a). Groups 2 was seen in PC789 as light blue (Figure 3.5b). Groups 3 was seen with PCs 127 as dark blue (Figure 3.5c). Groups 4 and 8 were seen in PCs 236 where group 4 was pink and group 8 was yellow (Figure 3.5d). Group 5 and group 7 are seen with PC134 where Group 5 was pink/green and Group 7 was dark green (Figure 3.5e). Finally, group 6 was seen in PC combination 234 as orange/pink (figure 3.5f).

3.4.5 Species discrimination

3.4.5.1 Linear Discriminant Analysis

Linear discriminant analysis (LDA) was performed on each group except groups 7 and 8 because they only have one species (Table 3.5). The goal of LDA was to discern species within groups. The analysis was performed using the entire spectral range (8.5 -11 μm). The dependant variable was the species in a group and the independent variables were the spectral signatures. First a predictive model was build for each group and an error rate was calculated using a correction matrix for each species and then a total error rate for each group (Table 3.5, error rates results of correction matrices, matrices not shown). For validation, an independent model was created where the training data was the 2013 data set and the testing data was the data collected in 2014. The testing data was classified using the model from the training data. This was done evaluate the performance of the model and an error rate was reported per group and species. Table 3.5 displays the error rate (misclassification rate) of each species within a group and the total per

group before and after the independent validation. All errors before the cross validation were 0.00 and after the error rates ranged from 0.00 to 0.67 (Table 3.5)

Additional calculations and graphical representations were created for groups with 3 or more species (Groups 1, 3 and 6; Table 3.6, Figure 3.6). For these groups proportion of trace values were calculated. The proportion of trace is a ratio of "between class variability" to "within class variability". Each linear discriminant (LD) function will have a value of proportion of trace that accounts for as much of the ratio as possible. The proportion of trace is approximately equivalent to the total variance explained from PCA's. The number of LDs in a model is n-1, where n is the quantity of classes, in this case, n is the number species in a group. For this reason, groups with only 2 species will always have only one linear discriminant function. Therefore, no proportion of trace is reported because value will always be 1. In this investigation only the first two proportion of trace values were reported for LD1 and LD2 because this is where most of the variance is captured and these two LDs were used in the following analysis, scatter plots for the LDAs with groups of 3 or more species. The more of the variance captured in first two LDs the better the model performed. From that logic, group 1 performed the best where the first 2 LDs together equalled 0.94 seconded by group 6 at 0.84 and the least variance captured model of the three was group 3 covering 0.51 in the first two LDs.

Graphical representations of the LDAs were created for groups with only three species to visually demonstrate the clustering patterns of the species within a group and to examine where the uncertainties of the models are (Figure 3.6). The first two LDs were plotted against each other in three scatter plots, one per group, (groups 1, 3 and 6). The best model was for group 1 and from Figure 3.6 (G1) the reason is apparent; even with a larger x and y scale than that used for the G3 and G6 data the species are very tightly clustered (Figure 3.6). Group 6 also displayed

a high proportion of trace and clusters for species are clearly discernible (Figure 3.6). MT was separated into A and B (both one species, *Maclura tinctoria*) because in the LDA there are measurements from one tree individual that are quite separate from the other samples (Figure 3.6, G6). The reason for this is not known and requires further investigation. Group 3 had the lowest proportion of trace for the first 2 LD's at 0.51, and Figure 3.6 illustrates where the misclassification occurred. It is clear that 7 of the 11 species in this group are not the source of the uncertainty because they form relatively tight clusters that are separable (AG, BQ, CV, GU, SMO and TO and ZG). The four species that appear to be the source of misclassification were: CC, CAR, LS and LC as they form a large cluster in the center right of the panel (Figure 3.6 G3). Two of these species (LS and LC) are in the same *Luehea* genus and because of their likeliness even expert taxonomists have difficulty differentiating them.

Species discrimination within groups with 2 species (Groups 2, 4, 5) is represented graphically using histogram plots rather than scatter plots (Figure 3.7). As described above the total linear discriminant function for the LDA model of two species is 1. However, each data point has a linear discriminant function value and these were used to demonstrate the success of the model. Two histograms of the frequency of the LD function values were plotted on the same graph, an overlap of the histograms indicating classification errors and uncertainties in the model. Figure 3.7 shows that there is no overlap for any of the three groups. These results imply the LDA models to be good predictors of species within a given group.

Finally, species were separated into individual trees for each group and the LDAs were performed again with the separated individuals. This was done to demonstrate that the intra-crown variability is sufficiently mixed to argue that each leaf is its own independent sample rather than each tree as a sample with the leaves as pseudo-replicates. Only the LDA from group

6 is shown for simplicity (Figure 3.9). The sum of the proportion of traces for the first two LDs of each group are (with their respective group number in parentheses): 0.58 (G1), 0.75 (G2), 0.40 (G3), 0.89 (G4), 0.86 (G5) and 0.85 (G6).

3.4.5.2 Random Forest Boot-Strapping analysis

A random forest (RF) analysis was conducted on the species library. The goal of this analysis was to discriminate species without use of groupings. The training data set used to establish the predictive model was from the 526 spectra collected in 2013, and the validation data set was from 221 spectra collected in 2014. A correction matrix was built to estimate the accuracy of predicted species based on the training data set (Table 3.7). The error rate ranged from lowest for species BC, CC, ES, RT and SME to highest (e.g 0.37) for CV (Table 3.7). The out of bag error (OOB) rate and overall classification accuracy were determined to estimate the quality of the model with a 500 decision tree RF classifier. The out-of-bag (OOB) error rate was 0.11 with 500 decision trees. When a RF was performed on the raw reflectance as opposed to the wavelet representation (S345), the OOB error rate was 0.64 with 500 decision trees. Random forest proved to be more effective after the wavelet transformation compared to the raw reflectance data with out of bag error rates of 0.11 and 0.64 respectively (results of raw reflectance RF not reported in tables). In the CWT random forest analysis, the error class rates per species were very low and ranged from 0% to 30%. The low error of 0% could potentially be a result of the low sample size however the overall error rate of 0.11 suggests that the CWT is a rigorous pre-processing methodology for classification of such remotely sensed long-wave spectral data.

An index table (Figure 3.8) displaying the mean gini values and their corresponding wavelength was created to determine the relative importance of bands for the species classification. The

wavelengths are ranked based on the unitless gini co-efficient which is a measure of statistical dispersion; the higher the value the more important the band in classification of the RF. Some of the most significant bands shown as their wavelength in the RF were (with their respective gini co-efficient): 8.65 μm-8.75 μm (8.4-6.08), 8.93 μm-8.96 μm (6.05-4.84), 9.75 μm-9.79 μm (4.58-3.84) and 9.14 μm-9.17 μm (3.9-3.7) (Figure 3.8).

3.5 Discussion

Long-wave infrared spectroscopy can potentially be used to detect cuticular and cell wall constituents as a means for species discrimination. This investigation was able to accomplish: 1) the identification of spectral features of TDF tree species, 2) the grouping of species based on common features and the attribution of features to dominant compounds and, 3) the discrimination of species using LDA and RF classifiers.

3.5.1 Influence of cell wall and cuticle macromolecules on TDF species spectral signature

Spectral features are a result of molecular bonds from complex leaf compounds. There are variations exhibited within a feature of a certain compound as a result of the abundance, orientation and location of the compound in the leaf. To quantify these variations, the differences in leaf organization at cellular level must be understood. A crude explanation of the structure and composition of cell walls is that they are a cellulose micro-fibril matrix of glucose chains linked by hydrogen bonds and the crystalline matrix is bound by matrix glycans polysaccharides (Taiz and Zeiger 2006). Cellulose is an unbranched glucose polymer (1→4 β-D-glucan) linked by glycosidic bonds (Taiz and Zeiger 2006). There are many types of matrix glycans, however their basic structure is a repeated polysaccharide back bone with a different polysaccharide side chain from polymer sugar subunits. One particularly common polysaccharide is xylan (Taiz and Zeiger

2006). The cuticle is a hydrophobic outer waxy barrier that protects the leaf. It is more variable in its composition than cell walls however the basic organization is: a layer of cutin embedded in cuticular waxes (Taiz and Zeiger 2006). These complex matrices of sugars, waxes and large organic compounds appear as spectral features in the LWIR (Ribeiro da Luz and Crowley 2007; Kacurakova 2000; Wilson and Kacurakova 2001; Sene et al. 1994). In this investigation these compounds were identified from spectral features within a spectral signature.

The source of the spectral features in the LWIR has been found in a handful of molecules that make up the leaf internal machinery. In this investigation particular compounds were identified from a modified spectral library by Ribeiro da Luz (2013; cellulose, matrix glycans, cutin, O. Acid and lignin). Subtle shifts and variations in the feature positions were used to discriminate groups of species and species. Difference in abundance and structural organization of compounds amongst species is the key to meeting the objective of species classification. Some examples seen in the data set of this investigation that facilitated species identification were: subtle wavelength shifts between spectra of different tree species and variance in the amplitude of features (Figure 3.4). These shifts and amplitude variations are a result of vibrational masking or competition between bonds, functional groups and subunits (Kacurakova 2000; Wilson and Kacurakova 2001; Mouille et al.2003).

The most important molecule in this investigation was, not surprisingly, cellulose. In a third of the species in this investigation cellulose was the main driver in the spectral signatures (Figure 3.4). The reason for its significance is its role in cell walls as the main compound and its abundance of up to 30% of the dry weight material of leaves (Sene et al. 1994). The variance of cellulose spectral signatures has been examined through cell wall mutants, extraction and purification and manufacturing of known crystalline matrices (Kondo and Sawatari 1996; Sene et

al 1994; Abidi et al 2014). In this investigation, successful species classification in groups associated with cellulose was the result of features' shifts to longer wavelengths. Furthermore, the feature at 9.97 μm in group 3 is worth noting because it is present in species of this group, the largest group, but absent in the pure cellulose spectra from the compound library and absent in group 4, therefore its source remains unidentified (Figure 3.4). Since cellulose is the driver of group 3 & 4 and the most abundant compound in this spectral investigation I suggest further molecular analyses are required to understand the extent of the variations in each species. More specifically: what drives the horizontal shift of peaks in cellulose and what is the origin of Ft. f (figure 3.4c) in these species? Similar to our findings for cellulose, shifts to longer wavelengths in common spectral features within a group were the reasons for successful species discrimination. This phenomenon is apparent in the matrix glycan (xylan) polysaccharide family. This is because matrix glycans have a large variety of combinations of backbone and side chain sugar subunits. The most indicative feature of this compound class is the result of a α-glucan sugar bond positioned at 9.61 μm (1041cm^{-1}) and shifts and amplitude differences of this feature are a result of different species of matrix glycans (Kacurakova et al. 2000). For example the following matrix glycans have varying absorption wavelengths: glucuronoxylan and arabinoxylan at 9.55 μm (1047cm^{-1}), xyloglucan at 9.61 μm (1041 cm^{-1}), galactan at 9.72 μm (1078 cm^{-1}),or mannose at 9.39 μm (1064 cm^{-1}), (Kacurakova et al 2000). These bands locations are unique to the sugar subunits and are a result of ring or side group vibrations. Groups 5 and 6 exhibit features of matrix glycan with a similar pattern of the main feature of the α-glucan: large in amplitude, broad and distinct. A hypothesis for the reason for shifts between species in these groups (5 and 6) to be from different matrix glycans types however from the data of this investigation, the specific matrix glycans type cannot be identified.

In many of the spectral signatures in this investigation there are multiple compounds influencing the "fingerprint." This is a major source of intra-species variation of spectral signatures in this investigation however it is advantageous in regards to shedding light on the inter-specific variations among tree species. Such a perspective would not otherwise be possible in a sample size of 9 or 13 species such as that of Ribeiro da Luz and Crowley (2006) and Ullah et al. (2012) investigations. Multiple compounds in single spectra can also start to provide insights on the structural composition of the leaf. For instance: 1) spectra with lignin such as group 2 or lignin and cellulose as seen in group 7 suggest the presence of a hypodermis with a casparian strip or the detection of the sclerenchyme ; or 2) group 1's sole spectral driver of cutin and RT's (Group 8) unique O. acid signature both suggest these are a result of a thick cuticle.

A recommendation for future investigations is that the compound library should include pectin samples. Other studies have argued that pectin is a large player in the LWIR spectral features (Kacurakova et al. 2000; Wilson and Kacurakova 2000). It is possible that some of the features in this investigation may be mis-labeled and are potentially a result of pectin bonds influencing the spectra. A next step in LWIR vegetation research should be a more complete compound library that would include the addition of other complex cell wall/ cuticle molecules such as pectin or a variation in the matrix glycans types.

3.5.2 Species discrimination

The LDAs for each group provides information regarding where the variation in the data resides as a function of species, whether future research should focus on gathering information to characterize intra-species or inter-species variability. For instance, in group 1 the LDA model performed very well with the highest proportion of trace and an error rate of 0.00 (Table 3.6).

This suggests that the complexity of the cuticle tends to be quite species specific. However, there is a fair amount of variation in cuticular thickness during plant growth and valuable insights may be gained from by removing the cuticle at various leaf growth stages to examine the variation of spectral signatures. Group 6's most notable result is its unique intra-species variability that enabled the separation of MT into two groupings. This demonstrates a potential problem for species discrimination; that there could be enough intra-species variability to lead models to separate one species is two classes. This highlights the importance of mapping spectral features and having a strong species library for RS so that these types of variations can be accounted for and understood. Groups with two species classified successfully (Groups 2, 4 and 5), as seen from histograms with no overlap in discriminant functions distributions and error rates of 0 (Table 3.5). Smaller groups of species also are beneficial for RS when creating training data. If the average of a group with two species can be discriminated readily from the rest of the canopy, this will facilitate decision analysis in imagery classification. This also applies to the two species grouped alone (group 7 and 8); their unique spectra will facilitate their RS detection.

3.5.3 Remote sensing applications

Spectral decomposition and wavelet analysis are methods that have been widely utilized in vegetation spectroscopy (Jones and Vaughan 2010). In this investigation the use of wavelets reduced non-compositional spectral variance and enhanced the spectral features of macromolecules in the leaf spectra. The merits of CWT were highlighted when comparing the outcomes of the RF results from raw reflectance versus CWT spectra, with respective error rates of 64% and 11%.

Comprehensive spectral libraries exist in the field of RS mineral spectroscopy and are used extensively for mineral mapping. In comparison vegetation spectral libraries are poorly developed (Jones and Vaughan 2010). This is in part due the observed spectral variability in the VIS and NIR for vegetation thus most libraries to date are developed for specific sites and not transferable across sites or biome type (Jones and Vaughan 2010). However, there is likely value for compound libraries such as that of Ribeiro da Luz (2013). Her work in concert with the results of this investigation demonstrates cross biome applicability and the need for more LWIR spectral libraries of cell wall and cuticular compounds.

A common practice of RS of vegetation is the use of training data for image classification or spectral discrimination (Jones and Vaughan 2010). The effectiveness of such characterization techniques is dependent on the scope and quality of the training data. For example, these data are used for Principal component analysis (PCA), artificial neural networks (ANN), Support vector machine (SVM) regression, genetic algorithms, stepwise linear multiple regression (SLMR), partial least square means (PLSM). By grouping the species this investigation has created the foundation for LWIR training data sets particularly for TDFs. The averages of the groups could be used to develop class types for analysis of airborne imagery.

RF successfully demonstrated that use of LWIR spectra is a suitable avenue for species discrimination with an OOB error rate of 11%. The use of data from one year to predict that of another suggest that discrimination in the LWIR can possibly be applied successfully temporally and potential training data can be used over time. Furthermore, the mean decrease gini index will prove to be helpful in future RS investigations where band selection is necessary in such common practices as spectral angle mapping or in data sets where multispectral data is the only information available. However, there are some disadvantages to this statistical analysis in that it

is not currently readily applicable from a RS perspective as a classifier of spectral imagery. Most decision tree metrics used in imagery classification have 1 to 10 decision criteria thus complexity reduction is key.

3.6 Conclusions

Field reflectance measurements in conjunction with laboratory molecular-level compound spectra shed light on the drivers of long-wave infrared spectral signatures of vegetation species. Cell wall and cuticular compounds can be attributed to LWIR spectral features of tree species in a TDF. From this knowledge tree species were discerned using wavelet transformed reflectance spectra. This investigation focused on interspecific variations though it is known that many sources of intra-specific variations also exist and these need to be further explored both spatially and temporally.

This investigation expanded on the Ribeiro da Luz and Crowley (2006; 2007; 2010) experiments through the addition of increased species diversity, widened the identification of spectral features associated with internal leaf compounds, and demonstrating the success and applicability of species discrimination. Increased diversity enabled the exploration of inter- and intra- specific variations of LWIR spectral signatures.

Spectral feature characterization was more systematic and divulged deeper into the source of each feature associated with cuticular and cell wall compounds. The library published by Ribeiro da Luz (2013) was used to identify the source compounds and mostly the source bond for each feature from within the compound was identified. The use of the Ribeiro da Luz (2013) compound library to the species library of this investigation demonstrates the potential for successful application of standardized LWIR vegetation and compounds libraries. Future

research should aim to increase the sample size of compound spectra, attempt to get pure samples rather than proxies if possible and include other abundant compounds such as pectin or other species of matrix glycans.

Grouping species due to similarities was made possible from the spectral feature characterization results. This was done to facilitate species identification by subsetting the diversity of species. This exercise also provides the foundation for training data sets for RS application of species discrimination from airborne imagery. The averages of the groups could potentially be utilized in imagery classification.

This investigation was the first to classification as many as 26 TDF trees species in the LWIR. Previous studies were limited in their number of temperate species and their relative success in classification (Salisbury 1986; Ribeiro da Luz and Crowley 2007; Ullah et al. 2012). The use of the diversity of the tropics as the ecosystem of choice facilitated an understanding of the variations that exist in species discrimination in the LWIR. For instance, the bulk of the species are driven by cellulose which are readily discernible based on shifts in the cellulose features to longer wavelengths. The classification approaches, LDAs and RF, provide alternative perspectives, both with their own advantages and disadvantages. LDAs were quite labour-intensive and they can be used for imagery/pixel classification. While RFs, not are overly useful in imagery classification they provided support to the use of CWTs, the potential for spectral sub-setting or spectral angel mapping with the gini index and reduced spectral complexity for imagery.

With advances in LWIR sensors and concurrent improvements in their signal to noise, applications of species detection from airborne imagery appear feasible. LWIR sensors such as

the HyTES (Hyperspectral Thermal Emission Sensor) from the Jet Propulsion Lab (JPL) offer the next step for developments in this area of RS research.

3.7. References

Abidi, N., Cabrales, L., & Haigler, C. H. (2014). Changes in the cell wall and cellulose content of developing cotton fibers investigated by FTIR spectroscopy. *Carbohydrate Polymers*, *100*, 9–16.

Batcheler, C. L. (1985). Note on measurement of woody plant diameter distributions. *New Zealand Journal of Ecology*, *8*, 129–132.

Castro-Esau, K. L., & Sanchez-Azofeifa, G. A. (2008). Changes in Spectral Properties, Chlorophyll Content and Internal Mesophyll Structure of Senescing *Populus balsamifera* and *Populus tremuloides* Leaves. *Sensors*, *8*, 51–69.

Castro-Esau, K. L., Sanchez-Azofeifa, G. A., Rivard, B., Wright, S. J., & Quesada, M. (2006). Variability in leaf optical properties of mesoamerican trees and the potential for species classification. *American Journal of Botany*, *93*(4), 517–530.

Chen, L., Carpita, N. C., Reiter, W.-D., Wilson, R. H., Jeffries, C., & McCann, M. C. (1998). A rapid method to screen for cell-wall mutants using discriminant analysis of Fourier transform infrared spectra. *The Plant Journal*, *16*(3), 385–392.

Cheng, T., Rivard, B., & Sanchez-Azofeifa, A. (2011). Spectroscopic determination of leaf water content using continuous wavelet analysis. *Remote Sensing of Environment*, *115*(2), 659–670.

Cheng, T., Rivard, B., Sanchez-Azofeifa, G. A., Feng, J., & Calvo-Polanco, M. (2010). Continuous wavelet analysis for the detection of green attack damage due to mountain pine beetle infestation. *Remote Sensing of Environment*, *114*(4), 899–910.

Clark, M. L., & Roberts, D. A. (2012). Species-level differences in hyperspectral metrics among tropical rainforest trees as determined by a tree-based classifier. *Remote Sensing*, *4*(6), 1820–1855.

Clark, R. N., Despain, D. G., Kokaly, R. F., & Livo, K. E. (2003). Mapping vegetation in Yellowstone National Park using spectral feature analysis of AVIRIS data, *Remote Sensing of the Environment 84*, 437–456.

Feng, X., Zhang, X., Sun, C., Motamedi, M., & Ansari, F. (2014). Stationary Wavelet Transform Method for Distributed Detection of Damage by Fiber-Optic Sensors. *Journal of Engineering Mechanics*, *140*(4), 04013004.

Hespell, R. B. (1998). Extraction and characterization of matrix glycan from the corn fiber produced by corn wet-milling processes. *Journal of Agricultural and Food Chemistry*, *46*(97), 2615–2619.

Jetter, R., Junst, L., & Samuels, L. (2006) Annual plant reviews volume 23: biology of the plant cuticle. Blackwell Publishing, Oxford, UK.

Jones, H. G., Vaughan, R. A. (2010). *Remote sensing of vegetation*. Ch. 7.2 Spectral indices.164-182, Oxford, New York, *Oxford University Press*.

Kacuráková, M., & Wilson, R. H. (2001). Developments in mid-infrared FT-IR spectroscopy of selected carbohydrates. *Carbohydrate Polymers*, *44*(4), 291–303.

Kacuráková, M. (2000). FT-IR study of plant cell wall model compounds: pectic polysaccharides and hemicelluloses. *Carbohydrate Polymers*, *43*(2), 195–203.

Kiang, N. Y., Siefert, J., Govindjee, & Blankenship, R. E. (2007). Spectral Signatures of Photosynthesis. I. Review of Earth Organisms. *Astrobiology*, *7*(1), 222–251.

Kokaly, R. F., Asner, G. P., Ollinger, S. V., Martin, M. E., & Wessman, C. A. (2009). Characterizing canopy biochemistry from imaging spectroscopy and its application to ecosystem studies. *Remote Sensing of Environment*, 113:S78–S91.

Kokaly, R. F., & Clark, R. N. (1999). Spectroscopic determination of leaf biochemistry using band-depth analysis of absorption features and stepwise multiple linear regression. *Remote Sensing of Environment*, *67*(3), 267–287.

Kondo, T., & Sawatari, C. (1996). A fourier transform infra-red spectroscopic analysis of the character of hydrogen bonds in amorphous cellulose. *Polymer*, *37*(3), 393–399.

Lyder, D., Feng, J., Rivard, B., Gallie, A., & Cloutis, E. (2010). Remote bitumen content estimation of Athabasca oil sand from hyperspectral infrared reflectance spectra using Gaussian singlets and derivative of Gaussian wavelets. *Fuel*, *89*(3), 760–767.

McCann, M. C., Hammouri, M., Wilson, R., Belton, P. S., & Roberts, K. (1992). Fourier Transform Infrared Microspectroscopy Is a New Way to Look at Plant Cell Walls. *Plant Physiology*, *100*(4), 1940–1947.

Mouille, G., Robin, S., Lecomte, M., Pagant, S., & Höfte, H. (2003). Classification and identification of Arabidopsis cell wall mutants using Fourier-Transform InfraRed (FT-IR) microspectroscopy. *Plant Journal*, *35*(3), 393–404.

Muraki, S. (1995). Multiscale of Volume 3D Edge Representation Data by a DOG Wavelet. *Image (Rochester, N.Y.)*, *3*(lD), 35–42.

Poletto, M., Pistor, V., & Zattera, A. J. (2013). Structural Characteristics and Thermal Properties of Native Cellulose. *Cellulose – Fundamental Aspects*, 45–68.

Portillo-Quintero, C., Sanchez-Azofeifa, A., Calvo-Alvarado, J., Quesada, M., & do Espirito Santo, M. M. (2015). The role of tropical dry forests for biodiversity, carbon and water conservation in the neotropics: lessons learned and opportunities for its sustainable management. *Regional Environmental Change*, *15*(6), 1039–1049.

Ramirez, F. J., Luque, P., Heredia, A., & Bukovac, M. J. (1992). Fourier transform IR study of enzymatically isolated tomato fruit cuticular membrane. *Biopolymers*, *32*(11), 1425–1429.

Ribeiro da Luz, B. (2006). Attenuated total reflectance spectroscopy of plant leaves: A tool for ecological and botanical studies. *New Phytologist*, *172*(2), 305–318.

Ribeiro da Luz, B., & Crowley, J. K. (2007). Spectral reflectance and emissivity features of broad leaf plants: Prospects for remote sensing in the thermal infrared (8.0-14.0um). *Remote Sensing of Environment*, *109*(4), 393–405.

Ribeiro da Luz, B., & Crowley, J. K. (2010). Identification of plant species by using high spatial and spectral resolution thermal infrared (8.0-13.5 μm) imagery. *Remote Sensing of Environment*, *114*(2), 404–413.

Ribeiro da Luz, B. (2013). Spectral Library. spectrallibrary.blogspot.ca/2013/12/plants

Rivard, B., Feng, J., Gallie, A., & Sanchez-Azofeifa, A. (2008). Continuous wavelets for the improved use of spectral libraries and hyperspectral data. *Remote Sensing of Environment*, *112*(6), 2850–2862.

Rogge, D. M., & Rivard, B. (2010). Iterative spatial filtering for reducing intra-class spectral variability and noise. *2nd Workshop on Hyperspectral Image and Signal Processing: Evolution in Remote Sensing, WHISPERS 2010 - Workshop Program*, (1), 1–4.

Sanchez-Azoffeifa, G.A., Kalacska, M., Quesada, M., Calco-Alvarado, J. C., Nassar, J.M., Rodriguez, J.P. (2005). Need for Integrated Research for a Sustainable Future in Tropical Dry Forests, 19(2), 285–286.

Sanchez-Azofeifa, G. A., Castro, K., Wright, S. J., Gamon, J., Kalacska, M., Rivard, B., Feng, J. L. (2009). Differences in leaf traits, leaf internal structure, and spectral reflectance between two communities of lianas and trees: Implications for remote sensing in tropical environments. *Remote Sensing of Environment*, *113*(10), 2076–2088.

Salisbury, J. W. (1986). Preliminary measurements of leaf spectral reflectance in the 8-14 μm region. *International Journal of Remote Sensing*, *7*(12), 1879–1886.

Sammons, R. J., Labbe, N., Harper, D. P., Elder, T., & Rials, T. G. (2009). Characterization of lignins using thermal and FT-IR spectroscopic analysis. *Abstracts of Papers of the American Chemical Society*, *238*(2), 2752–2767.

Séné, C. F. B., Mccann, M. C., Wilson, R. H., & Crinter, R. (1994). Fourier-Transform Raman and Fourier-Transform lnfrared Spectroscopy '. *Plant Physiology*, *106*, 1623–1631

Seyed Hamidreaza Ghaffar, M. F. (2013). Structural analysis for lignin characteristics in biomass straw. Biomass and Bioenery 57: 264-279.

Szymanska-Chargot, M., Chylinska, M., Kruk, B., & Zdunek, A. (2015). Combining FT-IR spectroscopy and multivariate analysis for qualitative and quantitative analysis of the cell wall composition changes during apples development. *Carbohydrate Polymers*, *115*, 93–103.

Torrence, C., & Compo, G. P. (1998). A Practical Guide to Wavelet Analysis. *Bulletin of the American Meteorological Society*, *79*(1), 61–78.

Ullah, S., Schlerf, M., Skidmore, A. K., & Hecker, C. (2012). Identifying plant species using mid-wave infrared (2.5-6??m) and thermal infrared (8-14µm) emissivity spectra. *Remote Sensing of Environment*, *118*, 95–102.

Ullah, S., Skidmore, A. K., Ramoelo, A., Groen, T. A., Naeem, M., & Ali, A. (2014). Retrieval of leaf water content spanning the visible to thermal infrared spectra. *ISPRS Journal of Photogrammetry and Remote Sensing*, *93*, 56–64.

Ustin, S. L., & Gamon, J. A. (2010). Remote sensing of plant functional types. *New Phytologist*, *186*(4), 795–816.

Vyas, N., & Argal, A. (2014). Isolation and characterization of oleanolic acid from roots of Lantana camara. *Asian Journal of Pharmaceutical and Clinical Research*, *7*(SUPPL. 2), 189–191.

Wilson, R. H., Smith, A. C., Kac, M., Saunders, P. K., Wellner, N., & Waldron, K. W. (2000). The Mechanical Properties and Molecular Dynamics of Plant Cell Wall Polysaccharides Studied by Fourier-Transform Infrared Spectroscopy 1. *Plant Physiology*, *124*(September), 397–405.

Zhang, J., Rivard, B., Sánchez-Azofeifa, A., & Castro-Esau, K. (2006). Intra- and inter-class spectral variability of tropical tree species at La Selva, Costa Rica: Implications for species identification using HYDICE imagery. *Remote Sensing of Environment*, *105*(2), 129–141.

Tables Chapter 3

Table 3.1. *Species and their respective groups*

Species	**Abbreviation**	**Group**
Albizia adinocephala	AA	1
Astronium graveolens	AG	2
Ateleia herbert-smithii	AH	1
Bombacopsis quinata	BQ	2
Bursera simaruba	BS	3
Byrsonima crassifolia	BC	4
Calycophyllum candidissimum	CC	2
Casearia argute	CAR	2
Casearia sylvestris	CS	4
Cedrela odorata	CO	7
Cochlospermum vitifolium	CV	2
Curatella americana	CAM	3
Eugenia solanensis	ES	5
Guazuma ulmifolia	GU	2
Lonchocarpus minimiflorus	LM	6
Luehea candida	LC	2
Luehea speciose	LS	2
Machaerium biovulatum	MB	5
Maclura tinctoria	MT	7
Psidium guajava	PG	1
Rehdera trinervis	RT	8
Semialarium mexicanum	SME	7
Simarouba glauca	SG	1
Spondias mombin	SMO	2
Tabebuia ochracea	TO	2
Zuelania Guidonia	ZG	2

Table 3.2. *List of compounds*

Compound	Samples	Description	Sample Origin
Cutin	Tomato_skin_dry_Alcup1	Experiment of transparency. External side of dry tomato skin. Measured on Al foil.	
	Tomato_skin_dry_on_black	Experiment of transparency. External side of dry tomato skin. Measured on a black plate.	
	Tomato_skin_fresh_Al	Experiment of transparency. External side of fresh (wet) tomato skin. Measured on top of Al foil.	
	Tomato_skin_fresh_on_black	Experiment of transparency. External side of fresh (wet) tomato skin. Measured on a black plate	
	Lycopersicum_esculentum_fruit09a	Tomato fruit from Whole Foods. Proxy for cutin	
	Lycoperscion_esculentum	Tomato fruit from Whole Foods. Proxy for cutin	Lovettsville, VA
	Lycopersicon esculentum fruit 2005	Fruit, Adaxial, Feb 23 2005, Solanaceae, Tomato fruit skin	Lovettsville, VA
	Lycopersicon esculentum fruit 2006	Fruit, Adaxial leaf, Jan 6 2006, Solanaceae, Tomato fruit skin	Microcrystalline Baker TLC reagent.
Cellulose	Cellulose_2006	Thick layer (full cup)	Microcrystalline Baker TLC reagent.
	Cellulose_packed	Cellulose microcrystaline packed by hand	Microcrystalline Baker TLC reagent.
	Cellulose_purged	Cellulose microcrystaline fried with purge	Microcrystalline Baker TLC reagent.
	Cellulose_vaccum	Cellulose microcrystaline dried in vacuum	Microcrystalline Baker TLC reagent.
	Cellulose_and_xylan	Cellulose Mixed with Xylan 1:1	Microcrystalline Baker TLC reagent.
	Cellulose_dried_100C	Cellulose microcrystaline	Microcrystallin

		dried in the oven for 2 days at 100° C	e Baker TLC reagent.
	Cellulose_dried_90C	Cellulose microcrystaline dried in the oven for 2 days at 90° C	Microcrystallin e Baker TLC reagent.
	Cellulose_dried_hot	Cellulose microcrystaline purged for 2.5 days and then dried at 90C for three hours. Measured while still hot	Microcrystallin e Baker TLC reagent.
	Cellulose_dried_cold	Cellulose microcrystaline purged for 2.5 days and then dried at 90C for three hours. Measured when cold	from oat spelts[9014-63-5]
Xylan	Zea mays 214 adaxial	Adaxial leaf, Poaceae, corn	Lovettsville, VA
	Zea mays 215 adaxial	Adaxial leaf, Poaceae, corn	Lovettsville, VA
	Zea mays 216 adaxial	Adaxial leaf, Poaceae, corn	Lovettsville, VA
	Zea_mays_217_adaxial	Adaxial leaf, Poaceae, corn	Lovettsville, VA
Terpenes	Oleanolic_acid_thick	Triterpenoid.	Sigma minimum 97%
	Oleanolic acid thin	Triterpenoid.	Sigma minimum 97%
	Prunus serotina 238 adaxial Aug	Adaxial leaf, Rosaceae, Black cherry, August 11, 2004	Lovettsville, VA
	Prunus serotina 238 adaxial June	Adaxial leaf, Rosaceae, Black cherry, June 7, 2004	Lovettsville, VA
	Prunus serotina 3216	Adaxial leaf, Rosaceae, Black cherry, July 17, 2008	State Arboretum of Virginia
	Prunus serotina 3824	Adaxial leaf, Rosaceae, Black cherry, July 18, 2008	State Arboretum of Virginia
	Prunus serotina	Adaxial leaf, Rosaceae, Chinese Qince, July 18, 2007	Lovettsville, VA
Lignin	Lignin_hydrolotic_Aldrich	Sugar Cane bagasse. Thick layer	Aldrich

Table 3.3. *Compound features and probable origin*

Compound	Ft. Label	band	Probable origin
Cutin	a	8.65	asymmetrical stretching modes of ester C-O-C bonds (Ribeiro da Luz and Crowley 2007)
	b	9.14	symmetrical stretching modes of ester C-O-C bonds (Ribeiro da Luz and Crowley 2007)
	c	10.01	C-O alcohol stretching (weak and broad; Ramirez 1992)
	d	10.75	Unknown
Cellulose	a	8.19	Unknown
	b	8.62	asymmetric COC bridge stretching (Poletto 2013)
	c	9.02	anhydroglucose ring asymmetric stretching (Poletto 2013)
	d	9.44	the C-O stretching of primary alcohol functional groups (Ribeiro da Luz and Crowley 2007)/ CO stretching (Poletto 2013)
	e	9.67	the C-O stretching of secondary alcohol functional groups (Ribeiro da Luz and Crowley 2007)/ inplane CH deformation of cellulose (Poletto 2013)
	f	10.75	unknown (Kacurakova 2000)
Xylan	a	8.35	Unknown potentially alternative compound from corn spectra(Ribeiro da Luz and Crowley 2007)
	b	8.67	Unknown; potentially alternative compound from corn spectra (Ribeiro da Luz and Crowley 2007)
	c	9.03	CO, CC Stretching (arabinoxylans; Kacurakova 1994)
	d	9.67	COH bending (Ribeiro da Luz and Crowley 2007); (most likely: Xyloglucan, present in many matrix glycan very strong band; Kacurakova 2000)
Lignin	a	8.60	C=O stretching in ester group of HGS lignin (Sammons 2016)
	b	9.29	C-O stretching of secondary alcohols and aliphatic ethers (Sammons 2016)
	c	10.06	CH=CH bending (Sammons 2016)
	d	10.96	aromatic ring (Sammons 2016)
Oleanolic acid	a	8.67	Unknown
	b	9.00	Stretching vibrations of C-O group of carbonic acid Vyas and Argal 2014)
	c	9.27	Unknown
	d	9.70	Unknown
	e	10.36	Unknown
	f	10.75	Unknown

Table 3.4. *Key features of each group and their probable compound of origin*

Group	Feature	band(μm)	compound
1	a	8.61	Cutin
	b	9.19	Cutin
	c	9.58	Shoulder
	d	10.03	Cutin
	e	10.75	Cutin
2	a	8.20	Cellulose
	b	8.75	Cellulose
	c	9.10	Cellulose
	d	9.55	Cellulose
	e	9.67	Cellulose
	f	9.97	Unknown
	g	10.5	Cellulose
3	a	8.36-8.60	Xylan
	b	9.12-9.60	Xylan
	c	10.30-10.77	Xylan
4	a	8.58	Lignin
	b	9.25	Lignin
	c	9.75	Shoulder
	d	10.08	Cutin
	e	10.32	Cutin
	f	10.88	Cutin
5	a	8.25	Cellulose A
	b	8.54	Cellulose A
	c	8.84	Cellulose A
	d	9.30	Cellulose A
	e	9.56	Cellulose A
	f	10.20	Cellulose A
	g	10.67	Cellulose A
6	a	8.38-8.71	Lignin
	b	9.17	Cellulose
	c	9.51	Cellulose
	d	9.75	Cellulose
	e	10.20	Cellulose
	f	10.65	Cellulose
7	a	8.20-8.49	Unknown
	b	8.62-8.88	Cutin
	c	9.17-9.65	Xylan
	d	10.02	Lignin
	e	10.55	Lignin
8	a	8.13	Oleanolic acid
	b	8.61	Oleanolic acid

	c	8.90	Oleanolic acid
	d	9.30	Oleanolic acid
	e	9.61	Oleanolic acid
	f	10.24	Oleanolic acid
	g	10.71	Oleanolic acid

Table 3.5. *LDA model error rates and independent validation error rates for each species and total per group*

Group	Species	Error rates from model	Error rate cross validation
1	AA	0	0.27
	AH	0	0.50
	PG	0	0.50
	SG	0	0.50
Total		**0**	**0.46**
2	BC	0	0.33
	CS	0	0.75
Total		**0**	**0.33**
3	AG	0	0.06
	BQ	0	0.26
	CAR	0	0.27
	CC	0	0.13
	CV	0	0.06
	GU	0	0.24
	LC	0	0.53
	LS	0	0.67
	SMO	0	0.11
	TO	0	0.21
	ZG	0	0.29
Total		0	**0.56**
4	ES	0	0.00
	MB	0	0.33
Total		**0**	**0.17**
5	BS	0	0.00
	CAM	0	0.00
Total		**0**	**0.00**
6	CO	0	0.00
	MT-A	0	1.00
	MT-B	0	0.50
	SME	0	0.00
Total		**0**	**0.13**

Table 3.6. *LDA proportion of trace values*

Group	Proportion of trace	
	LD1	LD2
1	0.6761	0.2705
3	0.2804	0.2296
6	0.5335	0.309

Table 3.7. *Random forest species error rates*

Species	Error rate
AA	0.188
AG	0.100
AH	0.105
BC	0.000
BQ	0.056
BS	0.053
CAM	0.095
CAR	0.154
CC	0.000
CO	0.036
CS	0.333
CV	0.313
ES	0.000
GU	0.100
LC	0.154
LM	0.125
LS	0.250
MB	0.130
MT-A	0.100
MT-B	0.211
PG	0.400
RT	0.000
SG	0.053
SME	0.000
SMO	0.214
TO	0.069
ZG	0.154
OOB error total	0.110

Figures Chapter 3

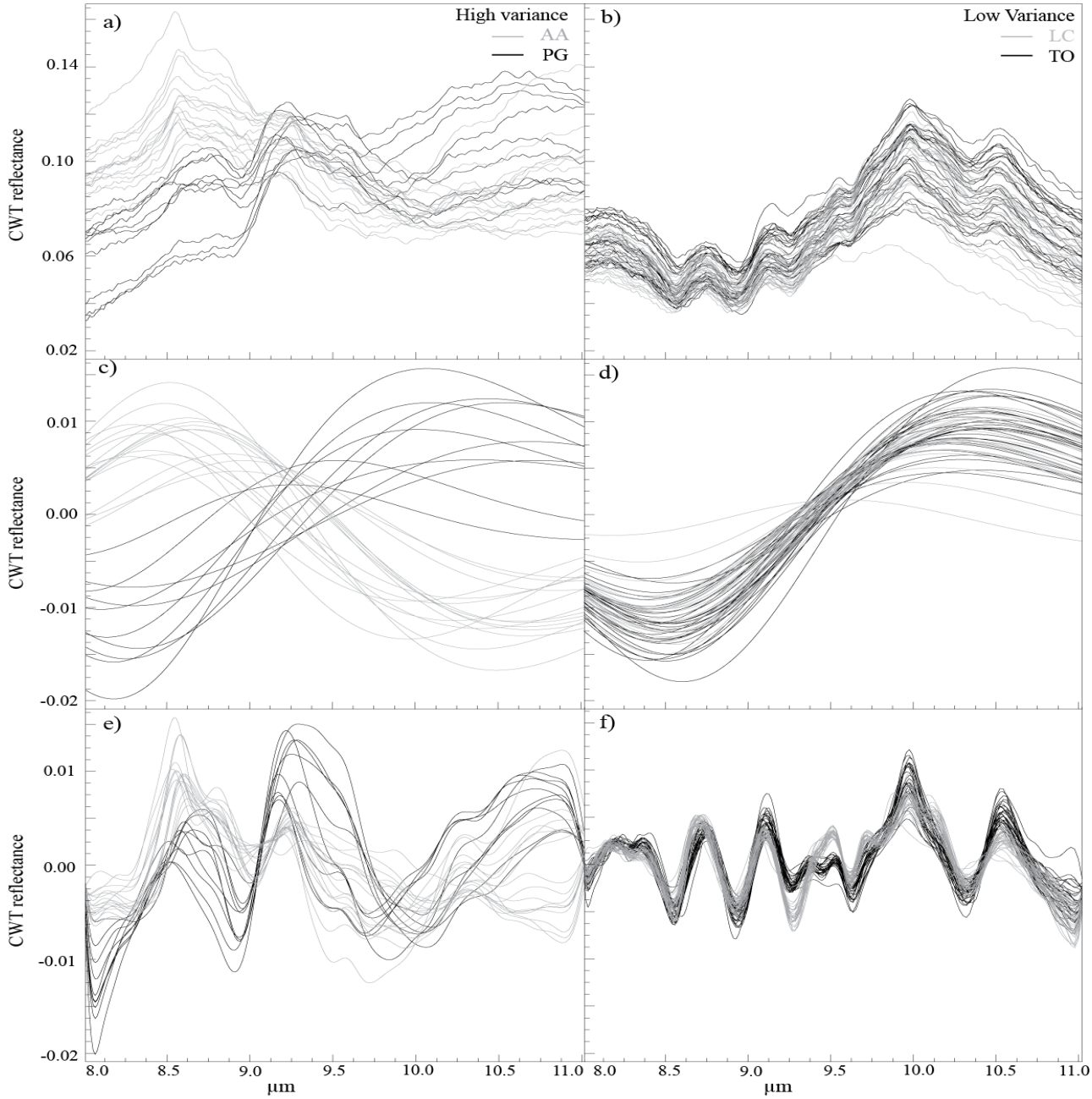

Figure 3.1. *Comparison of reflectance spectra and their wavelet representations for two groups of species. The left column shows spectra for two species displaying relatively high spectral variance (AA: Albizia adinocephala and PG: Psidium guajava). The right column shows spectra for two species displaying relatively low spectral variance (LC: Luehea candida and TO: Tabebuia ochracea). In each case the top panel displays reflectance spectra while the middle and lower panels display wavelet scales S78 and S345 respectively*

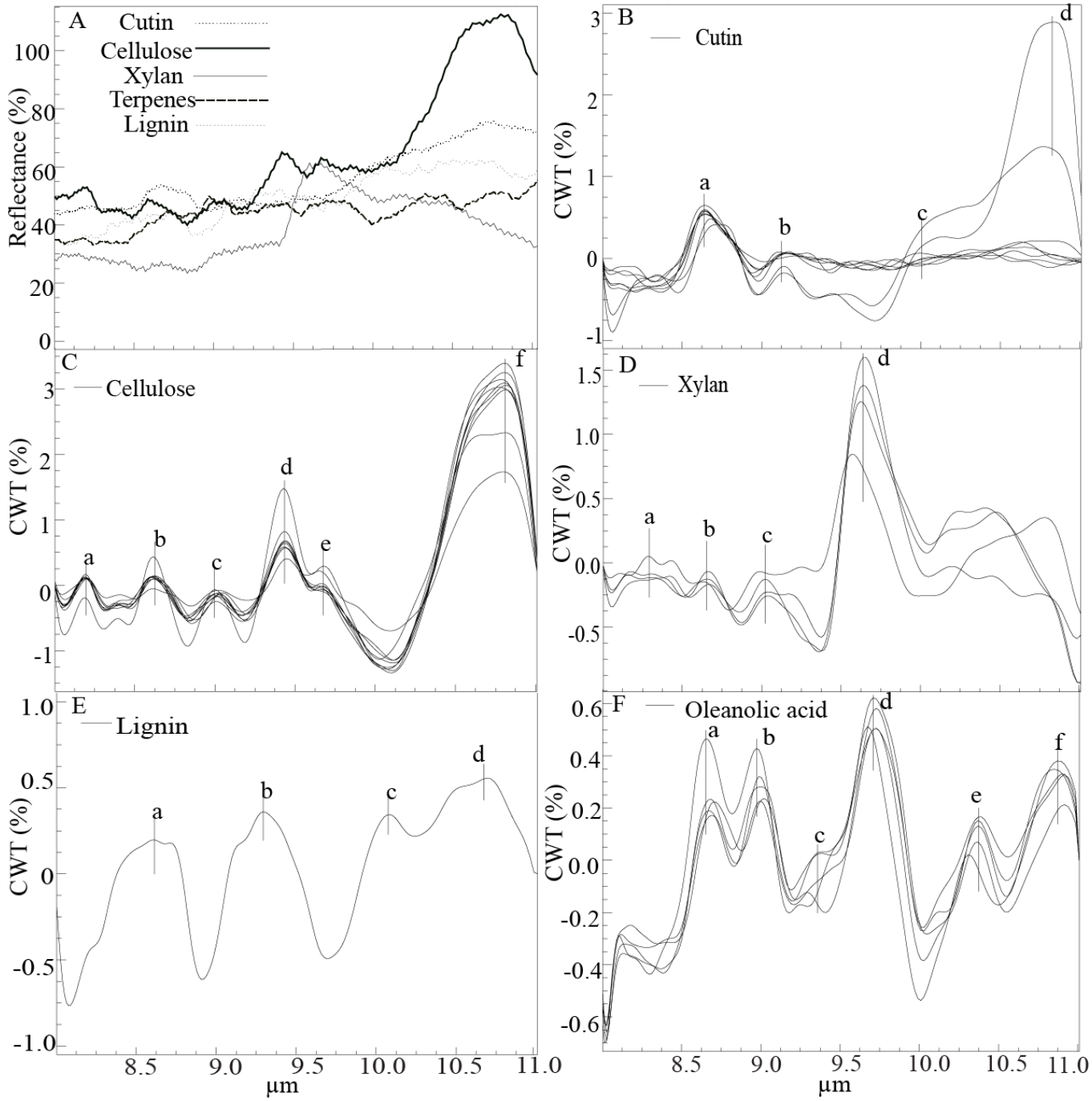

Figure 3.2. *Reflectance and CWT spectra of compounds. a) Averages reflectance spectra of each compound. CWT spectra of all samples of b) cellullose, c) cutin, d) xylan, e) lignin and f) oleanolic acid (or terpenes). Lines denote feature maxima that are indicative of the compound in question labelled by letters.*

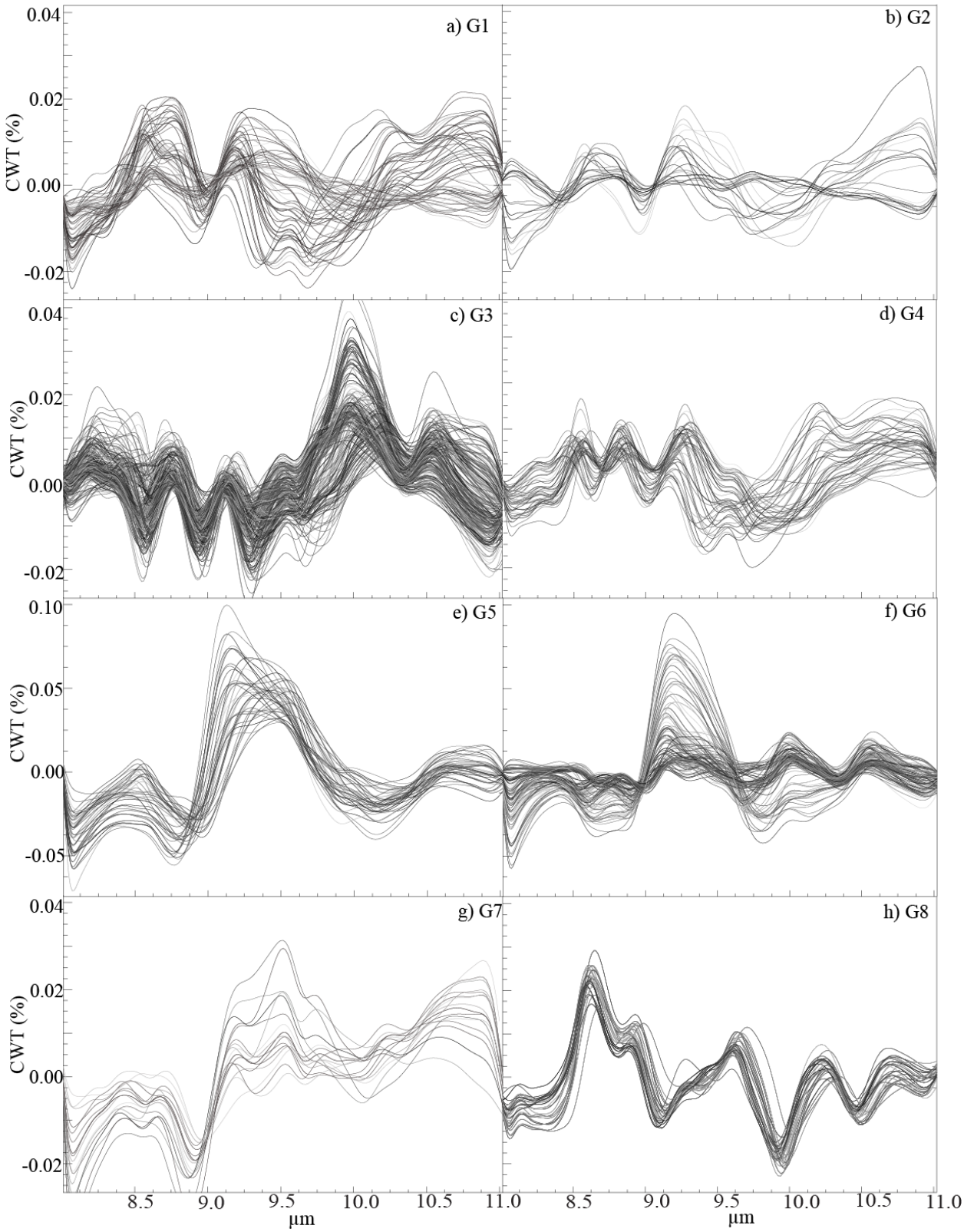

Figure 3.3. *CWT spectra of all leaf samples displayed in 8 grouping of species. Numbers at the top left of each panel indicate the group number. Species are not differentiated but a list of species in each group can be found in Table 3.1.*

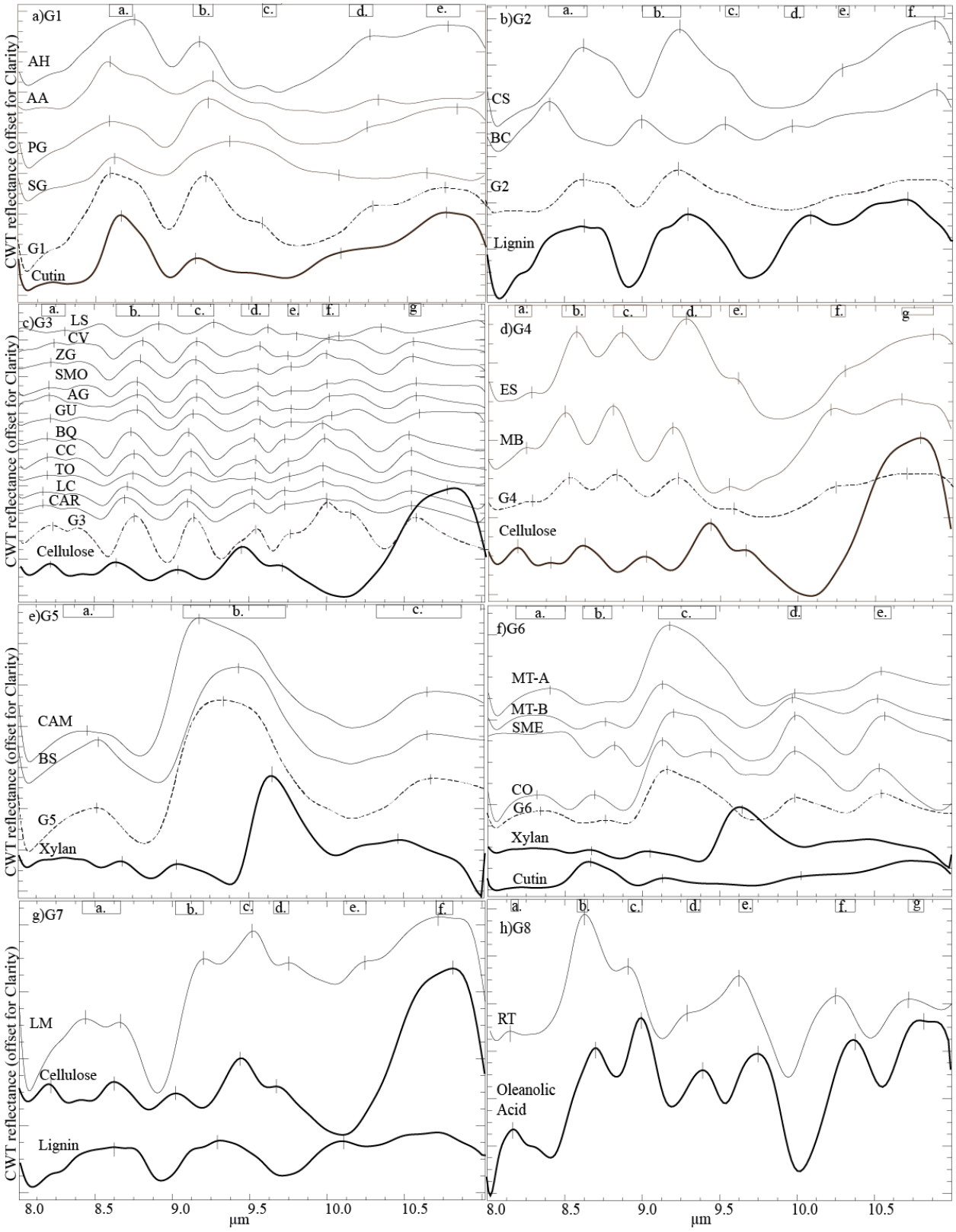
a)G1
AH
AA
PG
SG
G1
Cutin
b)G2
CS
BC
G2
Lignin
c)G3
LS
CV
ZG
SMO
AG
GU
BQ
CC
TO
LC
CAR
G3
Cellulose
d)G4
ES
MB
G4
Cellulose
e)G5
CAM
BS
G5
Xylan
f)G6
MT-A
MT-B
SME
CO
G6
Xylan
Cutin
g)G7
LM
Cellulose
Lignin
h)G8
RT
Oleanolic
Acid
CWT reflectance (offset for Clarity)
8.0
8.5
9.0
9.5
10.0
10.5
µm

Figure 3.4. *Average CWT leaf LWIR spectra per species organized by group shown along with average CWT spectra of attributed compounds. Solid lines denote the average spectra of each species with each panel representing a group. Dashed lines denote the group average spectrum and bold solid lines denote average spectrum for individual compounds attributed to each group. Vertical lines denote prominent spectral features and white boxes represent approximate full-width for each reflectance feature. Shaded boxes represent subset region of greatest spectral differences between species within a group.*

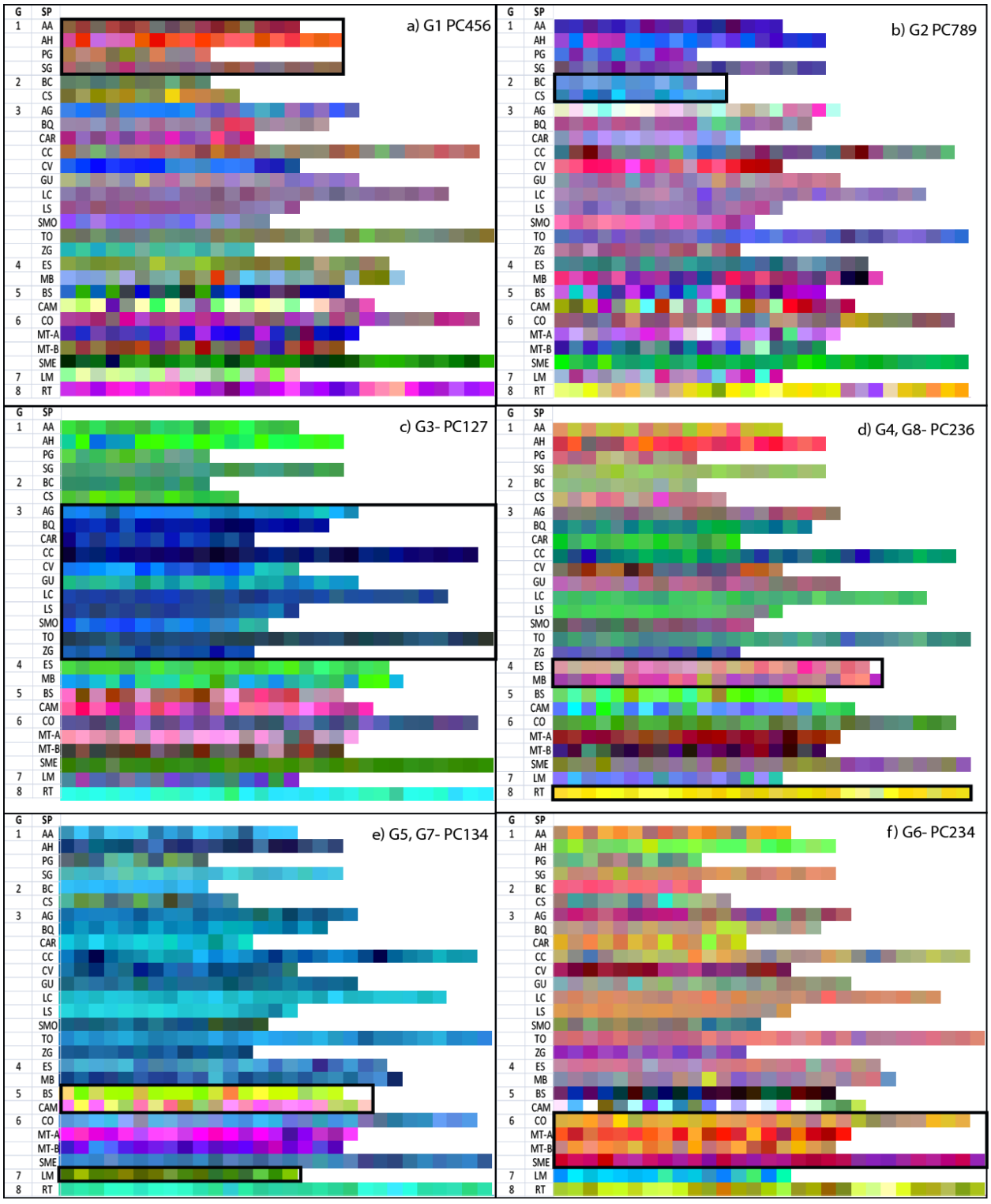

Figure 3.5. *Color composites of principal component combinations for each grouping. Grouping number and principal component numbers forming the RGB composite are written in top right corner of each. Color and brightness indicated similarity and difference distances.*

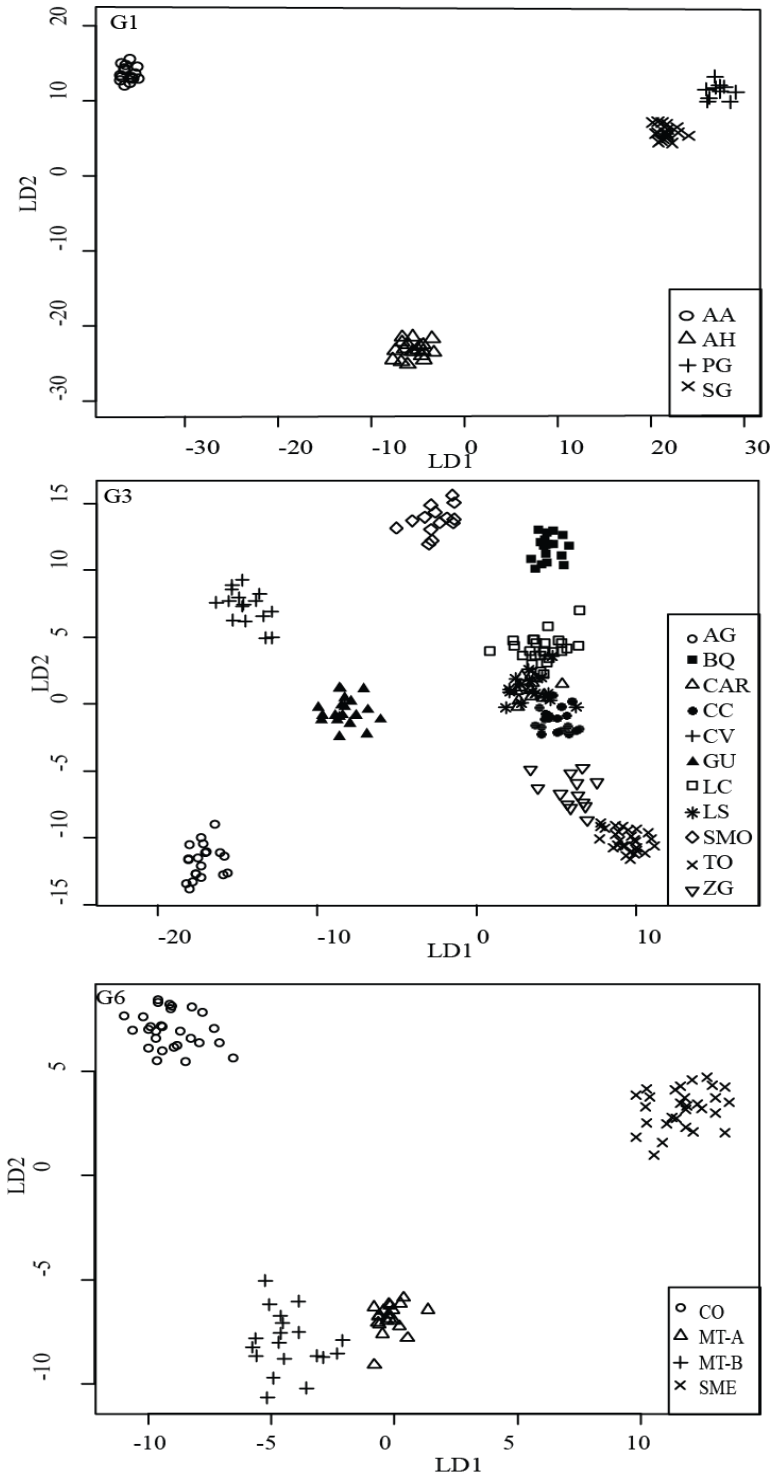

Figure 3.6. *Linear discriminate analysis scatter plots. First two linear discriminants on the x and y axes. Each symbol denotes a species. Scatter plots created for groups 1, 3 and 6 that encompass over three species.*

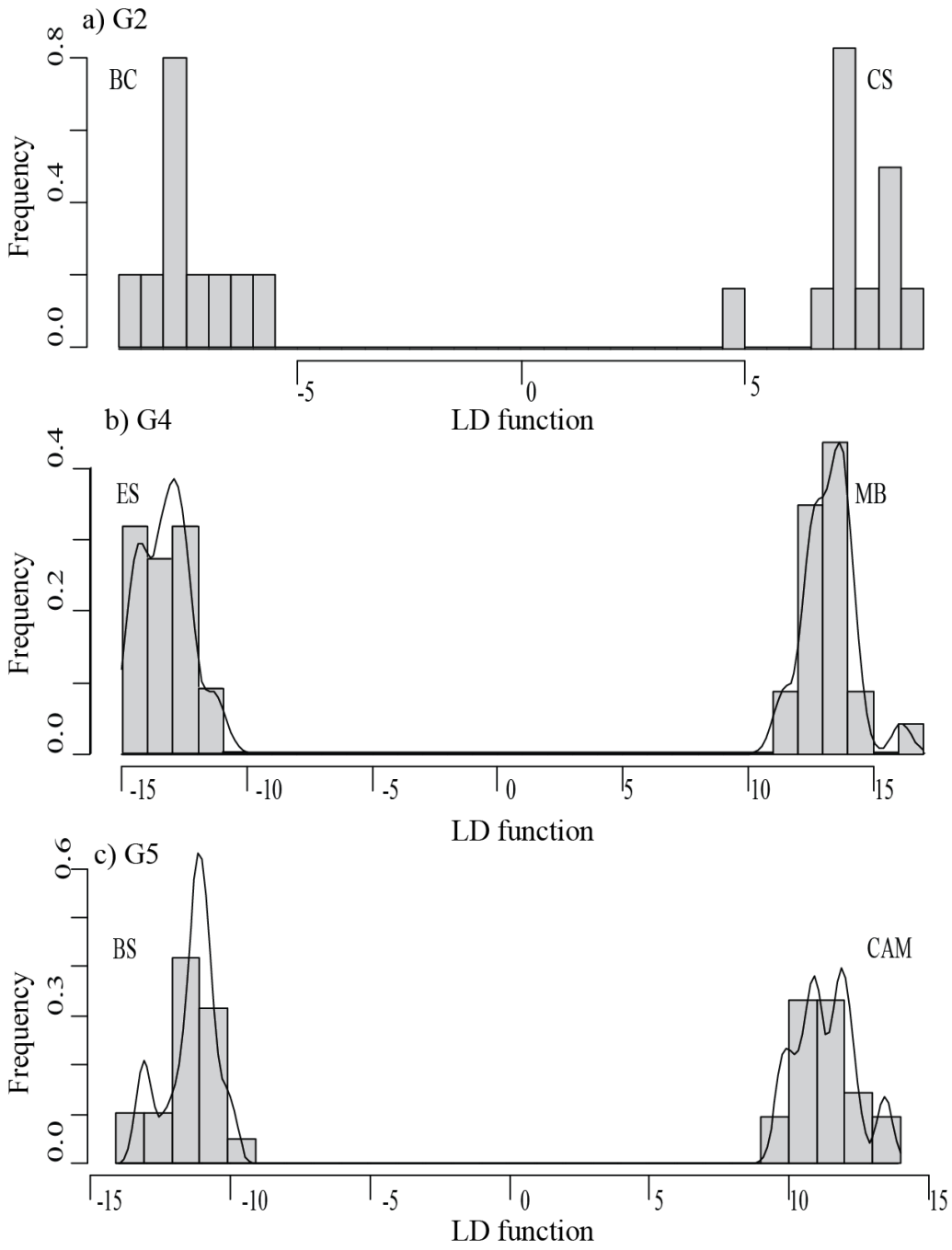

Figure 3.7. *Histograms of Linear Discriminant function values of groups with 2 species. X axis is the discriminant function of each data point and the y-axis is the frequency of the LD function value. a) group 2, b) group 4 and c) group 5.*

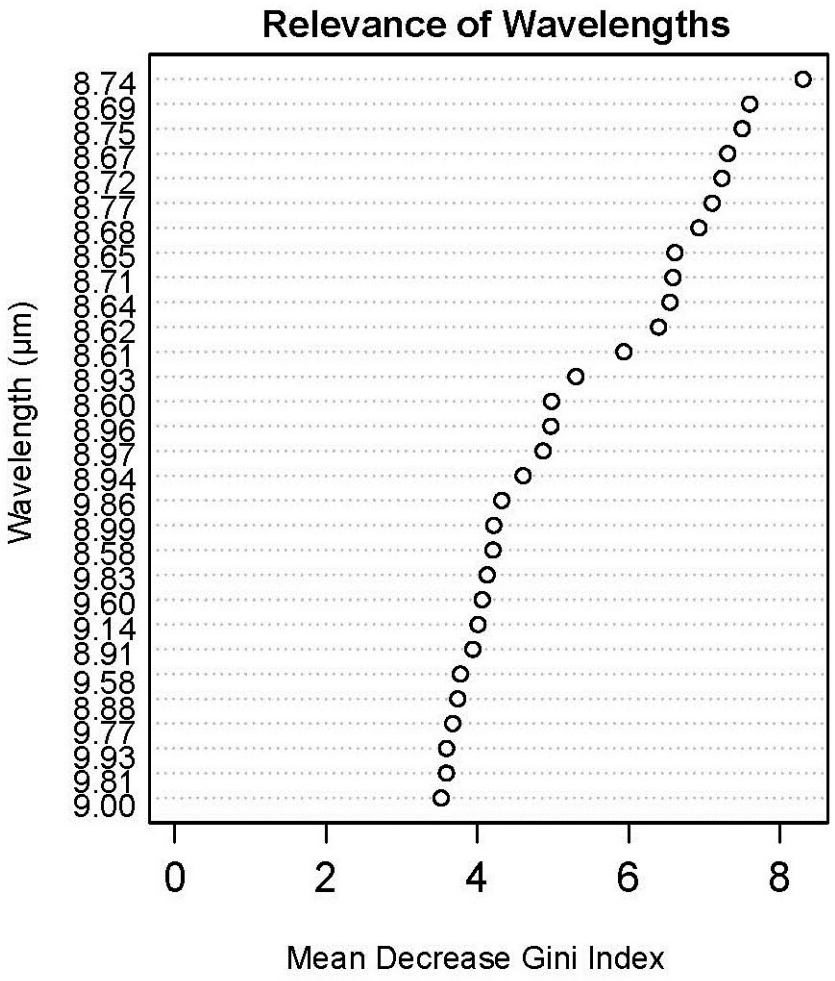

Figure 3.8. *Mean Decrease Gini Index. Index denotes relevance of wavelength from Random forest analysis. Higher numbers on the x axis are most relevant. The y axis shows the wavelength with most influence on RF.*

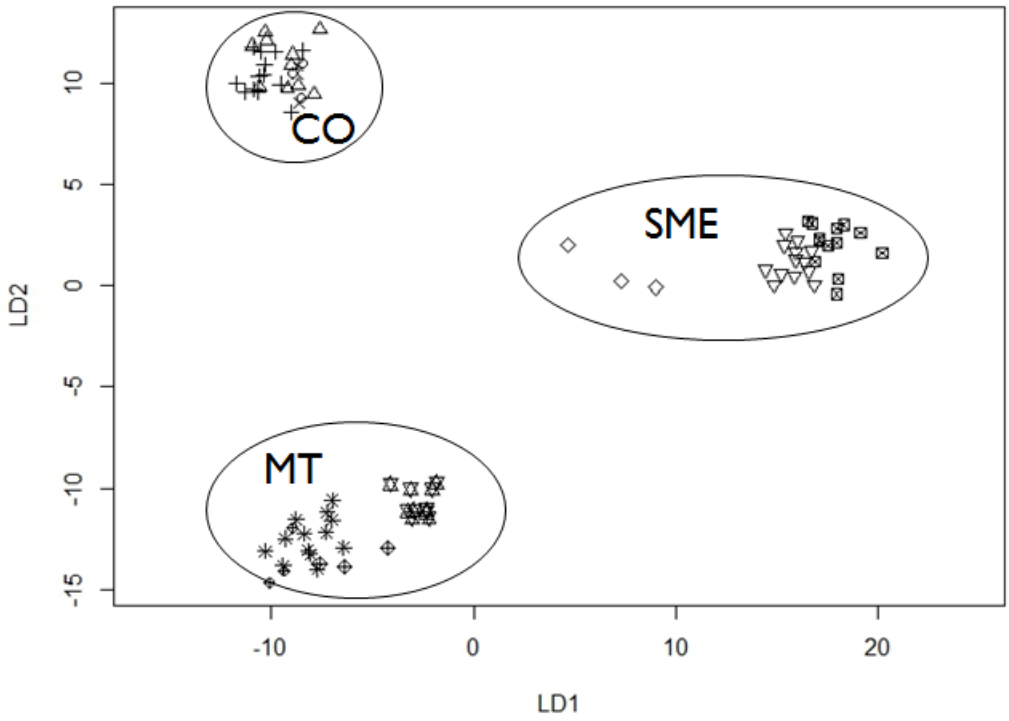

Figure 3.9. *Linear Discriminant Analysis of group 6 with individual trees. Each symbol represents an individual crown and each point represents a leaf. Each species is circled with its respective abbreviation. The first two linear discriminants (LD) are plotted against each other (LD1 and LD2). The proportion of trace for each LD is: 0.52 and 0.34 for LD1 and LD2, respectively.*

4.0 Conclusions

4.1 Summary & Contributions

The research of this investigation sought to advance the field of vegetation classification by contributing to the gap in pre-existing methodologies and by creating new avenues to discern tree species. This was accomplished by first integrating traditional whole-leaf traits with newly quantified anatomical traits along the leaf economic spectrum (LES) to differentiate between two plant functional groups (PFG), lianas and trees in two different sites, a tropical wet forest and a tropical dry forest. The second objective was accomplished by using the novel application of long-wave infrared (LWIR; 8.5 -12 μm) spectral signature characterization to discriminate species for later application to remote sensing (RS).

The focal ecosystems were tropical forests because they hold the majority of the world's biodiversity (Myers et al 2000). Tropical forests cover 7% of earth's terrestrial surface and contain 50% of the plant and animal species (Urquhart 2001). With the pressures of deforestation and climate change resulting in increased rates of species extinction it is pertinent that the dynamics of these biodiversity hotspot are understood and quantified (Myers et al 2000). This thesis aided in the advancement of vegetation classification at a local scale in hopes of later application to a regional or global scale through remote sensing.

In an attempt to understand plant functional group (PFG) classification Chapter 2: "**An anatomical application to Leaf Economic Spectrum through liana and tree whole-leaf trait analyses"** accomplished the implementation of anatomical traits into the LES. This was done through exploring the interactions of anatomical and whole-leaf traits between PFGs and site types. There is a lack of mechanistic explanations and functional consequences to whole-leaf traits in the literature (Reich 2014; Wright et al. 2004). Moreover, the LES does not attempt to

explore the consequential functions in anatomical variations in physiological and morphological traits .The use of functional traits is restricted to whole-leaf function without addressing the anatomical locality (Reich 2014).

Chapter 2 fills this gap in the LES by providing mechanistic explanations of the trends observed between lianas and trees. This was accomplished by examining the interactions between anatomical traits and whole-leaf traits at two different sites, a tropical wet forest and a tropical dry forest. Traits combinations were made based on the functions occurring at different location within the leaf (i.e. upper and lower epidermises, palisade and spongy mesophyll).

For the first time the integration of anatomy and whole-leaf traits were combined to understand the separation of lianas and trees at two different sites. The addition of anatomical traits support the hypothesis that lianas are resource acquisitive and trees are resources conservative but also provides a mechanistic view towards this hypothesis. Lianas exhibit a high metabolism and inexpensive infrastructure. Conversely, trees have a slow metabolism to support an expensive infrastructure. Finally, this chapter concluded that water availability significantly affects the resource strategies of each functional group. Drier environments have fewer water resources and therefore smaller leaves with less physiological investment and the inverse conclusions were found regarding wet sites.

The classification of PFGs is important in order to understand how different group of plants will respond to climate change. In the case of liana and tree dynamics, there is a consensus that ecosystem structure between the two groups is changing in some tropical forests (Schnitzer 2005; Schnitzer and Bonger 2005; Sanchez-Azofeifa et al. 2009, Schnitzer et al. 2015). Therefore, to fully comprehend the ecosystem consequences to climate change and deforestation

there needs to be a strong understanding of the foliar level micro-mechanisms and how they will respond.

Chapter 3 "**Long-wave infrared spectral feature characterization of tropical dry forest tree species and use for species discrimination**" of this thesis collected local-scale hyperspectral data from tropical dry forest (TDF) tree species with the intent of later applications to regional and global-scale environmental monitoring. This was accomplished through the identification of cuticle and cell wall compounds using the LWIR spectral signatures of leaves of 26 dry forest tree species and ensuing species discrimination from spectra. Species discrimination for remote sensing purposes have long been a difficulty due to such issues as atmospheric windows, a lack of speciation in visible light or water absorption features dominating the SWIR (Kokaly et al. 2003). However, a novel study in from Ribeiro da Luz and Crowley (2006; 2007; 2010) demonstrated that with advances in technology the LWIR is a promising region of the EM spectrum for vegetation discrimination.

This investigation found the best approach to species classification in the LWIR was through spectral feature identification and from these findings species discrimination. For the first time TDF tree species were classified using their respective long-wave infrared spectral signature. This was achieved through the decomposition of the spectral features to their most probably origin, 1 of 5 essential cell wall or cuticular compounds (cellulose, matrix glycan, cutin, lignin or oleanolic acid). After deciphering spectral features, the spectral signatures were used to discern species with linear discriminant analysis and random forest boot-strapping analysis.

The purpose of environmental monitoring through RS is to provide information regarding changes and processes of ecosystem structure and function. This then provides information for

impact assessments, to mitigate and manage nature resources and to extend conservation efforts in biodiversity and its subsequent ecosystem services. The limitations in environmental monitoring in the tropics are the results of unstable technical, institutional and political infrastructures (Houghton et al 2001). Furthermore, farming, poverty and vulnerable areas are at most risk and are often concentrated in biodiversity hotspots where destructive techniques such as slash and burning occur. The implementation of cheap and consistent monitoring techniques is a start to attempt to solve the issues presented above.

4.2 Future work

4.2.1 Anatomical traits applications

PFG were described in detail in this thesis; they are a classification technique based on phenology, physiology and structure (Ustin and Gamon 2010). The addition of anatomy enabled the first steps of classification from the perspective of locality dictating functionality. The groups used in this investigation were lianas and trees. Currently lianas are increasing in abundance as a result of drier and warmer conditions associated with climate change. Furthermore, the increase in abundance of lianas causes an increase in tree mortality and suppression of tree growth (Schnitzer 2005; Schnitzer and Bonger 2005). Since this investigation was at a very local scale in only two sites, future investigations should focus on replication, to quantify the anatomical variations in more species of trees and lianas and at more sites. This would advance our understanding of lianas' expansion associated with climate change and aid in the mitigation efforts directed at this problem of biodiversity loss. From a methodological point of view the inclusion of anatomy could be applied to other PFGs other than of lianas' and tree to explore the potential of these traits as a common practice in ecology; future work could be to add anatomical traits into the LES as standard in the field vegetation classification. Just as metrics

such as leaf mass area (LMA), leaf longevity and other whole traits, are standards so too should anatomical parameters.

4.2.2 Long-wave infrared remote sensing applications

Remote sensing provides a novel monitoring technique at a variety of scales. At the local scale, the decomposition of the LWIR spectra into organic compounds aids in the comprehension of leaf molecular structure and additionally helps species discrimination. This was an *in-situ* experiment and a very early study in the exploration of LWIR research. LWIR has been use quite extensively in micro-spectroscopy but this application to RS was the result of advances in technology. The next steps will be application to airborne surveys since the technology is now publicly and commercially available though further advances in signal to noise of data would be particularly beneficial to remote sensing of vegetation.

This has been a step forward in the field of remote sensing of vegetation. Advances in technology will enable species discrimination at the landscape scale. Mapping tropical ecosystems from a global perspective will aid in the understanding of biodiversity distribution and quantification; this will ultimately help in decision making in policies towards combating climate change effects on ecosystem structure and biodiversity degradation. Future investigations opportunities are broad since this field of research is in its infancy and technology is constantly improving. Therefore, the next research efforts should focus on 1) a more complete spectral library of cuticle and cell wall compounds for feature identification and; 2) a scale-up study that could be conducted from an airborne hyperspectral survey over a TDF in an attempt to discriminate species in imagery at a regional scale.

4.2.3 Synthesis Conclusions

Human impacts on other species extinct rates have increased as much as 1000 times over the past 100 years when compared to pre-industrial anthropogenically-caused extinction rates (Collen et al. 2013); and yet there is still a lack of information on biological systems that hinders our understanding of the impacts of these species loss (Winter 2012). What is known, however, is that the loss of biodiversity impacts are anthropogenically and environmentally detrimental to ecosystem services, structure and function (Collen et al. 2013). Therefore, the emphasis should focus on the need to fully comprehend and manage climate change and its repercussions on biodiversity. Ecosystem monitoring is an essential and crucial field to fully exploit before the impacts of biodiversity loss, if they are not already, are irreparable. Classification systems and environmental monitoring are necessary tools to best understand the dynamics of the ecosystem.

This thesis took two alternative approached to the betterment of classification methodologies; the incorporation of anatomy into the LES and the exploration of long-wave infrared as a discrimination metric. The contribution of these two chapters furthers the solution to the predicament of advancing environmental monitoring to the point of fully understanding our impacts on biodiversity. Future investigations and movement in this field should focus on: standardization in classification techniques and an emphasis on the global perspective remote sensing has to offer.

4.1 References

Collen, B., Pettorelli, N., Bailie, J. E. M., Durant, S. 2013. *Biodiversity monitoring and conservation: bridging the gap between global commitment and local action*. Wiley-Blackwell publications.

Houghton, J. T., Ding, Y., Griggs, D. J., Noguer, M., Van der Linden, P. J., Dai, X., Johnson, C. A. (2001). Climate Change 2001: The Scientific Basis. *Climate Change 2001: The Scientific Basis (IPCC)*, 881.

Kokaly, R., Despain, D. G., Clark, R. N., & Livo, E. (2003) Mapping vegetation in Yellowstone National Park using spectral feature analysis of AVIRIS data. Remote Sensing of the Environment 84: 437-456

Kokaly, R. F., Asner, G. P., Ollinger, S. V., Martin, M. E., & Wessman, C. A. (2009). Characterizing canopy biochemistry from imaging spectroscopy and its application to ecosystem studies. *Remote Sensing of Environment*, *113*(SUPPL. 1), S78–S91.

Kokaly, R. F., & Clark, R. N. (1999). Spectroscopic determination of leaf biochemistry using band-depth analysis of absorption features and stepwise multiple linear regression. *Remote Sensing of Environment*, *67*(3), 267–287.

Myers, N., Mittermeier, R. A., Mittermeier, C. G., da Fonseca, G. A. B., & Kent, J. (2000). Biodiversity hotspots for conservation priorities. *Nature*, *403*(6772), 853–858.

Reich, P. B. (2014). The world-wide "fast-slow" plant economics spectrum: A traits manifesto. *Journal of Ecology*, *102*(2), 275–301.

Ribeiro da Luz, B. (2006). Attenuated total reflectance spectroscopy of plant leaves: A tool for ecological and botanical studies. *New Phytologist*, *172*(2), 305–318.

Ribeiro da Luz, B., & Crowley, J. K. (2007). Spectral reflectance and emissivity features of broad leaf plants: Prospects for remote sensing in the thermal infrared (8.0-14.0μm). *Remote Sensing of Environment*, *109*(4), 393–405.

Ribeiro da Luz, B., & Crowley, J. K. (2010). Identification of plant species by using high spatial and spectral resolution thermal infrared (8.0-13.5 [mu]m) imagery. *Remote Sensing of Environment*, *114*(2), 404–413.

Sanchez-Azofeifa, G. A., Castro, K., Wright, S. J., Gamon, J., Kalacska, M., Rivard, B., Feng, J. L. (2009). Differences in leaf traits, leaf internal structure, and spectral reflectance between two communities of lianas and trees: Implications for remote sensing in tropical environments. *Remote Sensing of Environment*, *113*(10), 2076–2088.

Sanchez-Azoffeifa, G.A., Kalacska, M., Quesada, M., Calco-Alvarado, J. C., Nassar, J.M., Rodriguez, J.P. (2005). Need for Integrated Research for a Sustainable Future in Tropical Dry Forests, 19(2), 285–286.

Schnitzer, S. A. (2005). A mechanistic explanation for global patterns of liana abundance and distribution. *The American Naturalist*, *166*(2), 262–276.

Schnitzer, S, Bongers, F., Burham, R. J., & Putz, F. E., (2015) *Ecology of lianas*. John Wiley & Sons Blackwell, Oxford UK.

Schnitzer, S., & Bongers, F. (2002). The ecology of lianas and their role in forests. Trends in Ecology & Evolution, 17(5), 223–230.

Ustin, S. L., & Gamon, J. A. (2010). Remote sensing of plant functional types. *New Phytologist*, *186*(4), 795–816.

Urquhart, G., Chomentowski, W.S. (2001). Tropical deforestation. Technical report, NASA Earth Observatory (Burgess)

Winter, S. (2012). Forest naturalness assessment as a component of biodiversity monitoring and conservation management. *Forestry*, *85*(2), 291–304.

Wright, I. J., Reich, P. B., Westoby, M., Ackerly, D. D., Baruch, Z., Bongers, F., Gulias, J. (2004). The worldwide leaf economics spectrum, Nature, 12, 821–827.

5.0 Thesis References

5.1 Introduction References

Asner, G. P., & Martin, R. E. (2012). Contrasting leaf chemical traits in tropical lianas and trees: Implications for future forest composition. *Ecology Letters*, *15*(9), 1001–1007.

Batcheler, C. L. (1985). Note on measurement of woody plant diameter distributions. *New Zealand Journal of Ecology*, *8*, 129–132.

Burgess, K. S., Fazekas, A. J., Kesanakurti, P. R., Graham, S. W., Husband, B. C., Newmaster, S. G., Barrett, S. C. H. (2011). Discriminating plant species in a local temperate flora using the rbcL+matK DNA barcode. *Methods in Ecology and Evolution*, *2*(4), 333–340.

Burgess, R., Hansen, M., Olken, B. A., Potapov, P., & Sieber, S. (2012). The political economy of deforestation in the tropics. *Quarterly Journal of Economics*, *127*(4), 1707–1754.

Castro-Esau, K. L., & Sanchez-Azofeifa, G. A. (2008). Changes in Spectral Properties, Chlorophyll Content and Internal Mesophyll Structure of Senescing Populus balsamifera and Populus tremuloides Leaves. *Sensors*, *8*, 51–69.

Castro-Esau, K. L., Sanchez-Azofeifa, G. A., Rivard, B., Wright, S. J., & Quesada, M. (2006). Variability in leaf optical properties of mesoamerican trees and the potential for species classification. *American Journal of Botany*, *93*(4), 517–530.

Chazdon, R. L. (2008). Beyond deforestation: restoring forests and ecosystem services on degraded lands. *Science (New York, N.Y.)*, *320*(5882), 1458–1460.

Clark, R. N., Despain, D. G., Kokaly, R. F., & Livo, K. E. (2003). Mapping vegetation in Yellowstone National Park using spectral feature analysis of AVIRIS data, *Remote Sensing of the Environment 84*, 437–456.

Collen, B., Pettorelli, N., Bailie, J. E. M., Durant, S. 2013. *Biodiversity monitoring and conservation: bridging the gap between global commitment and local action*. Wiley-Blackwell publications.

De Cáceres, M., Font, X., Vicente, P., & Oliva, F. (2009). Numerical reproduction of traditional classifications and automatic vegetation identification. *Journal of Vegetation Science*, *20*(4),

Domingues, T. F., Martinelli, L. A., & Ehleringer, J. R. (2007). Ecophysiological traits of plant functional groups in forest and pasture ecosystems from eastern Amazonia, Brazil. *Plant Ecology*, *193*(1), 101–112.

Dybzinski, R., Fargione, J. E., Zak, D. R., Fornara, D., & Tilman, D. (2008). Soil fertility increases with plant species diversity in a long-term biodiversity experiment. *Oecologia*, *158*(1), 85–93.

Féret, J. B., & Asner, G. P. (2012). Semi-supervised methods to identify individual crowns of lowland tropical canopy species using imaging spectroscopy and lidar. *Remote Sensing*, *4*(8), 2457–2476.

Gardner, T. A., Barlow, J., Chazdon, R., Ewers, R. M., Harvey, C. A., Peres, C. A., & Sodhi, N. S. (2009). Prospects for tropical forest biodiversity in a human-modified world. *Ecology Letters*, *12*(6), 561–582.

Houghton, J. T., Ding, Y., Griggs, D. J., Noguer, M., Van der Linden, P. J.,Dai, X., Johnson, C. A. (2001). Climate Change 2001: The Scientific Basis. *Climate Change 2001: The Scientific Basis*

Jensen, M., & Bourgeron, P. (1994). Volume II: ecosystem management: principles and applications. *General Technical Report PNW-GTR 318*, 376.

Jones, H. G., Vaughan, R. A. (2010). *Remote sensing of vegetation*. Ch. 7.2 Spectral indices.164-182, Oxford, New York, *Oxford University Press*.

Kiang, N. Y., Siefert, J., Govindjee, & Blankenship, R. E. (2007). Spectral signatures of photosynthesis I review of earth organisms. *Astrobiology*, *7*(1), 222–251.

Kokaly, R. F., Asner, G. P., Ollinger, S. V., Martin, M. E., & Wessman, C. A. (2009). Characterizing canopy biochemistry from imaging spectroscopy and its application to ecosystem studies. *Remote Sensing of Environment*, *113*(SUPPL. 1), S78–S91.

Kokaly, R. F., & Clark, R. N. (1999). Spectroscopic determination of leaf biochemistry using band-depth analysis of absorption features and stepwise multiple linear regression. *Remote Sensing of Environment*, *67*(3), 267–287.

Mucina, L. (1997). Classification of vegetation: Past, present and future, Journal of Vegetation Science 8 751–760.

Myers, N., Mittermeier, R. A., Mittermeier, C. G., da Fonseca, G. A. B., & Kent, J. (2000). Biodiversity hotspots for conservation priorities. *Nature*, *403*(6772), 853–858.

Peterson, G., Allen, C. R., Holling, C. S. (1997). Ecological resilience, Biodiversity and Scale. Ecosystems 1: 6-18.

Pierce, S., Brusa, G., Vagge, I., & Cerabolini, B. E. L. (2013). Allocating CSR plant functional types: The use of leaf economics and size traits to classify woody and herbaceous vascular plants. *Functional Ecology*, *27*(4), 1002–1010.

Reich, P. B. (2014). The world-wide "fast-slow" plant economics spectrum: A traits manifesto. *Journal of Ecology*, *102*(2), 275–301.

Ribeiro da Luz, B. (2006). Attenuated total reflectance spectroscopy of plant leaves: A tool for ecological and botanical studies. *New Phytologist*, *172*(2), 305–318.

Ribeiro da Luz, B., & Crowley, J. K. (2007). Spectral reflectance and emissivity features of broad leaf plants: Prospects for remote sensing in the thermal infrared (8.0-14.0um). *Remote Sensing of Environment*, *109*(4), 393–405.

Ribeiro da Luz, B., & Crowley, J. K. (2010). Identification of plant species by using high spatial and spectral resolution thermal infrared (8.0-13.5 [mu]m) imagery. *Remote Sensing of Environment*, *114*(2), 404–413.

Sanchez-Azofeifa, G. A., Castro, K., Wright, S. J., Gamon, J., Kalacska, M., Rivard, B., … Feng, J. L. (2009). Differences in leaf traits, leaf internal structure, and spectral reflectance between two communities of lianas and trees: Implications for remote sensing in tropical environments. *Remote Sensing of Environment*, *113*(10), 2076–2088.

Sanchez-Azoffeifa, G.A., Kalacska, M., Quesada, M., Calco-Alvarado, J. C., Nassar, J.M., Rodriguez, J.P. (2005). Need for Integrated Research for a Sustainable Future in Tropical Dry Forests, *19*(2), 285–286.

Salisbury, J. W. (1986). Preliminary measurements of leaf spectral reflectance in the 8-14 μm region. *International Journal of Remote Sensing*, *7*(12), 1879–1886.

Schläpfer, F., & Schmid, B. (1999). Ecosystem Effects of Biodiversity : a Classification of. *Ecological Applications*, *9*(3), 893–912.

Schnitzer, S. A. (2005). A mechanistic explanation for global patterns of liana abundance and distribution. *The American Naturalist*, *166*(2), 262–276.

Séné, F. C., B., Mccann, M. C., Wilson, R. H., & Crinter, R. (1994). Fourier-Transform Raman and Fourier-Transform lnfrared Spectroscopy '. *Plant Physiology*, *106*, 1623–1631.

Sterk, F., Markesteijn, L., Chieving, F., & Poorter, L. (2011). Functional traits determine trade-offs and niches in a tropical forest community. Proceedings of the National Academy of Sciences 51: 2062-20632.

Urquhart, G., Chomentowski, W.S. (2001). Tropical deforestation. Technical report, NASA Earth Observatory (Burgess)

Ustin, S. L., & Gamon, J. A. (2010). Remote sensing of plant functional types. *New Phytologist*, *186*(4), 795–816.

Whittaker, R. H. 1998. *Ordination of plant communities*. Dr.W Junk Publishes. The Hague Boston-London.

Winter, S. (2012). Forest naturalness assessment as a component of biodiversity monitoring and conservation management. *Forestry*, *85*(2), 291–304.

Wright, I. J., Reich, P. B., Westoby, M., Ackerly, D. D., Baruch, Z., Bongers, F., Gulias, J. (2004). The worldwide leaf economics spectrum, Nature, 12, 821–827.

Zhang, J., Rivard, B., Sánchez-Azofeifa, A., & Castro-Esau, K. (2006). Intra- and inter-class spectral variability of tropical tree species at La Selva, Costa Rica: Implications for species identification using HYDICE imagery. *Remote Sensing of Environment*, *105*(2), 129–141.

5.2 Chapter 2 References

Armstrong, D. L., Griffin, K. P., Danner, M., Mees, C., Nguyen, D. (1998). *Better crops with plant food*. Potash & phosphate institute, Norcross, GA.

Asner, G. P., & Martin, R. E. (2012). Contrasting leaf chemical traits in tropical lianas and trees: Implications for future forest composition. *Ecology Letters*, *15*(9), 1001–1007.

Bancroft, J. D., Cook, H. C. (1984) Manual of Histology Techniques. New York, NY, Churchill Livingstone

Bongers, F., Popma, (1990). Leaf characteristics of the tropical rain forest flora of Los Tuxtlas, Mexico. Botanical Gazette 151: 354-365.

Cai, Z., Schnitzer, S. A., Bongers, F. (2009). Seasonal difference in leaf-level physiology give lianas competitive advantage over trees ina tropical seasonal forest. Oecologia 161: 25-33

Castellanos, J., Maass, M., Kummerow, J. (1991). Root biomass of a dry deciduous tropical forest in Mexico. Plant and Soil 131: 225-228

Castro-Esau, K. L., Sanchez-Azofeifa, G. A., Caelli, T. (2004) Discrimination of lianas and trees with leaf level hyperspectral data. Remote sensing of the Environment 90: 353-372

Castro-Esau, K. L., Sanchez-Azofeifa, G. A., Rivard, B., Wright, S. J., & Quesada, M. (2006). Variability in leaf optical properties of mesoamerican trees and the potential for species classification. *American Journal of Botany*, *93*(4), 517–530.

Castro, K. L., & Sanchez-Azofeifa, G. A. (2008). Changes in Spectral Properties, Chlorophyll Content and Internal Mesophyll Structure of Senescing *Populus balsamifera and Populus tremuloides* Leaves. *Sensors*, *8*, 51–69.

Chazdon, R. L. (2008). Beyond deforestation: restoring forests and ecosystem services on degraded lands. *Science (New York, N.Y.)*, *320*(5882), 1458–1460.

Choog, A., Lucas, P. W, Ong, J. S. Y., Perreira, B., Tan, H. T. W., Turner, I. M. (1992). Leaf fracture toughness and sclerophylly: their correlations and ecological implications. New phytologist 121: 597-610.

DeWalt, S.J., Schnitzer, S. A.,Chave, J., Bongers, F., Burnham R. J., Cai, Z., Chuyong, G., Clark, D. B., Ewango, C. E. N., Gerwing, J., Gortaire, E., Hart, T., Ibarra-Manrıquez, G., Ickes, K., Kenfack, D., Macıa, M. J., Makana, J. R., Martınez-Ramos, M., Mascaro, J., Moses, S., Muller-Landau, H. C., ParrenM. P., Parthasarathy, N.,Perez-Salicrup, D. R. Putz, F. E., Romero-Saltos, H., & Thomas, D. (2010). Annual rainfall and seasonality predict pan-tropical patterns of liana density and basal area. Biotropica 42: 309-317

Domingues, T. F., Martinelli, L. A., & Ehleringer, J. R. (2007). Ecophysiological traits of plant functional groups in forest and pasture ecosystems from eastern Amazonia, Brazil. *Plant Ecology*, *193*(1), 101–112.

Duran, S., & Sanchez Azofeifa, G. A. (2015). Lianas effects on carbon storage and uptake in mature and secondary tropical forests. *Biodiversity of Lianas, Sustainable Development.* Springer International Publishing Switzerland.

Ferreira, T., & Rasband, W. (2012). ImageJ user guide1.46r.

Fortunel, C., Fine, P. V A., Baraloto, C. (2012). Leaf stem and root tissue strategies across 758 neotropical tree species. Functional Ecology 26: 1153-1161.

Gilbert, B., Wright, S. J., Muller Landau, H. C., Kitajima, K., Hernandez, A. (2006). Life history trade-offs in tropical trees and lianas. Ecological Society of America 87: 1281-1288.

Granados, J. and Korner, C. 2002. In deep shade, elevated CO2 increases the vigor of tropical climbing plants. Global Change Biology 8: 1109-1117.

Hopkins, W. G. Hüner, N. P. A. (2004) *Introduction to plant physiology*. Ontario, John *Wiley & Son publishing*.

Hudson, A., Jeffree, C. (2001). Leaf and Internode. *Encyclopedia of Life Science 1,* 1-6.

John, G. P., Scoffoni, C., Sack, L. (2010). Allometry of cells and tissues within leaves. American Journal of Botany 100: 1936-1948.

Kazda, M., and K. Mehltreter. "Contrasting leaf nutrition, and leaf mass per unit area in lianas, and trees from the subtropical Island Martin Garcia, Argentina." *Diss Bot* 346 (2001): 131-139.

Kikuzawa, K., (1995). The basis for variation in leaf longevity of plants. Vegetatio 121:89-100

Letcher, S., & Chazdon, R. (2009). Lianas and self-supporting plants during tropical forest succession. Forest Ecology and Management 257: 2150-2156.

McCune, B. and J. B. Grace. 2002. *Analysis of Ecological Communities*. MjM Software, Gleneden Beach, Oregon, USA (www.pcord.com) 304 page

Mediavilla, S., Escudero, A., Heilmeier, H. (1999). Internal leaf anatomy and photosynthetic resource-use efficiency: interspecific and intraspecific comparisons. Tree Physiology 21: 251-259.

MBF Bioscience (2015) Autospine. http://www.mbfbioscience.com/autospine

Milla-Moreno, E. (2010). Structural properties related to mesophyll conductance and underlying variation in leaf mass area of Balsam Poplar (Populus balsamifera). MSc Thesis University of British Columbia.

Poorter, H.,Niinemets, U., Pooter, L., Wright, I. J., Villar, R., Causes and consequences of variation in leaf per mass area (LMA): a meta-analysis. New Phytologist 182: 565-588.

Popma, J., & Bongers, F., Werger, M. J. A. (1992). Gap-dependence and leaf characteristics of trees ina tropical lowland rain forest in Mexico. Oikos 63: 207-2014.

Portillo-Quintero, C., Sanchez-Azofeifa, A., Calvo-Alvarado, J., Quesada, M., & do Espirito Santo, M. M. (2015). The role of tropical dry forests for biodiversity, carbon and water conservation in the neotropics: lessons learned and opportunities for its sustainable management. *Regional Environmental Change*, *15*(6), 1039–1049.

Pyke, K., (2012) Mesophyll. In: eLS. John Wiley & Sons, Ltd: Chichester

Reich, P. B. (2014). The world-wide “fast-slow” plant economics spectrum: A traits manifesto. *Journal of Ecology*, *102*(2), 275–301.

Sanchez-Azofeifa, G. A., Castro, K., Wright, S. J., Gamon, J., Kalacska, M., Rivard, B., Feng, J. L. (2009). Differences in leaf traits, leaf internal structure, and spectral reflectance between two

communities of lianas and trees: Implications for remote sensing in tropical environments. *Remote Sensing of Environment*, *113*(10), 2076–2088.

Sanchez-Azoffeifa, G.A., Kalacska, M., Quesada, M., Calco-Alvarado, J. C., Nassar, J.M., Rodriguez, J.P. (2005). Need for Integrated Research for a Sustainable Future in Tropical Dry Forests, *19*(2), 285–286.

Schnitzer, S. A. (2005). A mechanistic explanation for global patterns of liana abundance and distribution. *The American Naturalist*, *166*(2), 262–276.

Schnitzer, S., & Bongers, F. (2002). The ecology of lianas and their role in forests. Trends in Ecology & Evolution, 17(5), 223–230.

Schnitzer. S., Bongers, F., Burnham, R. J., Putz, F. (2015). *Ecology of lianas*. John Wiley & Sons, Ltd, Chichester, UK

Slot, M., Wright S. J., Kitajima, K. (2013). Foliar respiration and its temperature sensitivity in trees and lianas: in situ measurements in the upper canopy of a tropical forest. Tree physiology 33: 505-515.

Sterk, F., Markesteijn, L., Chieving, F., & Poorter, L. (2011). Functional traits determine trade-offs and niches in a tropical forest community. Proceedings of the National Academy of Sciences 51: 2062-20632.

Swaine,, M. D., & Grace, J. (2007). Lianas may be favoured by low rainfall evidence from Ghana. Plant Ecology 192: 271-276.

Venables, W. N. & Ripley, B. D. (2002) Modern Applied Statistics with S. Fourth Edition. Springer, New York. ISBN 0-387-95457-0

Wright, I. J., Reich, P. B., Westoby, M., Ackerly, D. D., Baruch, Z., Bongers, F., Gulias, J. (2004). The worldwide leaf economics spectrum, *Nature, 12*, 821–827.

Zotz, Gerhard, and Klaus Winter. "Diel patterns of CO2 exchange in rainforest canopy plants." *Tropical forest plant ecophysiology*. Springer US, 1996. 89-113.

5.3 Chapter 3 References

Abidi, N., Cabrales, L., & Haigler, C. H. (2014). Changes in the cell wall and cellulose content of developing cotton fibers investigated by FTIR spectroscopy. *Carbohydrate Polymers*, *100*, 9–16.

Batcheler, C. L. (1985). Note on measurement of woody plant diameter distributions. *New Zealand Journal of Ecology*, *8*, 129–132.

Castro-Esau, K. L., & Sanchez-Azofeifa, G. A. (2008). Changes in Spectral Properties, Chlorophyll Content and Internal Mesophyll Structure of Senescing *Populus balsamifera* and *Populus tremuloides* Leaves. *Sensors*, *8*, 51–69.

Castro-Esau, K. L., Sanchez-Azofeifa, G. A., Rivard, B., Wright, S. J., & Quesada, M. (2006). Variability in leaf optical properties of mesoamerican trees and the potential for species classification. *American Journal of Botany*, *93*(4), 517–530.

Chen, L., Carpita, N. C., Reiter, W.-D., Wilson, R. H., Jeffries, C., & McCann, M. C. (1998). A rapid method to screen for cell-wall mutants using discriminant analysis of Fourier transform infrared spectra. *The Plant Journal*, *16*(3), 385–392.

Cheng, T., Rivard, B., & Sanchez-Azofeifa, A. (2011). Spectroscopic determination of leaf water content using continuous wavelet analysis. *Remote Sensing of Environment*, *115*(2), 659–670.

Cheng, T., Rivard, B., Sanchez-Azofeifa, G. A., Feng, J., & Calvo-Polanco, M. (2010). Continuous wavelet analysis for the detection of green attack damage due to mountain pine beetle infestation. *Remote Sensing of Environment*, *114*(4), 899–910.

Clark, M. L., & Roberts, D. A. (2012). Species-level differences in hyperspectral metrics among tropical rainforest trees as determined by a tree-based classifier. *Remote Sensing*, *4*(6), 1820–1855.

Clark, R. N., Despain, D. G., Kokaly, R. F., & Livo, K. E. (2003). Mapping vegetation in Yellowstone National Park using spectral feature analysis of AVIRIS data, *Remote Sensing of the Environment 84*, 437–456.

Feng, X., Zhang, X., Sun, C., Motamedi, M., & Ansari, F. (2014). Stationary Wavelet Transform Method for Distributed Detection of Damage by Fiber-Optic Sensors. *Journal of Engineering Mechanics*, *140*(4), 04013004.

Hespell, R. B. (1998). Extraction and characterization of matrix glycan from the corn fiber produced by corn wet-milling processes. *Journal of Agricultural and Food Chemistry*, *46*(97), 2615–2619.

Jetter, R., Junst, L., & Samuels, L. (2006) Annual plant reviews volume 23: biology of the plant cuticle. Blackwell Publishing, Oxford, UK.

Jones, H. G., Vaughan, R. A. (2010). *Remote sensing of vegetation*. Ch. 7.2 Spectral indices.164-182, Oxford, New York, *Oxford University Press*.

Kacuráková, M., & Wilson, R. H. (2001). Developments in mid-infrared FT-IR spectroscopy of selected carbohydrates. *Carbohydrate Polymers*, *44*(4), 291–303.

Kacuráková, M. (2000). FT-IR study of plant cell wall model compounds: pectic polysaccharides and hemicelluloses. *Carbohydrate Polymers*, *43*(2), 195–203.

Kiang, N. Y., Siefert, J., Govindjee, & Blankenship, R. E. (2007). Spectral Signatures of Photosynthesis. I. Review of Earth Organisms. *Astrobiology*, *7*(1), 222–251.

Kokaly, R. F., Asner, G. P., Ollinger, S. V., Martin, M. E., & Wessman, C. A. (2009). Characterizing canopy biochemistry from imaging spectroscopy and its application to ecosystem studies. *Remote Sensing of Environment*, 113:S78–S91.

Kokaly, R. F., & Clark, R. N. (1999). Spectroscopic determination of leaf biochemistry using band-depth analysis of absorption features and stepwise multiple linear regression. *Remote Sensing of Environment*, *67*(3), 267–287.

Kondo, T., & Sawatari, C. (1996). A fourier transform infra-red spectroscopic analysis of the character of hydrogen bonds in amorphous cellulose. *Polymer*, *37*(3), 393–399.

Lyder, D., Feng, J., Rivard, B., Gallie, A., & Cloutis, E. (2010). Remote bitumen content estimation of Athabasca oil sand from hyperspectral infrared reflectance spectra using Gaussian singlets and derivative of Gaussian wavelets. *Fuel*, *89*(3), 760–767.

McCann, M. C., Hammouri, M., Wilson, R., Belton, P. S., & Roberts, K. (1992). Fourier Transform Infrared Microspectroscopy Is a New Way to Look at Plant Cell Walls. *Plant Physiology*, *100*(4), 1940–1947.

Mouille, G., Robin, S., Lecomte, M., Pagant, S., & Höfte, H. (2003). Classification and identification of Arabidopsis cell wall mutants using Fourier-Transform InfraRed (FT-IR) microspectroscopy. *Plant Journal*, *35*(3), 393–404.

Muraki, S. (1995). Multiscale of Volume 3D Edge Representation Data by a DOG Wavelet. *Image (Rochester, N.Y.)*, *3*(lD), 35–42.

Poletto, M., Pistor, V., & Zattera, A. J. (2013). Structural Characteristics and Thermal Properties of Native Cellulose. *Cellulose – Fundamental Aspects*, 45–68.

Portillo-Quintero, C., Sanchez-Azofeifa, A., Calvo-Alvarado, J., Quesada, M., & do Espirito Santo, M. M. (2015). The role of tropical dry forests for biodiversity, carbon and water conservation in the neotropics: lessons learned and opportunities for its sustainable management. *Regional Environmental Change*, *15*(6), 1039–1049.

Ramirez, F. J., Luque, P., Heredia, A., & Bukovac, M. J. (1992). Fourier transform IR study of enzymatically isolated tomato fruit cuticular membrane. *Biopolymers*, *32*(11), 1425–1429.

Ribeiro da Luz, B. (2006). Attenuated total reflectance spectroscopy of plant leaves: A tool for ecological and botanical studies. *New Phytologist*, *172*(2), 305–318.

Ribeiro da Luz, B., & Crowley, J. K. (2007). Spectral reflectance and emissivity features of broad leaf plants: Prospects for remote sensing in the thermal infrared (8.0-14.0um). *Remote Sensing of Environment*, *109*(4), 393–405.

Ribeiro da Luz, B., & Crowley, J. K. (2010). Identification of plant species by using high spatial and spectral resolution thermal infrared (8.0-13.5 μm) imagery. *Remote Sensing of Environment*, *114*(2), 404–413.

Ribeiro da Luz, B. (2013). Spectral Library. spectrallibrary.blogspot.ca/2013/12/plants

Rivard, B., Feng, J., Gallie, A., & Sanchez-Azofeifa, A. (2008). Continuous wavelets for the improved use of spectral libraries and hyperspectral data. *Remote Sensing of Environment*, *112*(6), 2850–2862.

Rogge, D. M., & Rivard, B. (2010). Iterative spatial filtering for reducing intra-class spectral variability and noise. *2nd Workshop on Hyperspectral Image and Signal Processing: Evolution in Remote Sensing, WHISPERS 2010 - Workshop Program*, (1), 1–4.

Sanchez-Azoffeifa, G.A., Kalacska, M., Quesada, M., Calco-Alvarado, J. C., Nassar, J.M., Rodriguez, J.P. (2005). Need for Integrated Research for a Sustainable Future in Tropical Dry Forests, 19(2), 285–286.

Sanchez-Azofeifa, G. A., Castro, K., Wright, S. J., Gamon, J., Kalacska, M., Rivard, B., Feng, J. L. (2009). Differences in leaf traits, leaf internal structure, and spectral reflectance between two communities of lianas and trees: Implications for remote sensing in tropical environments. *Remote Sensing of Environment*, *113*(10), 2076–2088.

Salisbury, J. W. (1986). Preliminary measurements of leaf spectral reflectance in the 8-14 μm region. *International Journal of Remote Sensing*, *7*(12), 1879–1886.

Sammons, R. J., Labbe, N., Harper, D. P., Elder, T., & Rials, T. G. (2009). Characterization of lignins using thermal and FT-IR spectroscopic analysis. *Abstracts of Papers of the American Chemical Society*, *238*(2), 2752–2767.

Séné, C. F. B., Mccann, M. C., Wilson, R. H., & Crinter, R. (1994). Fourier-Transform Raman and Fourier-Transform lnfrared Spectroscopy '. *Plant Physiology*, *106*, 1623–1631

Seyed Hamidreaza Ghaffar, M. F. (2013). Structural analysis for lignin characteristics in biomass straw. Biomass and Bioenery 57: 264-279.

Szymanska-Chargot, M., Chylinska, M., Kruk, B., & Zdunek, A. (2015). Combining FT-IR spectroscopy and multivariate analysis for qualitative and quantitative analysis of the cell wall composition changes during apples development. *Carbohydrate Polymers*, *115*, 93–103.

Torrence, C., & Compo, G. P. (1998). A Practical Guide to Wavelet Analysis. *Bulletin of the American Meteorological Society*, *79*(1), 61–78.

Ullah, S., Schlerf, M., Skidmore, A. K., & Hecker, C. (2012). Identifying plant species using mid-wave infrared (2.5-6??m) and thermal infrared (8-14μm) emissivity spectra. *Remote Sensing of Environment*, *118*, 95–102.

Ullah, S., Skidmore, A. K., Ramoelo, A., Groen, T. A., Naeem, M., & Ali, A. (2014). Retrieval of leaf water content spanning the visible to thermal infrared spectra. *ISPRS Journal of Photogrammetry and Remote Sensing*, *93*, 56–64.

Ustin, S. L., & Gamon, J. A. (2010). Remote sensing of plant functional types. *New Phytologist*, *186*(4), 795–816.

Vyas, N., & Argal, A. (2014). Isolation and characterization of oleanolic acid from roots of Lantana camara. *Asian Journal of Pharmaceutical and Clinical Research*, *7*(SUPPL. 2), 189–191.

Wilson, R. H., Smith, A. C., Kac, M., Saunders, P. K., Wellner, N., & Waldron, K. W. (2000). The Mechanical Properties and Molecular Dynamics of Plant Cell Wall Polysaccharides Studied by Fourier-Transform Infrared Spectroscopy 1. *Plant Physiology*, *124*(September), 397–405.

Zhang, J., Rivard, B., Sánchez-Azofeifa, A., & Castro-Esau, K. (2006). Intra- and inter-class spectral variability of tropical tree species at La Selva, Costa Rica: Implications for species identification using HYDICE imagery. *Remote Sensing of Environment*, *105*(2), 129–141.

5.4 Conclusion References

Collen, B., Pettorelli, N., Bailie, J. E. M., Durant, S. 2013. *Biodiversity monitoring and conservation: bridging the gap between global commitment and local action*. Wiley-Blackwell publications.

Houghton, J. T., Ding, Y., Griggs, D. J., Noguer, M., Van der Linden, P. J., Dai, X., Johnson, C. A. (2001). Climate Change 2001: The Scientific Basis. *Climate Change 2001: The Scientific Basis (IPCC)*, 881.

Kokaly, R., Despain, D. G., Clark, R. N., & Livo, E. (2003) Mapping vegetation in Yellowstone National Park using spectral feature analysis of AVIRIS data. Remote Sensing of the Environment 84: 437-456

Kokaly, R. F., Asner, G. P., Ollinger, S. V., Martin, M. E., & Wessman, C. A. (2009). Characterizing canopy biochemistry from imaging spectroscopy and its application to ecosystem studies. *Remote Sensing of Environment*, *113*(SUPPL. 1), S78–S91.

Kokaly, R. F., & Clark, R. N. (1999). Spectroscopic determination of leaf biochemistry using band-depth analysis of absorption features and stepwise multiple linear regression. *Remote Sensing of Environment*, *67*(3), 267–287.

Myers, N., Mittermeier, R. A., Mittermeier, C. G., da Fonseca, G. A. B., & Kent, J. (2000). Biodiversity hotspots for conservation priorities. *Nature*, *403*(6772), 853–858.

Reich, P. B. (2014). The world-wide "fast-slow" plant economics spectrum: A traits manifesto. *Journal of Ecology*, *102*(2), 275–301.

Ribeiro da Luz, B. (2006). Attenuated total reflectance spectroscopy of plant leaves: A tool for ecological and botanical studies. *New Phytologist*, *172*(2), 305–318.

Ribeiro da Luz, B., & Crowley, J. K. (2007). Spectral reflectance and emissivity features of broad leaf plants: Prospects for remote sensing in the thermal infrared (8.0-14.0μm). *Remote Sensing of Environment*, *109*(4), 393–405.

Ribeiro da Luz, B., & Crowley, J. K. (2010). Identification of plant species by using high spatial and spectral resolution thermal infrared (8.0-13.5 [mu]m) imagery. *Remote Sensing of Environment*, *114*(2), 404–413.

Sanchez-Azofeifa, G. A., Castro, K., Wright, S. J., Gamon, J., Kalacska, M., Rivard, B., Feng, J. L. (2009). Differences in leaf traits, leaf internal structure, and spectral reflectance between two communities of lianas and trees: Implications for remote sensing in tropical environments. *Remote Sensing of Environment*, *113*(10), 2076–2088.

Sanchez-Azoffeifa, G.A., Kalacska, M., Quesada, M., Calco-Alvarado, J. C., Nassar, J.M., Rodriguez, J.P. (2005). Need for Integrated Research for a Sustainable Future in Tropical Dry Forests, 19(2), 285–286.

Schnitzer, S. A. (2005). A mechanistic explanation for global patterns of liana abundance and distribution. *The American Naturalist*, *166*(2), 262–276.

Schnitzer, S, Bongers, F., Burham, R. J., & Putz, F. E., (2015) *Ecology of lianas*. John Wiley & Sons Blackwell, Oxford UK.

Schnitzer, S., & Bongers, F. (2002). The ecology of lianas and their role in forests. Trends in Ecology & Evolution, 17(5), 223–230.

Ustin, S. L., & Gamon, J. A. (2010). Remote sensing of plant functional types. *New Phytologist*, *186*(4), 795–816.

Urquhart, G., Chomentowski, W.S. (2001). Tropical deforestation. Technical report, NASA Earth Observatory (Burgess)

Winter, S. (2012). Forest naturalness assessment as a component of biodiversity monitoring and conservation management. *Forestry*, *85*(2), 291–304.

Wright, I. J., Reich, P. B., Westoby, M., Ackerly, D. D., Baruch, Z., Bongers, F., Gulias, J. (2004). The worldwide leaf economics spectrum, Nature, 12, 821–827.